Derivatization of Amino Acids for Surface Assisted Laser Desorption/Ionization (SALDI) Mass Spectrometry Analysis

by

Jing Ji

A thesis submitted in partial fulfillment of the requirements for the degree of

Doctor of Philosophy

Department of Chemistry
University of Alberta

© Jing Ji, 2019

Abstract

Metabolites with low molar mass, such as amino acids, are of great importance in disease diagnosis. The rapid and accurate detection of amino acids and other small metabolites in biological samples has become significantly important. Surface assisted laser desorption/ionization (SALDI) has been applied in this area for detecting small metabolites, and nanostructure-based surfaces for SALDI provide reduced background noise and improved intensity in mass spectrometry. However, salts and other matrices in biological samples are a key challenge for accurate quantification of amino acids. In this thesis, we describe an approach to matrix-free SALDI strategies on nanoporous silicon surfaces for quantitative analysis of amino acids in complex biofluid samples. The approach removes interference through a simple on-chip cleanup method utilizing hydrophobic interactions.

This thesis investigates the application of nanoporous silicon films fabricated by glancing angle deposition (GLAD) technique for matrix-free SALDI mass spectrometry. The GLAD chips have controllable morphology, stable chemical property, and long shelf life, which are suitable for SALDI-MS. We investigate a silanization method to perfluoro modify the surface of GLAD chips, and utilize the affinity of perfluoro coated surfaces to fluorous labeled analytes for on-chip

purification. In chapter 2, different fluorous propanol as derivatizing reagents are tested to label carboxyl groups in amino acids, followed by SALDI-MS measurements on perfluoro coated GLAD films. The fluorous derivatization raises the mass of analytes to less background-obscured higher mass regions, and enables separation of fluorous labeled compounds from unlabeled ones on perfluoroalkyl-silylated GLAD chips through F-F interactions. A simple on-chip cleanup step is applied to remove unlabeled compounds, while the fluorous derivatives are retained, resulting in improved sensitivity in SALDI-MS. In chapter 3, the fluorous propanol based derivatization reaction is used for the quantification of amino acids in serum. C18 beads solubilized in methanol are used to remove proteins from the serum samples, the samples are then labeled by 3-(perfluorohexyl)propan-1-ol and measured by SALDI-MS. The quantitative results show good consistency with normal human ranges, and compare well with other studies.

In the second segment of this thesis, 4-chloro-3,5-dinitrobenzotrifluoride (CNBF) and 1H-perfluorohexane-1,1-diol are evaluated as the derivatization reagents to label amine groups in amino acids. The quantitative results of 1H-perfluorohexane-1,1-diol labeled derivatives provide reliable linear regression, and the relative standard deviations in the intensity ratios between the analyte and

the internal standard are low, indicating a great potential for precise quantitative analysis of amino acids in real samples.

Preface

The glancing angle deposition (GLAD) chips referred to in this thesis were fabricated by Aaron Hryciw of nanoFAB, University of Alberta. The perfluoro silanization method for modifying SALDI chips and SALDI-MS instrument settings for low mass analytes were developed by Chen Peng.

The literature review of Chapter 1 is my original work. The development of the surface washing and derivatization methods, the detection of samples by SALDI-MS, and data collection and analysis in Chapters 2, 3, 4, and 5 are my original work. A portion of Chapter 3 of this thesis will be submitted for publication. My role includes experimental design, data collection, data analysis, and manuscript drafting. Rupasri Mandal contributed to the NMR analysis. Randy Whittal contributed to LC-MS analysis.

The fluorous diol derivatization method in Chapter 4 was developed by Yohei Sakaguchi of Fukuoka University. The work in Chapter 5 was done in collaboration with Yuting Hou. I was responsible for off-chip derivatization, SALDI-MS detection on perfluoro coated GLAD films, and data collection and analysis. Yuting assisted with the sample preparation for whole blood on centrifugal discs.

Acknowledgements

At this moment, I would like to express my sincere gratitude for people who offered help and support to my PhD study.

First, I would like to thank my supervisor, Professor D. Jed Harrison, for his insightful guidance and constant support. For the past six years working with Jed, I was deeply influenced by his broad knowledge and rigorous attitude to scientific research. What I have learned from this experience is meaningful and valuable for my future career and life.

I would like to thank my supervisor committees, Professors Mark McDermott, Christopher Cairo for their guidance and suggestions to my graduate study. I am grateful to Professors Liang Li and Jie Chen for their attendance in my candidacy exam. I'd like to thank Professor Lekha Sleno to be my external examiner, and many thanks to Professors Nils Petersen and Jie Chen for attending my defense.

I would like to express my appreciation to the former and current members of Harrison's group, especially Chen Peng, Ya Zhou, and Yufeng Zhao for helping me in my research project. I am grateful to Randy Whittal, Jing Zheng from Mass Spectrometry Lab for their precious guidance. I would like to thank Rupa Mandal for her collaboration. I would like to thank the staff in Department of Chemistry and nanoFAB, especially Gareth Lambkin, Anita Weiler, Lin Ferguson, and Aaron Hryciw for their kind help and technical support to my research and study. I would like to express my thanks to Dr. Yohei Sakaguchi and Dr. Hitoshi Nohta for their kind help to my research.

Finally, I would like to express my gratitude to my family and friends, who always support me and encourage me in the past six years and my whole life.

Table of Contents

List of Tables

List of Figures

List of Abbreviations

AD	Alzheimer's disease
aCSF	Artificial cerebrospinal fluid
CNBF	4-Chloro-3,5-dinitrobenzotrifluoride
CRP	C-reactive protein
CSF	Cerebrospinal fluid
CVD	Chemical vapor deposition
DIOS	Desorption/ionization on silicon
DP	Dipeptides
DSS	Sodium 2,2-dimethyl-2-silapentane-5-sulfonate
EISA	Evaporation induced self-assembly
FAA	Free amino acids
GC	Gas chromatography
GLAD	Glancing angle deposition
HILIC	Hydrophilic interaction liquid chromatography
HOPG	Highly oriented pyrolytic graphite
IM	Ion-mobility
IS	Internal standard
LC	Liquid chromatography
LDI	Laser desorption/ionization
LOQ	Limit of quantitation
MALDI	Matrix-assisted laser desorption/ionization
MS	Mass spectrometry
MWCO	Molecular weight cut-off

MWNTs	Multi-walled carbon nanotubes
NALDI	Nano-wire assisted laser desorption/ionization
NDs	Nanodots
NMR	Nuclear magnetic resonance
NIMS	Nanostructure-initiator mass spectrometry
OAD	Oblique angle deposition
PFAA	Plasma free amino acids
PFG	Pulsed-field gradient
$pFSiCl_3$	(1H, 1H, 2H, 2H-perfluorooctyl) trichlorosilane
PGC	Nanoporous graphitic carbon
pSi	Porous silicon
PVD	Physical vapor deposition
R^2	Correlation coefficient
RSD	Relative standard deviation
SALDI	Surface-assisted laser desorption/ionization
SD	Standard deviation
SIM	Single ion monitoring
SIMS	Secondary-ion mass spectrometry
S/N	Signal to noise ratio
SNP	Silica nanoparticles
TOF	Time of flight
UTLC	Ultra-thin layer chromatography
UV	Ultraviolet

Chapter 1 Introduction

1.1 Laser desorption/ionization (LDI) mass spectrometry (MS) on nanoporous silicon

1.1.1 Surface-assisted laser desorption/ionization mass spectrometry (SALDI-MS)

Mass spectrometry (MS) is a widely used analytical chemistry technique for the identification and quantification of compounds. Ionization is very important in MS analysis for converting neutral molecules to charged ions.[1] The specific choice of ionization method depends on many factors, such as the chemical and physical properties of the sample, the molecular weight and mass range of the analytes, the fragmentation patterns, *etc.*[2,3] One ionization method, which is called laser desorption/ionization (LDI), is a soft ionization technique developed in the late 1960s.[4–7] A major breakthrough for LDI-MS was achieved when a chemical matrix was introduced in the 1980s.[8–10] The matrix-assisted laser desorption/ionization (MALDI) method relies on an organic matrix that is co-crystallized with the analytes, to transfer absorbed photon energy to surrounding analytes.[10,11] Hillenkamp and Karas published a MALDI method for ionization and desorption of biomolecules by using an organic matrix and a 266 nm laser.[10] In 1988, Tanaka *et al*. used 30 nm inorganic cobalt powders to mix with a liquid matrix of glycerol, and this combination enabled the analysis of protein and polymers with molecular weights as high as 34 kDa.[12] MALDI-MS reduces ion fragmentation and offers many advantages as a powerful tool for the analysis of biomolecules, but it also introduces background ions from the matrices. The matrix-related ions are highly

ionized in the low mass region, which can interfere with the detection of samples with low molecular weight.[13] Many efforts have been made to overcome this problem and to extend the application of MALDI-MS. Surface-assisted laser desorption/ionization (SALDI) is a newer method based on MALDI-MS and has been extensively studied during the past 25 years.

The concept of SALDI was originally proposed by Sunner *et al*. in 1995 from the inspiration of Tanaka's earlier work.[14] In their paper, 2-150 micron graphite particles were mixed with solutions of analytes in glycerol.[14] The electro-conductive graphite particles played a significant role in absorbing and transferring energy of the laser light in the desorption/ionization process.[15] Liquid glycerol was used to provide a proton source and to buffer the energy transfer.[16] With the assistance of the graphite surface, a spectrum with reduced background noise in the low mass region was obtained.[14] Since then, a number of surfaces and materials including nanomaterials have been reported to work in SALDI, such as silver thin films and silver particles,[13] titanium nitride (TiN) nanoparticle suspensions in glycerol,[17] and Al, Mn, Mo, Si, Sn, zinc oxide (ZnO), and titanium dioxide (TiO_2) particles as "inorganic matrices" in glycerol[18]. In these metal or inorganic surface aided strategies, less background noise is produced. However, the presence of liquid matrices still has some undesirable effects for sample analysis.[13]

Siuzdak's group reported the first truly matrix-free strategy, named desorption/ionization on silicon (DIOS) in 1999.[19] Porous silicon (pSi) was used to trap the analytes deposited on the surface, and to give assistance for the ionization process.[19,20] The matrix-free SALDI takes advantage of an active surface instead of using the chemical matrix of MALDI, to eliminate matrix interference, which

provides great advantages for the detection of analytes with low molecular weight.[15] Many nanoparticles of metals and metal oxides without a liquid matrix, such as magnetic iron oxide (Fe_3O_4) particles,[21] mesoporous WO_3-TiO_2,[22] gold (Au) nanoparticles,[23,24] and Fe_3O_4/TiO_2 core/shell nanoparticles,[25] were examined for SALDI-MS. Moreover, nano-wire assisted laser desorption/ionization (NALDI) has subsequently been reported.[26,27] The unique properties of nanomaterials greatly facilitate direct desorption/ionization of the analytes, and improve sensitivity and resolution in SALDI-MS.[14] Based on these studies, the SALDI technique has been widely applied in the analysis of biomolecules with low molecular mass, such as amino acids, lipids, peptides, and small proteins.[28–33]

The purpose of our research is to develop a method that can simultaneously detect small metabolites, especially amino acids, in complex biological samples with high sensitivity and selectivity. From this perspective, direct ionization in SALDI-MS is an ideal choice. The nanostructure-based surfaces in SALDI provide reduced background noise and improved intensity in MS detection.[14,26] Another important advantage is that nanostructured surfaces can be functionalized through simple chemical reactions. Many nanostructured surfaces and the techniques for producing nanostructured surfaces have been studied. Among those surfaces, glancing angle deposition (GLAD) chips have ordered structure, controllable morphology, and stable chemical and physical properties compared with other surfaces, which are proven to be suitable candidates in SALDI-MS.[34–36] The porous silicon surface of GLAD chips can be silylated, and a silanization method has been developed to modify porous silicon surfaces with perfluoro groups.[37,38] The perfluoro coated surface has an affinity to capture fluorous labeled analytes in complex samples. Thus fluorous derivatization is involved in our research for labeling target

molecules with fluorous tags. Different derivatization types and reactions have been reviewed to find a suitable derivatization reaction, and fluorous alkylation reactions have been selected. Several derivatization reagents are evaluated in this thesis, to label carboxyl groups and amine groups in amino acids. Derivatization provides clear advantages for raising the mass of analytes to higher mass regions and separating fluorous labeled species from unlabeled compounds through simple rinsing. The combination of derivatization reactions and perfluoro coated nanoporous surfaces enables rapid and sensitive quantification of amino acids in biological samples.

1.1.2 Laser desorption/ionization (LDI) on nanoporous silicon

1.1.2.1 Nanostructured surfaces in SALDI-MS

Nanostructured films and surfaces are widely exploited in nature, from plant leaves to butterflies, however, the manufacturing and development of nanostructured surfaces in the industry is relatively recent.[39] The high surface area to volume ratio, high photon absorption efficiency, and low heat capacity make nanostructured surfaces suitable candidates for realizing effective desorption/ionization of analytes in SALDI-MS.[26]

Carbon-based and semiconductor-based nanostructured surfaces are two important types of materials used in SALDI-MS.[15] For carbon-based nanomaterials, graphite particles have been applied in SALDI-MS since the 1990s.[14] Other carbon-based nanomaterials including multi-walled carbon nanotubes (MWNTs)[40,41],

buckminsterfullerene (C_{60})[40], highly oriented pyrolytic graphite (HOPG)[40], nanoporous graphitic carbon (PGC)[15,40], porous oxidized graphitized carbon[42], and graphitic carbon nitride nanosheets[43] have been explored and compared in SALDI analysis of small molecules. Tang *et al.* evaluated the LDI-MS performance of different carbon-based surfaces.[40] The scanning electron micrographs of HOPG surfaces and MWNTs surfaces revealed that destruction of their surfaces after laser irradiation occurred, as shown in Figure 1-1. Carbon surfaces were partially laser annealed on HOPG surfaces under high laser fluence, spherical clusters of ~ 10 nm diameter were formed after N_2 laser irradiation, as shown in Figure 1-1a.[40] A series of carbon cluster ions (differing by m/z 12.0) were found in the negative ion mass spectra of carbon-based surfaces, as shown in Figure 1-2. The carbon cluster ions suppress the signal of analytes, thus limiting the application of carbon-based SALDI.[40] However, the carbon cluster ions can be filtered out by ion-mobility (IM) mass spectrometry utilizing the different migration times between carbon cluster ions and biomolecules.[44] Nonetheless, the considerable variation in general background and specific cluster peaks illustrates the challenges associated with carbon-based nanomaterials.

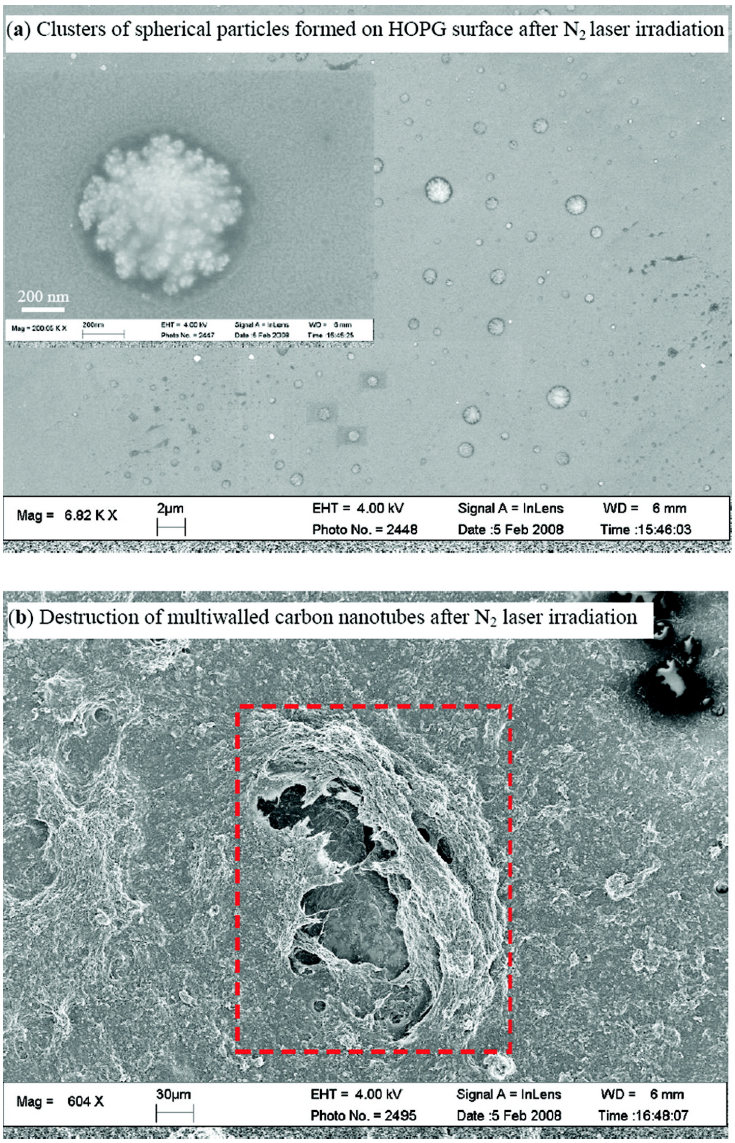

Figure 1-1: Scanning electron micrographs of (a) clusters of spherical particles formed on the surface of HOPG after N_2 laser irradiation (laser fluence = 109 mJ cm^{-2}) and (b) destruction of MWNT after N_2 laser irradiation (laser fluence = 43 mJ cm^{-2}). The carbon substrates were irradiated with the N_2 laser at a frequency of 10 Hz for 1000 laser pulses. Reprinted with permission from [40] © 2009 American Chemical Society.

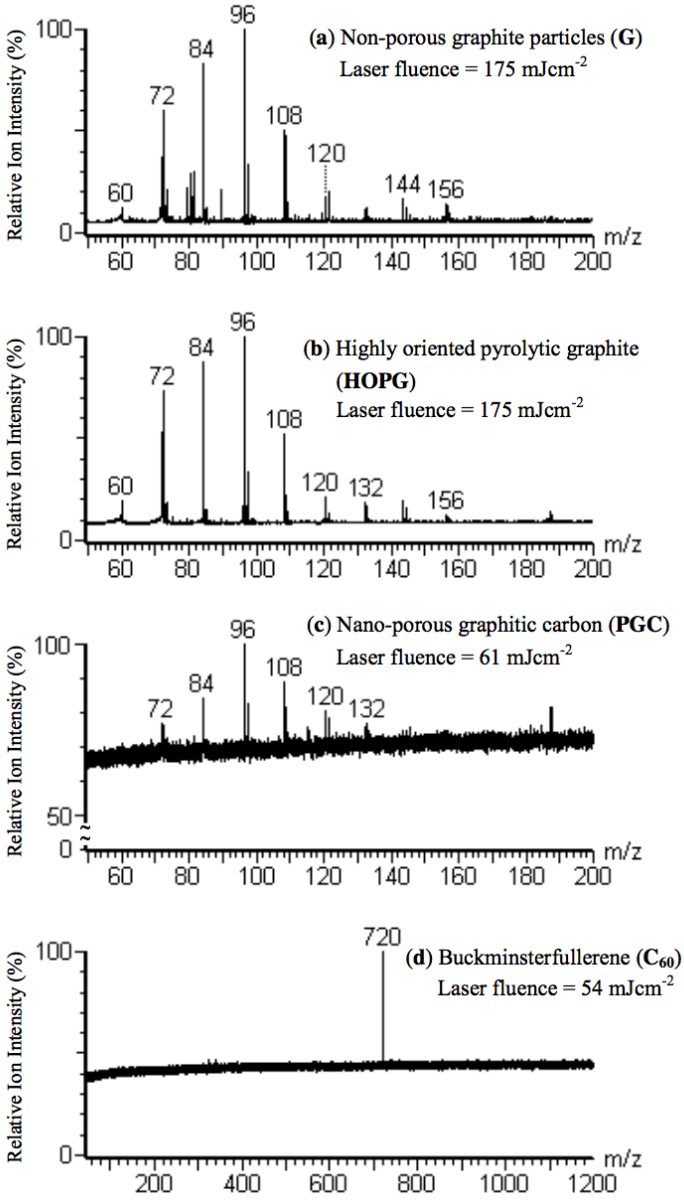

Figure 1-2: Negative SALDI mass spectra of (a) non-porous graphite particles, (b) highly oriented pyrolytic graphite, (c) nanoporous graphitic carbon and (d) buckminsterfullerene. Reprinted with permission from [40] © 2009 American Chemical Society.

Nanoporous silicon is a typical example of semiconductor-based nanostructured surfaces. The generation of nanoporous silicon surfaces extends the application of surface-assisted LDI-MS in metabolite analysis. Applying nanoporous silicon films in LDI-MS was first proposed by Siuzdak and his coworkers in 1999,[19] then a series of explorations for desorption/ionization on silicon mass spectrometry were presented by his group.[20,29,31,32] The porous structure provided a scaffold for trapping the analytes, and the desirable absorption capacity in the ultraviolet (UV) region of silicon substrates afforded effective transfer of laser energy to the adsorbates.[15,31]

Many other nanostructured surfaces are also studied in LDI-MS. ZnO, silicon carbide (SiC), tin (IV) oxide (SnO_2), and gallium nitride (GaN) nanowires grown on Si substrates have been employed to provide different desorption/ionization efficiencies.[26] Similarly, ZnO nanoparticles produced on Au substrates were reported by Park's group.[45] Silicon nitride nanoparticles suspended in trifluoroacetic acid (TFA) demonstrated improved capacity to desorb/ionize small drugs.[46] Tao's group developed a method using self-assembled germanium nanodots (GeNDs) to deposit on a silicon wafer by molecular beam epitaxy.[47,48] GeND-MS lowered the detecting limit to sub-femtomole level.[48] These nanostructured surfaces improve the detection dynamic range, improve the reproducibility and sensitivity in LDI-MS detection, but have not yet become a daily tool in biomolecular analysis.[49]

1.1.2.2 Nanoporous silicon surfaces in SALDI-MS

Nanoporous silicon surfaces offer remarkable advantages in SALDI-MS and have been studied in-depth since the late 1990s. The application of nanoporous silicon surfaces has been extended to the analysis of a wide range of compounds including metabolites, drugs, and peptides, with detection limits at femtomole and attomole levels.[19,20]

Nanoporous silicon films can be classified into two broad groups. One group is represented by a continuous structure, where all elements of the entire structure are linked together as a continuous three-dimensional network, such as a cellular-like or foam-like morphology.[39] Another group of nanoporous and nanostructured films shows an isolated structure, where the elements are free-standing from each other, forming a brush-like or hair-like structure.[39]

A vast number of methods have been developed to produce nanoporous surfaces, including chemical processing and physical processing methods. The porous silicon surfaces of DIOS-MS in Siuzdak's work were prepared by electrochemical etching silicon wafers to generate a continuous nanoporous structure. Characteristics such as thickness, morphology, and porosity are controllable by adjusting etching conditions and the type of silicon wafers.[19] The development of DIOS films started a new chapter of LDI-MS and enabled quantitative analysis of peptides and amino acids.[50] However, several problems still prevent accurate quantification in DIOS-MS. The freshly prepared surface is easy to oxidize, and the hydrogen-terminated porous silicon is chemically unstable. The wet chemical etched films have a high affinity for hydrocarbons from ambient air, which

introduces chemical noise in MS spectra.[15] In addition, surface restructuring of pSi during laser irradiation is also observed in the desorption/ionization process.[40,51] These undesirable properties limit the application of DIOS films in SALDI-MS.

Other chemical processing methods have been studied. Evaporation induced self-assembly (EISA) process uses sol-gel chemistry, a form of condensation polymerization using metal alkoxides as the monomer.[39,52] Nitta[53], Jain[54] and Ojha[55] described a two-step, acid-base catalysis scheme of tetraethyl orthosilane (TEOS) to produce a siloxane film on a silicon wafer. The surface structure and film thickness were controlled by the chemistry they used, the evaporation rate of the solvents, the fluid mechanics of coating, and polymerization interaction.[39] These chemically processed surfaces usually have a continuous porous structure,[56] such as the DIOS surface shown in Figure 1-3 and the nanoporous silica film shown in Figure 1-4. The structure of the material is random or partially random, instead of uniformly ordered.

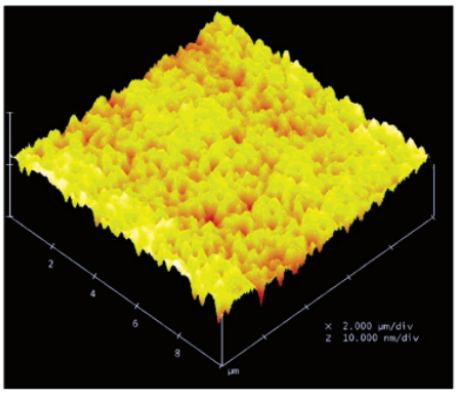

a

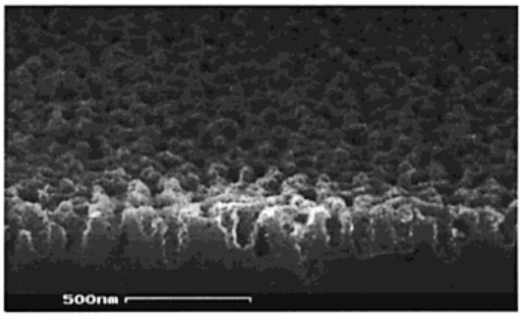

b

Figure 1-3: (a) Topography of a 10 × 10 µm part of the DIOS surface from AFM measurements. Considering that the tip curvature is 20 nm, the image indicates that a significant number of the pore entrances are smaller in diameter. Reprinted with permission from [56] © 2005 American Chemical Society. (b) SEM analysis of the "double-etched" porous silicon surface prepared from low-resistivity n^+-Si material (0.001-0.005 Ω, cm). Reprinted with permission from [31] © 2001 American Chemical Society.

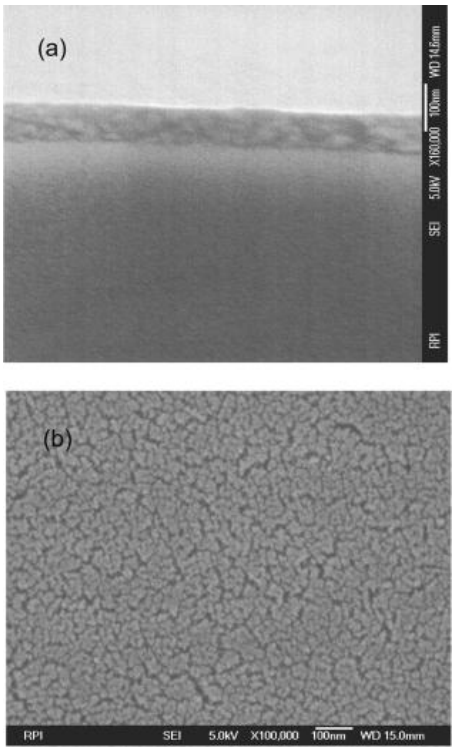

Figure 1-4: (a) Cross section (160000 × zoom) and (b) top view (1000000 × zoom) images of the 105 nm thick nanoporous silica film by SEM. A crack-free surface can be imaged. Reprinted with permission from [55] © 2006 AIP Publishing.

In addition, the wet chemical processed films require water in the reaction. The water is hard to remove and affects the dielectric constant of the surface.[39] Vapor deposition methods require no water, produce hybrid materials with enhanced mechanical properties, and are easy to integrate into processing methods.[39] Grill reported a plasma enhanced chemical vapor deposition (CVD) method to produce porous surfaces.[57] The SiCOH films were produced via a sacrificial technique in which the cyclic tetrasiloxane precursor was deposited with a porogen, the porogen

was then removed by thermal annealing due to its thermal instability.[57]

Physical processing methods for producing nanoporous films are based on physical vapor deposition (PVD), including oblique angle deposition (OAD) and glancing angle deposition (GLAD). In OAD, the technique is used to grow porous, sculptured thin films with a fixed substrate, typically. GLAD was invented by Brett's group in the 1990s as an extension of OAD, wherein the position of the substrate is manipulated during film deposition.[58–60]

The angle between the substrate normal and the incident vapor flux is defined as the deposition angle α. A flux of atoms is produced by the vapor source. Many vapor sources such as electron-beam evaporation, thermal evaporation, sputtering, several co-sputtering techniques, and pulsed-laser deposition have been used for GLAD.[58] The arrival of the vapor flux forms random nuclei on the surface. The nuclei grow into nanocolumns upon ballistic shadowing. Substrate rotation alters the normal growth of the nanocolumns relative to the substrate. A schematic presentation of nanocolumn formation is shown in Figure 1-5. Azimuthal rotation about the substrate normal is measured by the angle φ. A motor is used to control the deposition/rotation rate. A schematic of a GLAD-capable physical vapor deposition system is shown in Figure 1-6.

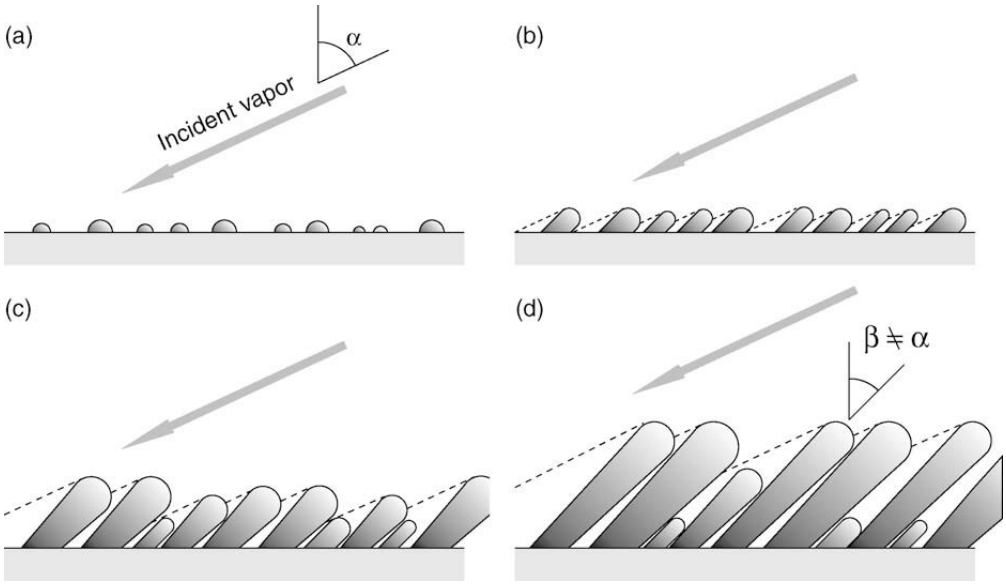

Figure 1-5: Schematic view of GLAD growth: (a) initial arrival of vapor flux at an angle α, producing a random distribution of nuclei on substrate surface; (b) nuclei grow, casting shadows across substrate; (c) columns develop, partially shadowing smaller neighbors and suppressing their growth; (d) columns grow at an inclined angle. Some columns have become extinct, fully shadowed by larger neighbors. Further growth is restricted to the top of columns. Reprinted with permission from [58] © 2010 Peter M. Martin. Published by Elsevier Inc.

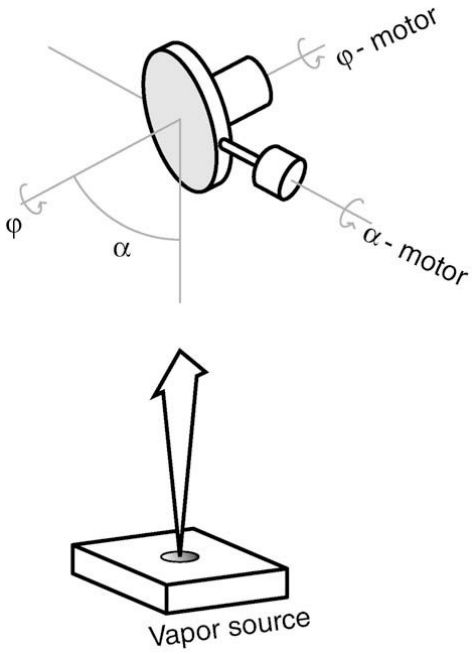

Figure 1-6: Schematic of GLAD apparatus and characteristic angles. Reprinted with permission from [58] © 2010 Peter M. Martin. Published by Elsevier Inc.

Surfaces produced by GLAD have an ordered structure with controllable porosity, thickness, density, and topology, obtained with high reproducibility. The variation of α and φ during deposition provides GLAD films different basic structures. Both α and φ have three designations, including a constant designation in which the substrate remains stationary at a fixed angle during deposition, a discrete designation wherein the substrate undergoes periodic changes in a given angle, but is stationary otherwise, and a continuous designation with the substrate in motion continuously during a deposition at a specified angle.[58] These designations yield GLAD films with different structural architecture such as slanted posts, vertical posts, and so on.[58,60–62]

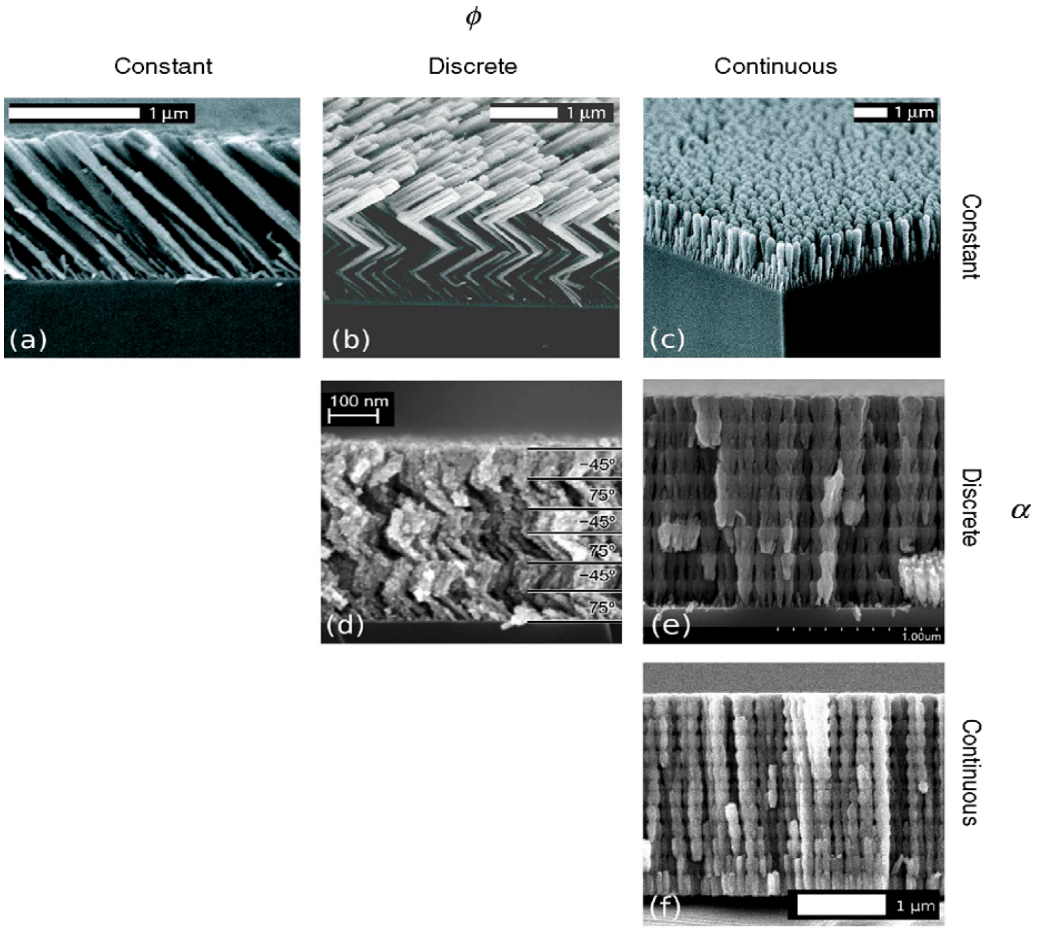

Figure 1-7: The basic GLAD structures: (a) slanted post; (b) chevron; (c) vertical post; (d) slanted post stack; (e) high-low stack and (f) rugate. These structures are fabricated using constant, discrete and continuous motion in α and β. Reprinted with permission from [58] © 2010 Peter M. Martin. Published by Elsevier Inc.

1.1.3 Improved LDI-MS on silylated porous silicon surfaces

The development of surface chemistry for a porous silicon surface adds a new dimension to LDI-MS. The mechanism of nanoporous surface assisted laser

desorption/ionization has not been fully understood, since complex factors are involved in the energy transfer pathway, ionization, and various interactions. However, the thermal, electronic, and chemical properties of the substrates are believed to be three of the most important factors in SALDI-MS.[49] The electronic property of the surfaces facilitates efficient energy transfer. The thermal conductivity of pSi substrates is involved in the laser induced heating desorption process.[63] Thermal induced desorption is not the only pathway for SALDI-MS, the surface area and porosity also affects adsorption, retention of the analytes, and the desorption process.[15] The presence of residual solvent molecules on or in a porous surface plays an important role in analyte desorption. The vaporization of solvent reduces analyte-analyte collision, stabilizes analyte ions, and promotes ionization by providing active proton sources.[49] These make porous surfaces a desirable platform for LDI-MS.

Chemical modification via hydrosilylation[64–68] or via silanization[37,69] for porous silicon surfaces has provided some success. Buriak and her coworkers presented and compared Lewis acid-mediated hydrosilylation and white light-promoted hydrosilylation of alkenes and alkynes on non-oxidized porous silicon.[65,66,68] The cathodic electrografting reaction directly attaches alkynyl residues through reduction of a silicon hydride bond.[67,68] Modification of pSi by silanization on oxidized pSi surface has been studied. In Trauger's work, silylation chemistry on porous silicon provides ultra-high sensitive analysis of analytes through hydrophobic interactions for direct analyte extraction.[37] Chemically functionalized pSi surfaces provide better performance in surface stability, sample preparation, and selective analyte capture.[37] Different modification reagents were evaluated by Trauger, the perfluoro silane best improved the ionization efficiency of pSi. Based

on this study, a former group member, Chen Peng proposed a simple modification method for GLAD silanization.[38] GLAD films were silylated by immersing in reactive silane solution in methanol for 30 min. It has been proved that the concentration of silane solution and the reaction time affects the hydrophobicity and stability of the GLAD films.[35,38,70] The silylated GLAD films enhance the sensitivity in SALDI-MS and enable accurate quantification of small metabolites.[35]

1.1.4 Application of nanoporous silicon surfaces in biomolecular analysis

Nanoporous silicon surfaces have been a powerful tool in chemical and biological analysis in LDI-MS. A DIOS chip allows for direct identification of low molecular weight compounds in the presence of potentially interfering compounds, as well as distinguishing and identifying specific biopolymers from complex biological media.[20,71] Approaches in metabolomics are obtained through nanostructured surfaces. An automated DIOS-MS system was developed in Shen's work to increase the throughput for monitoring thousands of inhibitors.[31] In Trauger's work, the detection limit of des-Arg^9-bradykinin molecules was decreased to less than 500 using a perfluorophenyl-modified surface, which provided ultra-sensitive analysis of analytes.[37] Vaidyanathan *et al.* generated metabolic footprinting of haploid yeast single-gene deletants (mutants) using DIOS-MS, 26 of the 30 metabolites could be covered between positive and negative ion modes.[72] Liu described a two-dimensional matrix-free DIOS imaging method to map small molecules on mouse liver tissues based on secondary-ion mass spectrometry (SIMS).[73] DIOS-MS is also refined as nanostructure-initiator mass spectrometry

(NIMS). NIMS is a surface-based MS technique in which liquid (initiator) compounds were trapped to nanostructured surfaces.[74,75] The perfluoro siloxanes were selected as good initiators for ion-NIMS in tissue MS imaging on electrochemically etched DIOS chip, resulting in a 1000-fold enhancement in sensitivity for high-resolution label-free analysis of peptide microarrays.[76,77] NIMS on porous silicon also allows for direct mass analysis of single cell and tissue imaging, and direct characterization of blood and urine.[76]

The physical vapor deposition of GLAD films gives improved quality with increased shelf life in ambient conditions, compared to many other porous substrates. Our former group member, Jemere, demonstrated that silicon GLAD films are a good nanoporous surface in SALDI for small molecules between 150 ~ 2500 Dalton.[34] Singh established an ultra-thin layer chromatography (UTLC) based LDI-MS method on silicon and silica GLAD films. UTLC separation and detection were performed on a single platform, higher ionization efficiencies were obtained in her work compared with other substrates.[36] Singh also presented the results of the GLAD film based SALDI mass spectrometry imaging for rat tissue sample in her work, some lipids and fatty acids were successfully detected.[36] Zhou[35] and Zhao[78] presented their methods for quantifying metabolites in serum on silylated GLAD films.

Nanoporous and nanostructured surfaces have been extensively studied and applied to biochemical analysis, imaging mass spectrometry, metabolic profiling, as well as to environmental pollutants.[79] Compared to other SALDI-MS methods, better laser desorption/ionization efficiency and higher sensitivity are observed on the nanoporous silicon surface.[49] These advantages mean that the exploration of

nanostructured surface assisted LDI-MS will be continued by many researchers.

1.2 Metabolomics for diagnosis

Metabolites are the intermediate end products of important metabolic functions.[80] Many studies have demonstrated that fluid samples from patients with specific diseases exhibit quantitative changes of a panel of metabolites, including amino acids, as biomarkers.[81–95] Although the effects of disease progression on amino acid metabolism are still unclear, the quantitative changes in amino acids provide important information for disease diagnosis. Suliman and coworkers compared cysteine levels of ninety-three patients with signs of inflammation (CRP > 1mg/dL) with 157 non-inflamed patients, and found patients had significantly lower levels of cysteine.[89] Fonteh measured free amino acids (FAA) and dipeptides (DP) in cerebrospinal fluid (CSF), plasma, and urine from probable Alzheimer's disease (AD) patients.[81] Histidine, ornithine, glycine, carnosine, *etc*. accounted for the major changes between control group and patients, indicating that antioxidants or FAA associated urea metabolic pathway may be important in preventing AD progression.[81] Lai compared 13 studies on plasma free amino acids (PFAA) profiles with malignant tumors in 2005 and concluded that the sensitivity of PFAA profile for cancer diagnosis was relatively high, but the specificity is low.[90] In 2011, Miyagi's work measured PFAA from patients diagnosed with one of five types of cancer: lung, gastric, colorectal, breast, or prostate cancer.[92] The results show that PFAA analysis has great potential to determine the diagnosis of various diseases and to understand the pathogenesis of the disease from a single blood sample.[92]

Poschke concluded that preoperative serum levels of 8 out of 15 amino acids were significantly higher in breast cancer patients than healthy donors, but after surgery, only 2 out of 15 amino acids (glutamic acid and valine) were still higher in patients.[91] However, in Gu's study, the level of histidine was significantly lower in patients with breast cancer, while the level of arginine and threonine were higher compared with healthy donors.[83] These studies demonstrate that changes in amino acid levels in human biological samples provide critical information for diagnosis.

Amino acids are among the most suitable candidates for studying metabolomics as they are either obtained through diet or endogenous synthesis, and play critical physiological roles both as basic metabolites and metabolic regulators.[92,96] The basal level of amino acids in blood, cerebrospinal fluid (CSF), and saliva samples is at μM levels, therefore developing a sensitive and selective method for determining amino acid levels in biofluid samples is of great importance.

A challenge for accurate quantitative analysis of amino acids is the interference from complex biological samples. Many methods using liquid chromatography (LC) with fluorescence, UV, or mass spectrometry (MS) have been reported utilizing column separation.[97–104] To protect the instrument, proper sample preparation procedure is required. After optimization of the elution method, certain analytes can be measured simultaneously by LC-MS.[103] However, LC-MS is often a relatively time consuming technique. Developing more rapid, sensitive and selective methods for quantifying amino acids is potentially useful. Direct analysis of amino acids in biological samples was achieved based on silylated DIOS chips in Trauger's work[37]. Further studies on GLAD films have been reported by Peng and Zhou.[35,38]

1.3 Derivatization reactions of metabolites

1.3.1 Introduction of analytical derivatization

Derivatization has extended the application of many analytical tools such as gas chromatography (GC) and mass spectrometry to new fields, and has been an integral part of medical, forensic, and environmental analysis.[105] Derivatization reactions are applied to transform analytes which are not amenable to direct instrumental analysis, or to improve the analysis of target molecules by improving separation efficiency, chromatographic behavior, or detectability.[105,106]

For GC analysis, the volatility of the sample is an important factor to consider. In small molecules, hydrogen bonding between polar groups contributes to strong intermolecular attraction. Chemical derivatization can replace active hydrogens in polar groups, hence increasing the volatility of analytes.[105] In some cases, analytes are too sensitive to be volatilized or thermally unstable in gas chromatography, so derivatization is applied to yield less volatile products or more stable derivatives for improving chromatographic performance.[105]

In liquid chromatography, the most common use of derivatization is to improve detection, such as labeling target molecules with certain functional groups for increasing UV absorption[98,100] or fluorescence[97–99], or improving separation properties in an LC column[103].

For MS analysis, chemical derivatization also modifies target molecules to make them more detectable by mass spectrometry, usually by making them easier to volatilize and ionize. Derivatization also shifts the target peaks to less

background-obscured higher mass regions, which can enhance sensitivity of MS analysis.[37,50,105] Moreover, after suitable derivatization, mass shifts and fragmentation patterns can provide important information for structural determination. Thermal or catalytic decomposition in mass spectrometric analysis can be reduced, and the ions formed during MS detection can be stabilized.[105] Many reports have proved that derivatization methods can increase sensitivity and selectivity, and are useful for both qualitative and quantitative MS analysis.[105,107–110] The derivatization reaction in Keough's work promoted efficient fragmentation of the backbone amide bonds in MALDI detection.[108] Garcia and coworkers described a method for the characterization of histone modifications using chemical derivatization and tandem mass spectrometry, relative quantification was included and the results were in high reproducibility.[107]

Chemical derivatization can also be used to convert a target analyte to both un-isotope-labeled and stable isotope-labeled derivatives. Precise quantification may be gained by having specially synthesized analogs or analogs labeled with stable isotopes in a mixture.[111] This modification facilitates the identification of particular compound types within a complex mixture.

1.3.2 Types and reagents of analytical derivatization

Chemical derivatization modifies a compound to a new product, which has suitable properties for GC, LC or MS analysis. For traditional GC-MS and LC-MS analysis, modification of the functional group of a compound increases the analytical efficiency, detectability, and stability of the compound. Various kinds of

derivatization have been used in the study of many drugs, poisons, and their metabolites as well as other biologically active substances, which are frequently presented in trace amounts in biological fluids.[111] Many of these compounds can be detected and quantified only after extraction and derivatization by highly-sensitive methods.[111] In recent studies, particular biomolecules such as organic acids, amides, amino acids, pesticides, and other persistent organic compounds, new reactions, for example, fluorinated alkylation reactions and polycyclic aromatic derivatization continue to emerge and are extensively explored.[104,106,112,113] Fluorinated alkylation derivatization has been used in a wide range of studies including the analysis of amines and amino acids in MS detection.[113,114]

Here alkylation derivatization reactions including fluorinated alkylation derivatization are introduced. Except alkylation, silylation and acylation are another two common types applicable to many functional groups in derivatization reactions. Silylation and acylation reactions can be used in conjunction with alkylation. The introduction and typical reagents of these three types are discussed below.

1.3.2.1 Alkylation derivatization reactions

Alkylation reaction replaces the active hydrogen in carboxylic acids (R-COOH), sulfonic acids (R-SO_2H), alcohols and phenols (R-OH), mercaptans (R-SH), primary (R-NH_2) and secondary amines (R-NH-R'), amides (R-$CONH_2$) and N-substituted amides (R-CONH-R'), sulfonamides (R-SO_2N_2) and CH-acids (of the type RCO-CH_2-COR') with alkyl (sometimes aryl) groups.[115] The reactions

produce a new compound suitable for further analysis or further derivatization, or serves to protect certain active hydrogens. Derivatization reagents can be used alone to form esters, ethers, and amides.[105] In the case of acids, the reaction is known as esterification.[115] The alkylation reagents can also be used in conjunction with acylation or silylation reagents. The principal reaction for the formation of alkylation derivatives is shown in equation 1.

$$Sample - OH + R' - X \xrightarrow{base} Sample - O - R' + HX \quad (1)$$

X is a halogen or other leaving group.

Reagents commonly used for alkylation derivatization are discussed here. For choosing a suitable derivatization reagent, many factors should be taken into consideration. No rearrangements or structural alterations of a compound should occur during derivatization reactions. The reaction yield should be over 95 %, and the reagent should not contribute to sample loss during the reaction. The derivative should be stable, without interaction with the GC or LC column.[106]

Common derivatization reagents used for alkylation reactions are dialkylacetals, diazoalkales, pentafluorobenzyl bromide (PFBBr), pentafluorobenzyl-hydroxylamine hydrochloride (PFBHA), benzylbromide, tetrabutylammonium hydroxide (TBH), and boron trifluoride (BF_3) in methanol or butanol.[106] The reaction conditions vary from strongly acidic to strongly basic, depending on the formation of stable derivatives.[106]

Fluorinated alkylation derivatization has been applied in the analysis of general metabolites by mass spectrometry.[116,117] Fluoro-alkyl derivatization reagents have

many good properties, such as high electronegativity, low polarizability, and good thermal and chemical stabilities, which make them a good candidate for masking target molecules for MS detection.[118] Many studies applying fluorous reagents for identification and quantification by MS have been reported.[112,119,118,114,120,121,113,104] The target molecules were labeled with high selectivity and the sensitivity in MS detection was dramatically improved.

1.3.2.2 Silylation derivatization reactions

Silylation reactions are also commonly used in GC and LC-MS analysis. Silylation derivatization reactions replace active hydrogens in OH (alcohols, phenols, carboxylic acids, oximes, sulfo-acids, borous acids, phosphorous acids, enols), NH (amines, amides, imines), and SH (thiols, thiolcarboxylic acids) groups with a silyl group, to reduce the polarity of the compound and hydrogen bonding.[105,106,111] This is the simplest, quickest, and most versatile method of derivatization for GC, MS, or GC-MS analysis.[111,122,123] Trimethylsilyl derivatives are often applied, other silyl groups such as dimethylsilyl [$SiH(CH_3)_2$], t-butyldimethylsilyl [$Si(CH_3)_2C(CH_3)_3$], and chloromethyldimethylsilyl [$SiCH_2Cl(CH_3)_2$] are also used for different purposes.[105,106] The silylation reaction occurs through nucleophilic attack (SN2), and is driven by the leaving group. The properties of a good leaving group include low basicity, ability to stabilize a negative charge in the transitional state, and little or no back bonding between the leaving group and silicon atom.[105] The general reaction for the formation of trialkylsilyl derivatives is shown in equation 2, here X represents a good leaving group.

$$Sample - OH + R_3Si - X \longrightarrow Sample - O - SiR_3 + HX \quad (2)$$

Reagents used for silylation derivatization include bistrimethylsilylacetamide (BSA), bistrimethylsilyltrifluoroacetamide (BSTFA), N-methyltrimethylsilyltrifluoroacetamide (MSTFA), hexamethyldisilzane (HMDS), trimethylchlorosilane (TMCS), trimethylsilylimidazole (TMSI), trimethylsilyldiethylamine (TMS-DEA), N-methyl-N-t-butyldimethylsilyltrifluoroacetamide (MTBSTFA), and halo-methylsilyl derivatization reagents.[106] These reagents are influenced by both the solvent system and the addition of a catalyst.[106] Silylation is most commonly used to derivatize non-volatile samples for GC analysis, the silylated derivatives are more volatile and more stable, rather narrow and symmetrical peaks are observed.[106,124] Halket and coworkers reported trimethylsilylated derivatization of samples with BSTFA, followed by GC-MS analysis.[125] Mass spectra obtained after deconvolution were compared with a special user library containing both the mass spectra and retention indices of the target components, to achieve efficient identification of many polyols, mono- and dicarboxylic acids, keto- and hydroxy-acids, various N-acylamino acids, and even carbohydrates.[111,125]

1.3.2.3 Acylation derivatization reactions

Acylation is a useful alternative or complementary to silylation reactions.[106] Acylation derivatization reactions introduce an acyl group to an organic compound. Active hydrogens in OH, SH, and NH groups can be converted into esters,

thioesters, and amides, respectively, through acylation.[126] Equation 3 shows an example of acylation reaction between acetic anhydride and alcohol.

$$Sample - OH + CH_3OCOCOCH_3 \xrightarrow{H^+(Catalyst)} Sample - OCOCH_3 + HOCOCH_3 \quad (3)$$

Acylation improves the stability of compounds that are thermally labile by inserting protecting groups into the molecule. Acylation reactions are popular in producing volatile derivatives of highly polar organic materials, which enable efficient separation of extremely polar materials such as sugars by GC.[106,127] In addition, acyl derivatives tend to produce fragmentation patterns of target molecules in MS analysis, which can provide useful structural information of these compounds.[106,127] Acylation can also be used to form chromogenic derivatives for high performance liquid chromatography.[105] However, interference of other reaction products (acid by-products) exists in acylation derivatization, these acid by-products must be removed before GC separation to avoid destructive effects on the column.[105,106,127]

Common reagents for acylation derivatization reactions include fluorinated anhydrides, fluoracylimidazoles, N-methylbis(trifluoroacetamide) (MBTFA), pentafluorobenzoyl chloride (PFBCI), pentafluoropropanol (PFPOH), and 4-carbethoxyhexafluorobutyryl chloride (4-CB).[106] Compounds that are multi-functional with high polarities, such as carbohydrates and amino acids, can be readily modified with these acyl anhydride, acyl halide, and activated acyl amide reagents.[105,106] Among these acylating reagents, fluorinated acyl groups offer clear advantages of introducing electron-capturing properties, and have been widely used in the detection by electron capture detector (ECD) and GC-MS for

the enhancement of detectability.[106,124]

1.3.2.4 Other derivatization reactions

Other derivatization reactions that are more specific are also reported. For monofunctional compounds such as unsaturated compounds, alcoholic and carboxylic groups, special methods of derivatization is required to enhance the structural information content of electron ionization and chemical ionization mass spectra.[128] For example, preliminary chemical and physical-chemical degradation for structure elucidation of high molecular weight compounds (biopolymers, synthetic polymers) was described by Black and coworkers.[129] For compounds containing two or more functional groups, mixed derivatives are synthesized. Thus certain reaction procedures are used to modify one type of functional group, while other groups are protected to be unaffected.[105,111,115,126,127] Cyclic derivatives are also involved for multifunctional compounds which have functional groups in close proximity. Many reports mentioned that some mass spectral features of particular cyclic derivatives provided helpful information in their structure identification.[130–132]

1.3.3 Fluorous derivatization and the application in metabolite analysis

In recent studies, fluorous derivatization has been proven to be extremely useful for both qualitative and quantitative mass spectrometry. For achieving accurate and precise identification and quantification of analytes in complex biological samples,

a big challenge is the isolation of target analytes from biological matrices. With the improvement of analytical instruments and detecting methods, the sensitivity and selectivity for analytes of interest have been enhanced remarkably in recent years. Chemical derivatization modifies analytes into compounds that are more suitable for the investigation by analytical methods, and can be applied not only with EI or CI, but also with newly developed ionization and combined techniques.[111] Fluorous derivatization reagents have good thermal and chemical stabilities and an affinity for a fluorous media, which makes them a good candidate for masking target molecules and isolating derivatives through solid phase extraction and retention.[29] Fluorous derivatization has been widely used in MS analysis with high selectivity and sensitivity. Nohta's group developed a series of fluorous derivatization methods for sensitive analysis of metabolites, including biogenic amines, sialic acids, 5-hydroxyindoles, and amino acids in biological samples.[104,112–114,119,121] The pre-column fluorous derivatization and sample purification permit simultaneous determination of analytes. The derivatization reactions are high selective and these methods provide accurate quantitative results of human plasma and urine samples with detection limits at femtomole levels.[113,114]

1.4 Fluorous derivatization combined with fluorinated GLAD surfaces for SALDI-MS

In 2007, Siuzdak's group developed a method in which compounds of interest were first selectively derivatized with perfluoroalkyl groups, and then applied to a perfluoroalkyl-silylated porous silicon surface for desorption/ionization on silicon

MS detection.[133] In their work, the target molecules with fluorous affinity tags were retained on the surface of perfluoro coated DIOS chips in the washing step, leading to the purification and enrichment of target molecules from complex mixtures.[133] It has been proved that the fluorophilic interaction between the fluorous labeled compounds and the perfluorinated stationary phase enables strong retention of the fluorous labeled species, while non-fluorous molecules are eluted.[104,112,119,133,134] However, no quantification results for amino acids in biological samples have been presented by direct LDI-MS analysis. Based on these studies, our work combines fluorous derivatization reaction with fluorinated GLAD films for the quantitative analysis of amino acids in real samples. GLAD films, with their more stable chemical properties and controllable morphologies as discussed previously, were used for SALDI-MS. Our former group members successfully determined the amino acid levels in serum samples, and the results were consistent with LC-MS and nuclear magnetic resonance (NMR) measurements.[35,78] With the assistance of fluorous derivatization, our method has great potential in SALDI-MS on fluorinated GLAD surfaces.

1.5 Thesis outline

This thesis work was designed to address the problem of desalting biofluid samples without using chromatographic methods, in order to offer a rapid batch analysis format for MS detection of metabolites. More specifically, other members of the Harrison group showed that salt desegregation can be accomplished on perfluoro coated GLAD films, but that rinsing steps immediately removed the ionic target

analytes. This work has sought to evaluate the use of fluorous interactions between a SALDI surface and a labeled analyte to allow rinsing for salt removal. The goal was to improve the analytical performance relative to the previously developed salt desegragation process on a perfluoro coated GLAD surface.

In chapter 2, we evaluate different fluorous propanol as derivatizing reagents for amino acids, determined by SALDI-MS analysis on perfluoro coated GLAD films. A simple rinse is effective in removing unlabeled compounds, while fluorous derivatives are retained on the surface of perfluoroalkyl-silylated GLAD films due to F-F interaction. The sensitivity of analytes is enhanced in SALDI-MS, and the quantitative analysis of amino acids in artificial samples shows high intensity and good reproducibility. In chapter 3, we develop a method combining fluorous derivatization and SALDI-MS for the quantification of amino acids in serum. The sample is first prepared by C18 beads solubilized in methanol to remove proteins, and then labeled by 3-(perfluorohexyl)propan-1-ol, followed by SALDI-MS detection on perfluoro coated GLAD films. The nonfluorinated biomolecules and salts are removed through simple on-chip washes. The quantitative results show good consistency with normal human ranges, and compare well with other studies, suggesting this method works well for accurate quantification of amino acids in biological samples. In chapter 4, 4-chloro-3,5-dinitrobenzotrifluoride (CNBF) and 1H-perfluorohexane-1,1-diol are evaluated to label amine groups in amino acids. The quantitative results of 1H-perfluorohexane-1,1-diol derivatives provide reliable linear regression, and the RSD values are less than 10%, suggesting great potential for precise quantitative analysis of amino acids in real samples. Chapter 5 extends our method to the quantification of amino acids in blood samples with the preparation of centrifugal devices and proposes future research.

Chapter 2 Derivatization with fluorous affinity tags for surface assisted laser desorption/ionization mass spectrometry (SALDI-MS) analysis

2.1 Introduction

Matrix-assisted laser desorption/ionization (MALDI) mass spectrometry (MS) is a technique widely used in biomolecular analysis. Traditional MALDI uses an organic matrix to transfer energy to analytes,[10,11] which improves the ionization efficiency and works well for analytes with high molecular weight. However, background chemical noise from the matrix is also observed in the low mass region, causing undesirable interference for the detection of low molar mass molecules.[13] Surface-assisted laser desorption/ionization (SALDI) takes advantage of an active surface to replace the chemical matrix of MALDI, so the interference can be greatly reduced.[13–15,21] Siuzdak's group developed a matrix-free desorption/ionization on silicon (DIOS) strategy in 1999.[19] The porous silicon (pSi) surface for DIOS facilitates the ionization process and reduces background noise in MS analysis.[19] However, the low chemical stability and short shelf life of wet etching prepared surfaces for DIOS-MS still have drawbacks for quantitative analysis.[13] The studies of nanostructure-based SALDI methods prove that nanostructured surfaces offer many advantages for SALDI-MS analysis, due to the large surface area and the thermal and electronic properties.[34,135] In 2010, Jemere *et al.* reported a SALDI-MS method using silicon films fabricated by glancing angle deposition (GLAD) technique.[34] The GLAD films are prepared by depositing the

vapor flux through an electron beam with a fixed deposition angle.[34,35,39] The porous silicon surfaces generated by GLAD have controllable film porosity and thickness.[39] Moreover, the pSi surfaces can be further modified with functional groups by simple chemical reactions,[35,37] which broadens the application of GLAD films as a SALDI-MS platform for quantitative analysis of low molar mass analytes.

In recent years, the importance of small metabolites, especially amino acids as biomarkers in disease diagnosis, has gained a lot of attention.[81–89,93,95,136] The changes in amino acid levels in human blood, urine, and other body fluid samples have proved to be early indicators of various diseases, such as Alzheimer's disease, Parkinson's disease, breast cancer, kidney cancer, lung cancer, gout, *etc.*[81–92] Therefore, accurate quantitative analysis of amino acids is of great importance today.

For amino acid quantification in SALDI-MS, derivatization of the analytes raises the mass of amino acids to a higher mass region, which reduces the interference from background ions. Derivatization with fluorous groups has been applied in liquid chromatography with mass spectrometry or tandem mass spectrometry (MS/MS), since fluorous groups have good thermal and chemical stability.[104,112–114,118–121,134,137] Besides, fluorous labeled species have a remarkable affinity for a fluorous environment, which is called "fluorophilicity".[118,133,138] This affinity enhances solid phase extraction and retention of fluoro-functionalized media.[133,139] In this regard, GLAD films, which can be coated with perfluoro groups by simple soaking in fluoro-silane solution,[35] are a good candidate for surface purification of fluorous derivatized analytes. The hydrophobic interactions between labeled amino

acids and the fluorocarbon on the nanoporous surface promote easy separation of fluorous labeled molecules from unlabeled ones.[37,75,140–142]

Fluorous derivatization combined with perfluoro coated pSi surface for SALDI-MS was demonstrated by Go and coworkers.[133] Fluorous propanol was proved to be a good fluorous labeling reagent, the derivatives of fluorous propanol exhibited significantly improved MS signals on a fluorous-silylated pSi surface.[133] Here fluorous propanol with different fluorous affinity tags are evaluated in our work, with 3-(perfluorohexyl)propan-1-ol found to be the best labeling reagent. We present a method using 3-(perfluorohexyl)propan-1-ol to label target amino acids for SALDI-MS analysis on perfluoro coated GLAD films. After derivatization, the labeled analytes are retained on the surface of perfluoro coated nanoporous silicon films due to F-F interaction, while the unlabeled species can be easily removed by simple rinsing. SALDI-MS results provide improved signal to noise ratio (S/N) of labeled molecules, and the sensitivity of low mass analytes is enhanced. The quantitative analysis of artificial samples shows high intensity and good reproducibility, indicating this method has great potential for determining the concentration of amino acids in real samples.

2.2 Experimental section

2.2.1 Materials and reagents

Methanol (purity > 99.9%), HCl (hydrochloric acid), histidine, arginine, lysine, cysteine, asparagine, tyrosine, serine, valine, threonine, leucine, (1H, 1H, 2H,

2H-perfluorooctyl) trichlorosilane ($pFSiCl_3$), NaCl (sodium chloride), KCl (potassium chloride), $CaCl_2 \cdot 2H_2O$ (calcium chloride dihydrate), $MgCl_2 \cdot 6H_2O$ (magnesium chloride hexahydrate), $Na_2HPO_4 \cdot 7H_2O$ (sodium monohydrogen phosphate heptahydrate), and $NaH_2PO_4 \cdot H_2O$ (sodium dihydrogen phosphate monohydrate) were purchased from Sigma-Aldrich Chemical Company (St. Louis, MO, USA). 3-(Perfluorobutyl)propan-1-ol, 3-(perfluorohexyl)propan-1-ol, and 3-(perfluorooctyl)propan-1-ol were purchased from Fluorous Technologies, Inc. (Pittsburgh, PA, USA).

Ultrapure water used for sample preparation was from a deionizing system (Millipore Canada, Mississauga, ON, Canada).

1% (v/v) silane/methanol solution for GLAD film silanization was prepared by adding 50 μL $pFSiCl_3$ into 5 mL methanol (purity > 99.9%), followed by 1 min of vortex mixing.

Stock solutions of analyte standards were prepared as aqueous solutions and diluted in water. Artificial cerebrospinal fluid (aCSF) solution was prepared following the protocol from ALZET (www.alzet.com) and aCSF samples were prepared by diluting analyte stock solutions in aCSF solution. The electrolyte concentrations in real and artificial CSF solution are list in Table 2-1. No other components are included in the ALZET protocol, only electrolytes.

Table 2-1: Electrolyte concentrations of real and artificial CSF (pH=7.3)

Ion/Compound	Cerebrospinal Fluid* (mM)	Artificial CSF (mM)
Na^+	154	150
K^+	3.0	3.0
Ca^{2+}	1.4	1.4
Mg^{2+}	0.9	0.8
PO_4^{3-}	0.4	1.0
Cl^-	136	155

Source: http://www.alzet.com/products/guide_to_use/cfs_preparation.html

*Cerebrospinal fluid concentrations are an average of the values of human, dog, cat and rabbit.

2.2.2 SALDI chip preparation

500 nm thick vertical silicon nano-columns were deposited on a clean silicon wafer substrate (Silicon Materials, prime grade, 500 μm thickness) by the GLAD technique. The substrate rotation was employed at a nominal deposition rate of 2.4 nm deposited/rotation when the substrate was at 0°. The deposition angle was fixed at 86°. Silicon (Kurt J. Lesker, p-type, 99.999% purity) was evaporated by a high vacuum electron beam with a column growth rate of ~ 5.5 nm/min. After deposition, the Si GLAD film was transferred into open air where a native oxide rapidly formed on the surface of silicon nano-columns.[34,143,144]

(1H, 1H, 2H, 2H-perfluorooctyl) trichlorosilane ($pFSiCl_3$, Gelest) was applied to modify the silicon GLAD chips by immersing the chips into 1% (v/v)

silane/methanol solution at room temperature for 30 min. The fluorinated chips were stored in a petri dish overnight and then rinsed with liquid CO_2 in a critical point dryer (Tousimis Research Corporation) to remove excess silane.

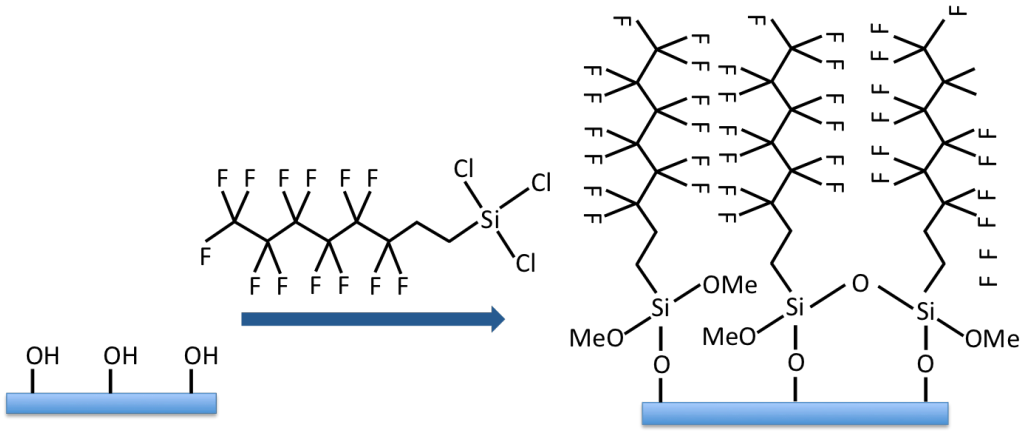

Figure 2-1: Silanization scheme on Si GLAD films by (1H, 1H, 2H, 2H-perfluorooctyl) trichlorosilane.

2.2.3 Sample preparation

Analyte standards of histidine and arginine were diluted in water to give 500 µM stock solutions. Dilute stock solutions of histidine and arginine were prepared and mixed in different ratios to give 5 µM of histidine and different concentrations of arginine in the mixtures. Artificial cerebrospinal fluid (aCSF) samples were prepared by diluting analyte stock solutions in aCSF solution to obtain mixtures containing 5 µM of histidine and different concentrations of arginine. Samples

containing histidine, arginine, lysine, cysteine, asparagine, tyrosine, serine, valine, threonine, and leucine in water and aCSF solution were also prepared.

200 µL of pure sample or aCSF sample solution was first dried in a small vial by water bath at 100 °C. Then 150 µL of fluorous propanol and 50 µL of concentrated HCl were added into the vial for fluorous derivatization reaction. The reaction mixture was incubated at 65 °C for 1 hour and then evaporated to dryness with heating by water bath, to remove excess reagent. The apparatus are shown in Figure 2-2b. The derivatized samples were reconstituted with 200 µL of 1:1 (v/v) methanol/H_2O.

a

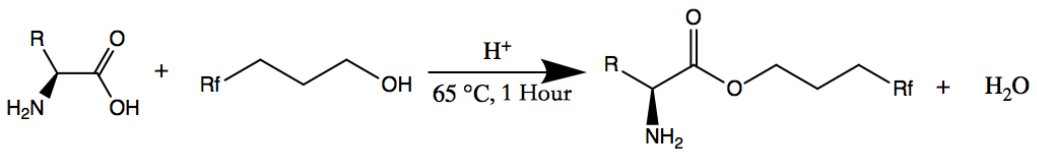

R-side chain
Rf-fluorous tag

Continued on next page

b

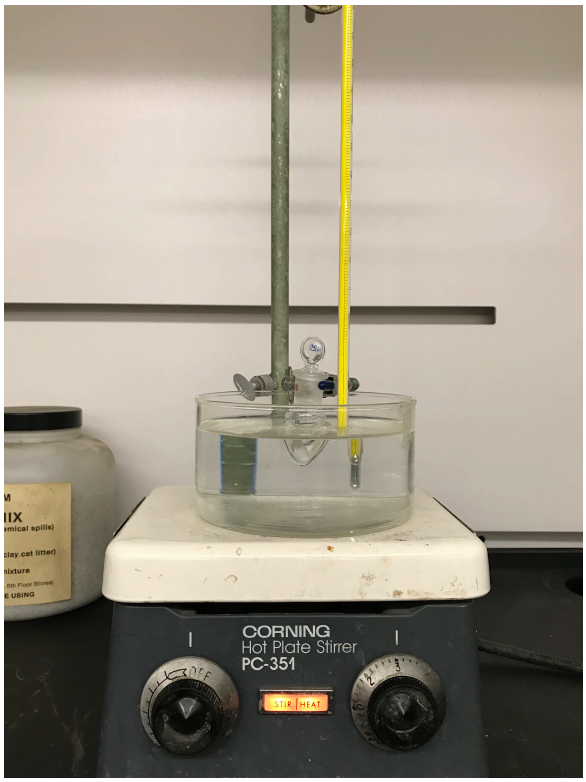

Figure 2-2: (a) Scheme of derivatization reaction with fluorous propanol, (b) The apparatus of derivatization reaction with water bath.

2.2.4 Mass spectrometry

Reconstituted, derivatized samples were spotted in 1 µL aliquots on $pFSiCl_3$ coated SALDI chips and open-air-dried for 1 hour at room temperature (in Figure 2-3a). SALDI chips with dry sample spots were attached to a modified matrix assisted laser desorption/ionization target plate with conductive double-sided carbon tape (Electron Microscopy Sciences, Hatfield, PA, USA), as shown in Figure 2-3b. Before SALDI-MS measurement, each spot was rinsed by applying 1 µL of 1:1

(v/v) methanol/H_2O as a standing droplet for 40 seconds, the methanol/H_2O droplets were then blown away to dryness of the GLAD surface by nitrogen gas (Figure 2-3c & d).

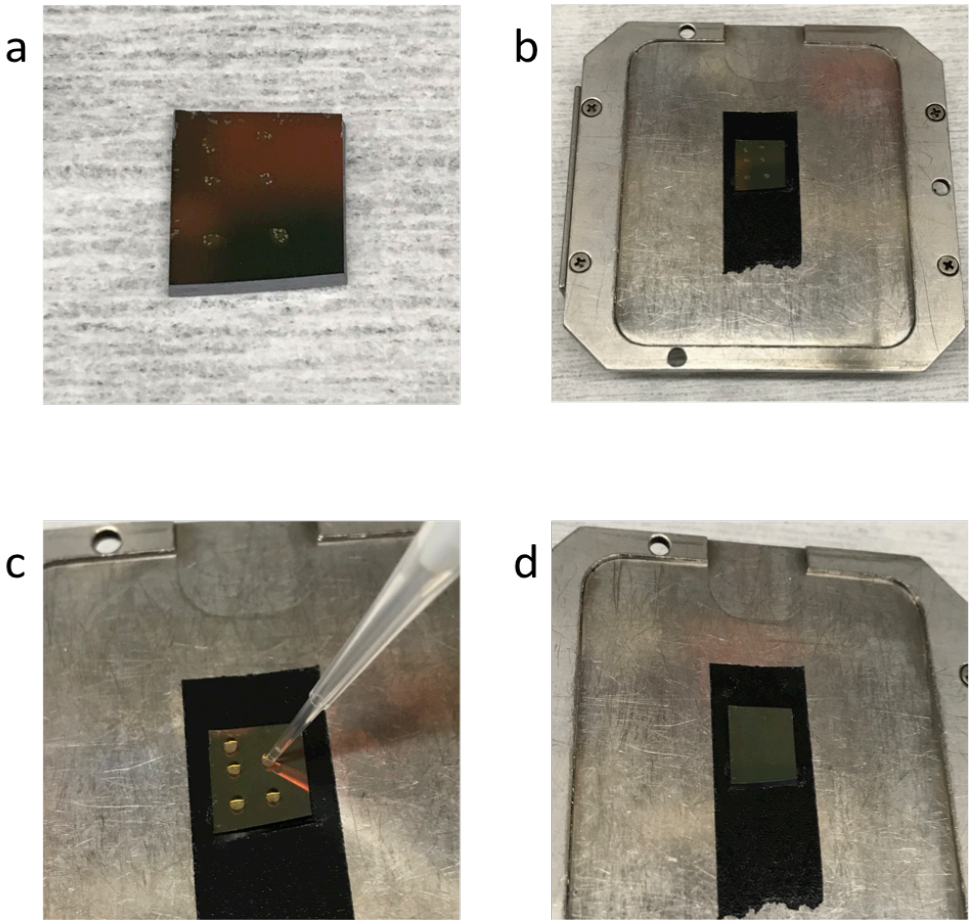

Figure 2-3: Picture of (a) samples dried on $pFSiCl_3$ coated SALDI chip, (b) SALDI chip attached to MALDI plate with double-ended conductive tape, (c) sample spots rinsed with 1µL 1:1 (v/v) methanol/water, and (d) dry chip ready for SALDI-MS measurements.

Figure 2-4: AB Sciex Voyager Elite MALDI-Time of Flight (TOF) mass spectrometer. Picture is downloaded from http://www.chem.ualberta.ca/~massspec/instr.htm.

MS measurements were performed on an AB Sciex Voyager Elite MALDI-TOF mass spectrometer (Figure 2-4) equipped with a pulsed nitrogen laser (wavelength 337 nm, 3 ns pulse) at a repetition rate of 3.0 Hz. Spectra were acquired in a reflector, delayed ion extraction mode and each spectrum is the accumulation of 100 laser shots. The operating parameters were first selected by a former group member, Chen Peng,[38] and then optimized in our method. Instrument settings of

MALDI-TOF-MS in positive and negative ion mode are listed in Table 2-2.

Table 2-2: Instrument settings of MALDI-TOF-MS

Ion mode	Accelerating voltage (kV)	Grid voltage (%)	Guide wire voltage (%)	Extraction delay time (nsec)	Laser intensity (a. u.)
Positive	20	69	0.07	250	1200
Negative	18	78	0.05	150	1800

2.3 Results and discussion

2.3.1 Optimization for washing step

The interaction of a fluorinated sample with the perfluoro coated surface of a SALDI chip should allow retention of the fluorous derivatives and removal of the unlabeled compounds. To explore the efficiency of rinsing steps, the SALDI-MS spectra in positive ion mode of a derivatized sample (pure histidine solution derivatized with 3-(perfluorobutyl)propan-1-ol) before rinse, and after rinsing for 40 or 80 seconds, are compared in Figure 2-5. For the rinsing step, each spot was rinsed by applying 1 μL of 1:1 (v/v) methanol/H_2O as a standing droplet for a corresponding time, the droplet was then blown away to dryness by nitrogen gas. Rinsing times of 10 to 100 second were tested. For less then a 30 second rinse, background signal remained significant. The intensity of the target peak showed no significant change for rinses between 30 to 60 second, similar to that shown for 40 second, while the background was low and clean in the mass range from 300 to 700

Dalton, indicating that the fluorous tagged analytes are strongly retained on the fluorinated GLAD film due to F-F interaction, and the washing procedure is effective in removing interference. When the rinsing step lasts 80 seconds or longer, there is a large drop of MS signal, which means even labeled species are removed from the surface. Similar results are observed when labeled with 3-(perfluorohexyl)propan-1-ol and 3-(perfluorooctyl)propanol, demonstrating that fluorous-silylated GLAD films enable on-chip capture of fluorous labeled molecules, and the optimized rinsing time in this method is 40 seconds.

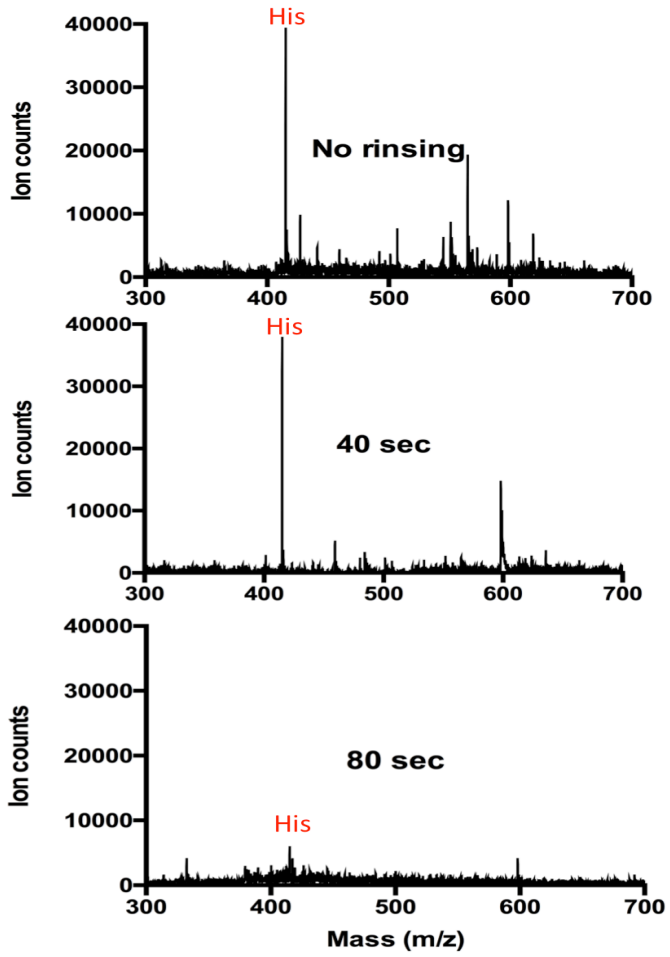

Figure 2-5: SALDI-MS spectra (positive ion mode) of 3-(perfluorobutyl)propan-1-ol derivatized histidine before rinse and after 40, 80 second rinse in the mass range of 300-700. Surface was coated with 1% $pFSiCl_3$.

2.3.2 SALDI-MS spectra of fluorous derivatized amino acids in positive and negative ion mode

We evaluated the quality of MS spectra for fluorous derivatives in positive and negative ion mode by using a mixture of 10 different amino acids (30 μM histidine, arginine, lysine, cysteine, asparagine, tyrosine, serine, valine, threonine, and leucine) in water. The mixture was first dried and then derivatized with 3-(perfluorohexyl)propan-1-ol. As shown in Figure 2-6a, multiple amino acids are fluorous labeled and identified in the SALDI-MS spectrum in positive ion mode, from left to right, the labeled peaks are serine, valine, threonine, cysteine, leucine, asparagine, lysine, histidine, arginine, and tyrosine. The target peaks of fluorous derivatized amino acids are raised to a higher mass region. High intensity with low and clean background is observed even at μM level, resulting in a higher signal to noise ratio in MS measurement. However, in negative ion mode, lower intensity is obtained with more background noise (Figure 2-6b) in SALDI-MS. No detectable peaks of derivatized tyrosine, cysteine, and asparagine are found in the spectra for concentrations below 30 μM. Therefore, MS detection in positive ion mode was used for further quantitative studies in this chapter. The decrease in negative ion yield is likely associated with the formation of an ester and the loss of an easily deprotonated carboxyl site.

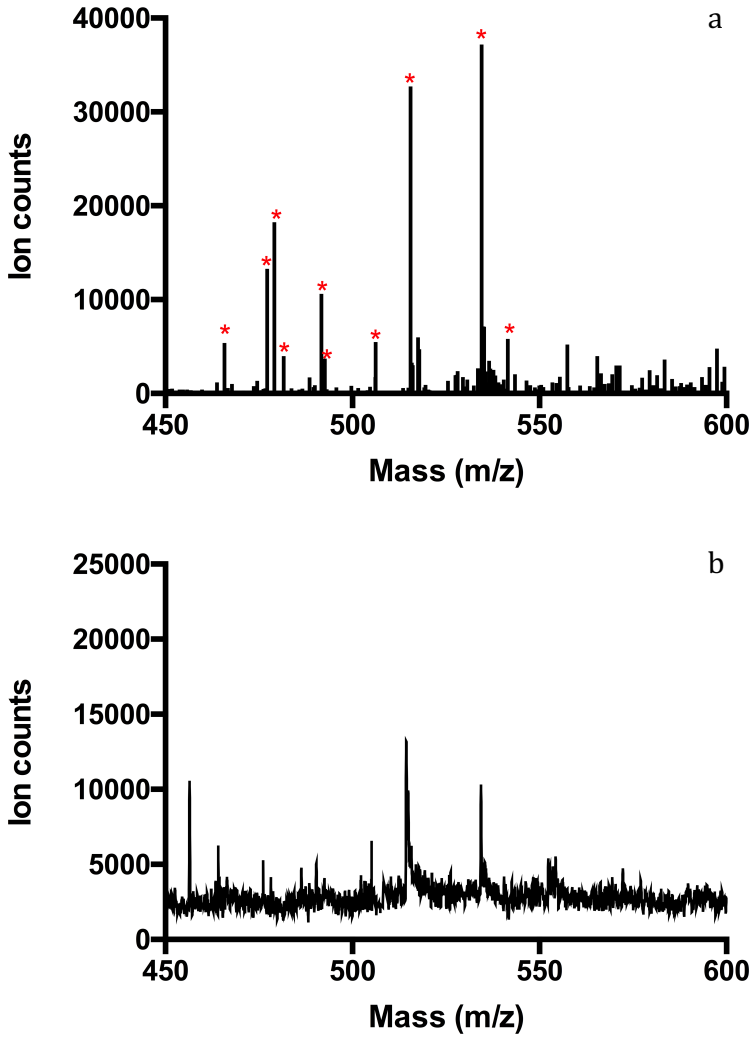

Figure 2-6: Perfluoro coated SALDI-MS spectra of 3-(perfluorohexyl)propan-1-ol derivatized sample (30 μM histidine, arginine, lysine, cysteine, asparagine, tyrosine, serine, valine, threonine, and leucine in water) in (a) positive ion mode and (b) negative ion mode in the mass range of 450-600. Identified amino acids after derivatization are labeled in (a) with star (*). From left to right, the labeled peaks are serine, valine, threonine, cysteine, leucine, asparagine, lysine, histidine, arginine, and tyrosine.

2.3.3 Selection of the labeling reagent

To explore the reaction and retention properties with different fluorous affinity tags, three different fluorous propanol were evaluated for this capture method. The reaction utilized for labeling is an acid catalyzed esterification of the carboxyl group, typically on the carboxyl attached to the α-carbon. Concentrated HCl is used to drive the reaction, as is elevated temperature, as is typical of esterification in presence of acid. For amino acid isomers, their derivatives can't be distinguished in SALDI-MS spectra. For several amino acids with nearly identical masses, such as glutamine (MW=146.14) and lysine (MW=146.19), better MS or MS/MS would be required to resolve the compounds. The hydroxyl side chains of amino acids would have side reactions, and multi-carboxyl amino acids could have multiple products.

3-(Perfluorooctyl)propan-1-ol (Tag: C_8F_{17}), as a solid under room temperature, has a melting point of 43 ~ 47 °C and a boiling point over 100 °C. The excess propanol can't be thoroughly removed by evaporation while heating in a water bath at 100 °C. The remaining propanol, with C_8F_{17} tagged derivatives, rapidly forms white precipitates in the vial during reconstitution or on pipet tips and on GLAD chips when applying sample spots, causing challenges for the rinsing process and quantitative analysis. When using 3-(perfluorobutyl)propan-1-ol (Tag: C_4F_9) or 3-(perfluorohexyl)propan-1-ol (Tag: C_6F_{13}) as the derivatization reagent, excess fluorous propanol is easily evaporated, obtaining clear and uniform reconstitution by adding 1:1 (v/v) methanol/H_2O. Both C_4F_9 and C_6F_{13} tagged derivatives show a high and stable intensity after rinsing. However, 3-(perfluorobutyl)propan-1-ol, with a fluorous tag of lower mass, does not raise some small amino acids (MW < 140 Dalton) to a high mass region (over 400 Dalton). When labeled with

3-(perfluorohexyl)propan-1-ol, different amino acids can be successfully derivatized and identified in SALDI-MS with strong retention on fluorinated GLAD chips even at low concentrations. The limit of quantitation (LOQ, defined as a signal to noise ratio of 10) of pure histidine in positive ion mode was 498 fmol for 1 μL sample volume or 0.5 μM, similar to other reports for quantitative analysis by desorption/ionization on pSi film.[33,35,50,116] Thus 3-(perfluorohexyl)propan-1-ol was selected as the labeling reagent in our work.

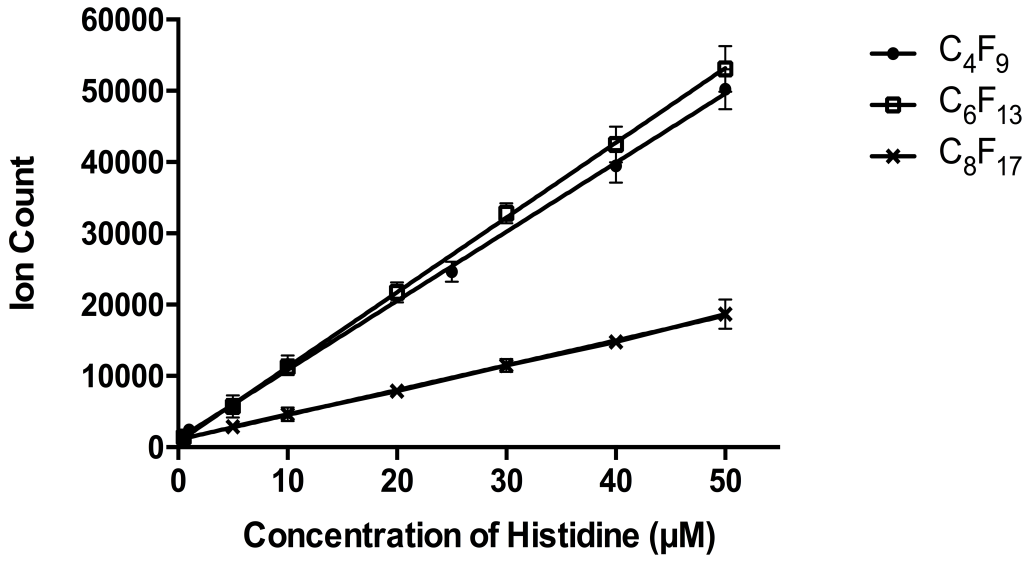

Figure 2-7: Ion count of histidine samples derivatized with different fluorous propanol *vs.* concentration of histidine. The linear range is 0.5 ~ 50 μM. The error bars represent standard deviation (SD) of 10 individual measurements.

2.3.4 Quantitative analysis of pure samples

Before applying this derivatization reaction to determine amino acid levels in sample matrices, pure standard solutions of amino acids were tested. To begin with, pure arginine was derivatized with 3-(perfluorohexyl)propan-1-ol, as was pure histidine. The products of these two amino acids were mixed by adding the derivatives of 5 μM histidine and the derivatives of arginine at different concentrations, and then detected by SALDI-MS. Separately labeled amino acids have no correlation effect in the labeling reaction, so the quantitative analysis represents the results for on-chip purification and SALDI-MS measurement. As shown in Figure 2-8, the MS spectrum in positive ion mode show high intensity with a clean background in the mass range from 100 to 700, suggesting the rinsing step provides effective removal of unlabeled species, while fluorous labeled compounds are retained on the chip with high and stable response in SALDI-MS.

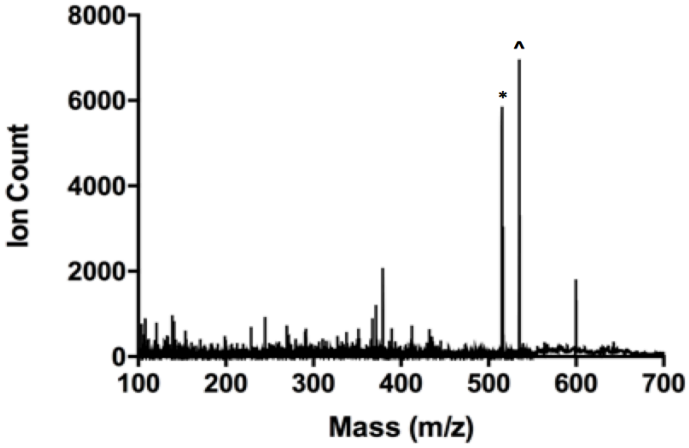

Figure 2-8: SALDI-MS spectrum of sample containing 3-(perfluorohexyl)propan-1-ol derivatives of 5 μM histidine (* m/z=516.2) and 5 μM arginine (^ m/z=535.3) in positive ion mode. The mass range is 100-700.

At high concentrations, ionization suppression has considerable effect in SALDI-MS detection, thus an internal standard (IS) is required for quantitative analysis. Histidine is an ideal internal standard for this SALDI-MS method based on its high and stable response in MS spectra. Here the MS signal of tagged histidine was used as the fixed standard, while the relative intensity of derivatized arginine increased with increasing concentration. The calibration curve is plotted as ion count ratio between labeled arginine and histidine *vs.* concentration of pure arginine in Figure 2-9. A linear regression is achieved in the range from 0.5 μM to 50 μM, with an R^2 of 0.99, and the LOQ of pure arginine samples is 470 fmol for 1 μL sample volume, indicating that individually fluorous labeled compounds at different concentrations have stable efficiency for desorption/ionization process in

SALDI-MS detection. The quantification results of SALDI-MS show high sensitivity across a wide concentration range.

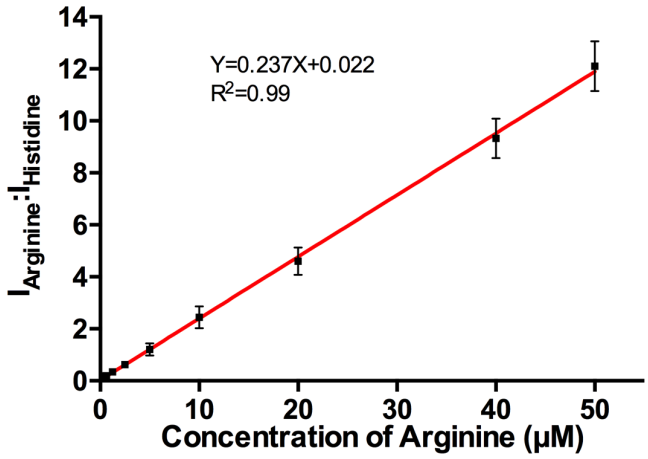

Figure 2-9: Ion count ratio between separately labeled arginine and histidine *vs.* the concentration of arginine in SALDI-MS. 5 μM histidine was used as the standard. Labeling was done in separate reactions and the products were then mixed. The linear range is 0.5 ~ 50 μM. The error bar represents SD of 10 individual measurements of different spots.

When the labeling reaction is performed in the presence of multiple amino acids, there is a risk of preferential labeling of one species versus another. As an initial test, a mixture of histidine and arginine was labeled. Samples containing 5 μM histidine as the internal standard and arginine at different concentrations were

prepared, the mixtures were derivatized with 3-(perfluorohexyl)propan-1-ol, and then measured by SALDI-MS. Intense MS signals with good reproducibility were obtained from the spectra. As shown in Figure 2-10, similar linear regression is observed from 0.5 μM to 50 μM with the R^2 of 0.99, indicating no selective labeling occurs for the derivatization reaction of these two amino acids. The estimated LOQ of pure arginine samples in histidine and arginine mixtures is 524 fmol. This fluorous derivatization reaction has the potential for analyzing amino acid mixtures, and histidine is a good internal standard in this method.

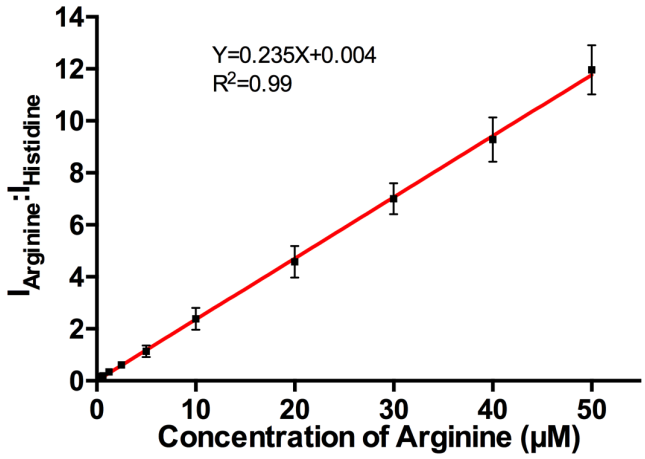

Figure 2-10: Internal standard calibration curve of arginine using 5 μM histidine as the internal standard. Labeling was performed in mixtures of the two compounds. The linear range is 0.5 ~ 50 μM. The error bar represents SD of 10 individual measurements.

2.3.5 Quantitative analysis of aCSF samples

Similar to pure samples, the mixtures of histidine and arginine in artificial cerebrospinal fluid (aCSF) solution were tested and compared. The aCSF samples containing arginine at different concentrations and 5 μM histidine as the internal standard were quantified in this work.

Salts from the artificial biofluid samples co-crystallize with analytes and cause undesirable interference in MS detection, which prevents accurate quantification of amino acids. Here aCSF samples with closely matched electrolyte concentrations of endogenous CSF were used to evaluate the efficiency of labeling and desalting in this method for complex biofluids. After open-air-drying of derivatized aCSF samples, many tiny crystals were formed on the surface of fluorinated GLAD films, as shown in Figure 2-11a, which notably reduced SALDI-MS quality. SALDI-MS spectrum for aCSF sample spots with salt crystals present on the perfluoro surface are shown in Zhou's work.[35] Zhou's results show substantial background noise in the 100-300 Dalton range for native amino acids, with few identifiable analyte signals. In contrast, after 40 seconds of washing, most salt crystals were removed from the perfluoro surface (Figure 2-11b), and the purified chip with fluorous labeled amino acids was ready for SALDI-MS measurement. The spectra for aCSF samples after 40 second rinse are discussed in the following text of this chapter, and the results show greatly reduced background noise and strong labeled analyte signal.

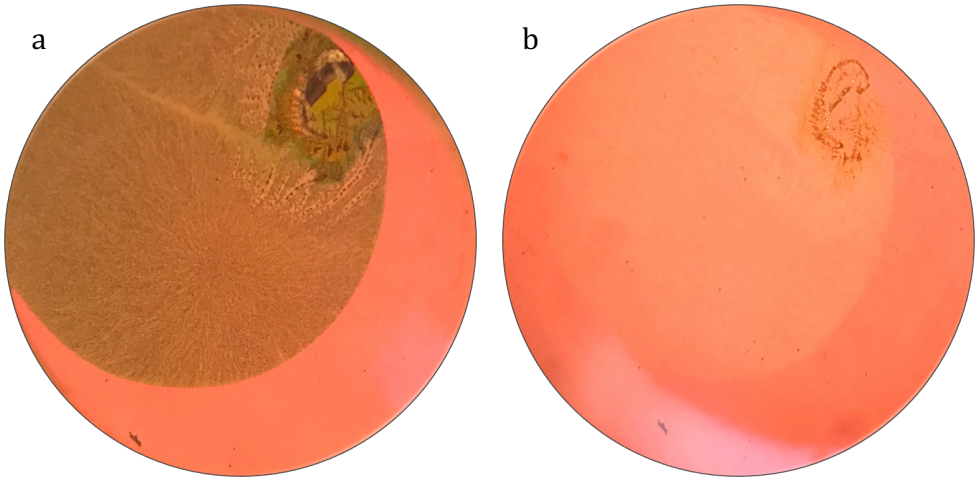

Figure 2-11: Microscopic photos of aCSF samples on $pFSiCl_3$ coated GLAD film (a) before and (b) after 40 second rinse.

In SALDI-MS spectra of arginine in aCSF solution using 5 μM histidine as the internal standard, the background is clean as shown in Figure 2-12. The ion count ratio between arginine and histidine linearly increased with increasing concentration of arginine (Figure 2-12 & 2-13). Good linear regression was observed from 0.5 μM to 50 μM with the R^2 of 0.98, as shown in Figure 2-13. The estimated LOQ of arginine in aCSF solution is 496 fmol for 1 μL sample volume. This linear regression equation closely fits previous regression for aqueous samples without salts in Figure 2-10, suggesting that the simple on-chip rinse effectively reduces the interference from salts and unfluorous labeled molecules, and provides reliable quantification results in SALDI-MS.

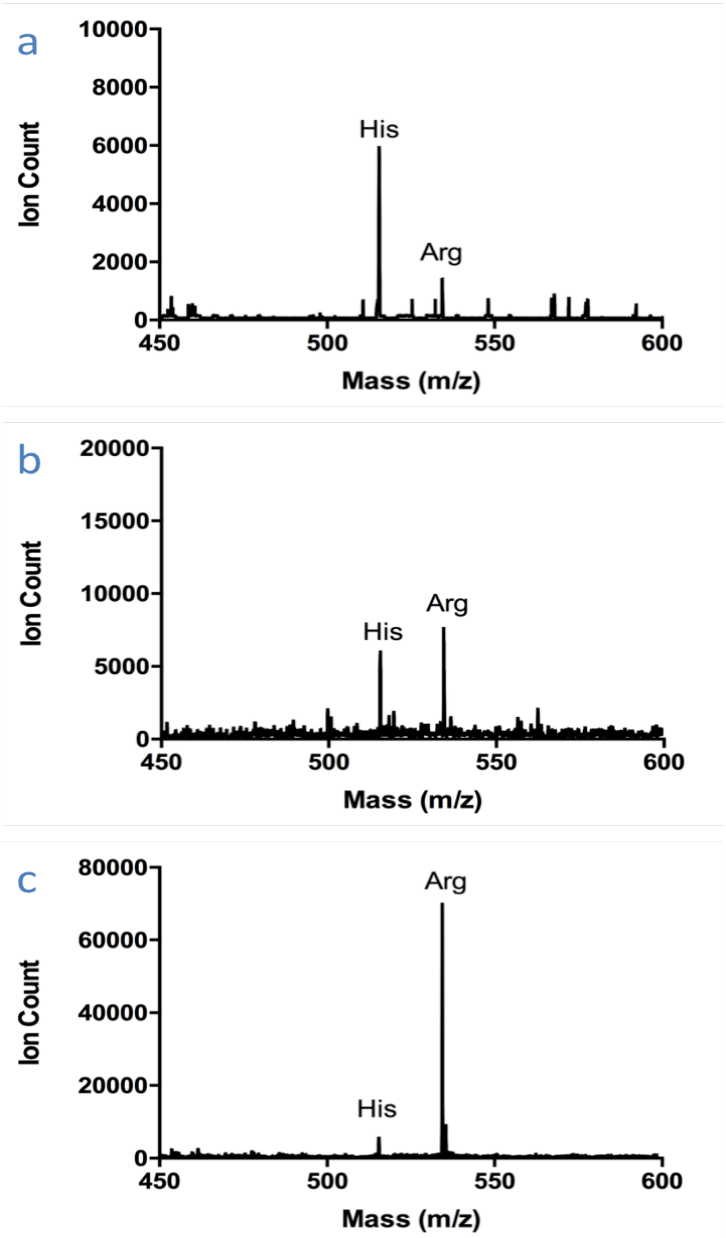

Figure 2-12: SALDI-MS spectra in positive ion mode of (a) 1 μM, (b) 5 μM, and (c) 50 μM arginine in aCSF solution using 5 μM histidine as the internal standard. The mass range is 450-600.

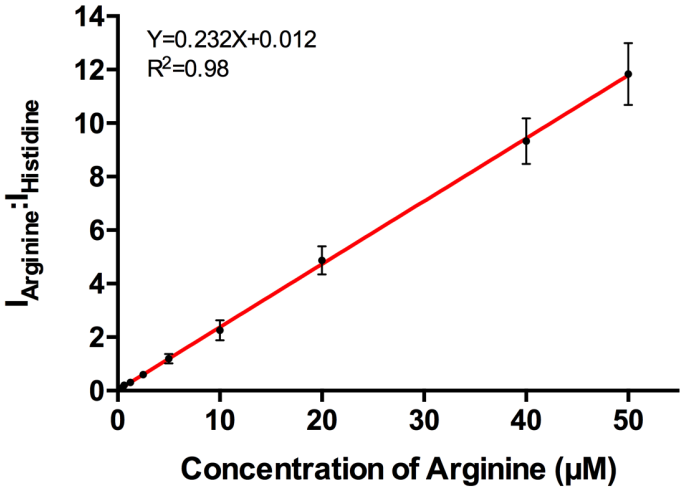

Figure 2-13: The internal standard calibration curve of arginine in aCSF solution using 5 μM histidine as the internal standard. The linearity range is 0.5 ~ 50 μM. The error bar represents SD of 10 individual measurements.

Ten amino acids (30 μM histidine, arginine, lysine, cysteine, asparagine, tyrosine, serine, valine, threonine, and leucine), which are identified above, were prepared in aCSF solution as a mixture. The mixture was labeled and then applied on perfluoro coated GLAD films following the procedures above. Sufficient removal of crystals from perfluoro coated GLAD films after rinse was also observed. The derivatives of these 10 amino acids were successfully identified in the SALDI-MS spectrum (Figure 2-14, from left to right, they are serine, valine, threonine, cysteine, leucine, asparagine, lysine, histidine, arginine, and tyrosine). The spectrum similarly matches the SALDI-MS data in Figure 2-6a with high intensity and good reproducibility. No sodium ion adduct peaks or salt component related peaks were found in the spectrum, indicating this method provides sufficient removal of salts

and avoids the need for a separate desalting step.

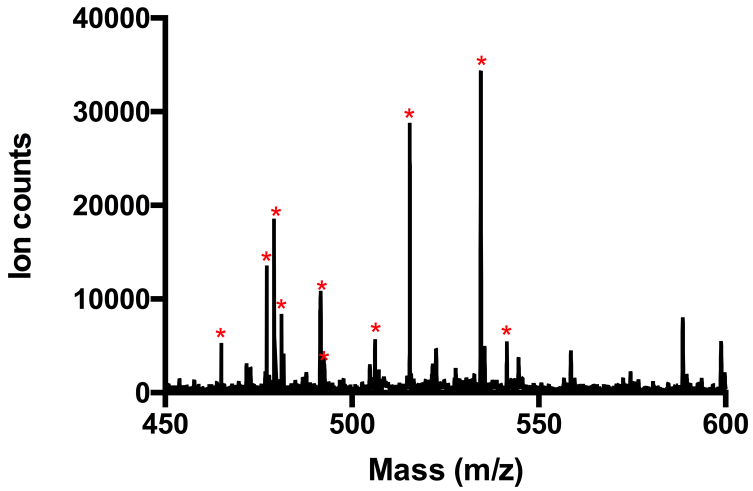

Figure 2-14: SALDI-MS spectrum (positive ion mode) of aCSF sample of 10 amino acids in the mass range of 450-600. The aCSF sample was prepared with 30 μM histidine, arginine, lysine, cysteine, asparagine, tyrosine, serine, valine, threonine, and leucine in aCSF solution as a mixture and then derivatized with 3-(perfluorohexyl)propan-1-ol. Amino acids after derivatization are identified and labeled with star (*) in the spectrum (from left to right, they are serine, valine, threonine, cysteine, leucine, asparagine, lysine, histidine, arginine, and tyrosine).

To further explore the quantitative performance of more complex samples containing salts and multiple amino acids in this SALDI-MS method, aCSF samples of 10 amino acid mixtures (20 μM lysine, cysteine, asparagine, tyrosine, serine, valine, threonine, leucine, 5 μM histidine as the internal standard and

arginine at different concentrations in aCSF solution) were prepared and fluorous labeled for SALDI-MS measurements. The calibration curve of arginine is plotted as the ion count ratio between arginine and histidine *vs.* concentration of arginine in Figure 2-15. The linear regression range is from 0.5 µM to 50 µM and the R^2 is 0.98. The estimated LOQ of arginine in 1 µL aCSF sample mixtures is 527 fmol. The results prove that this method has effective and stable reaction performance when there are multiple reactive species present, reduces the interference from salts and other unlabeled species by a simple on-chip rinse, and enables quantitative analysis for complex biofluid samples with fluorous derivatization in SALDI-MS.

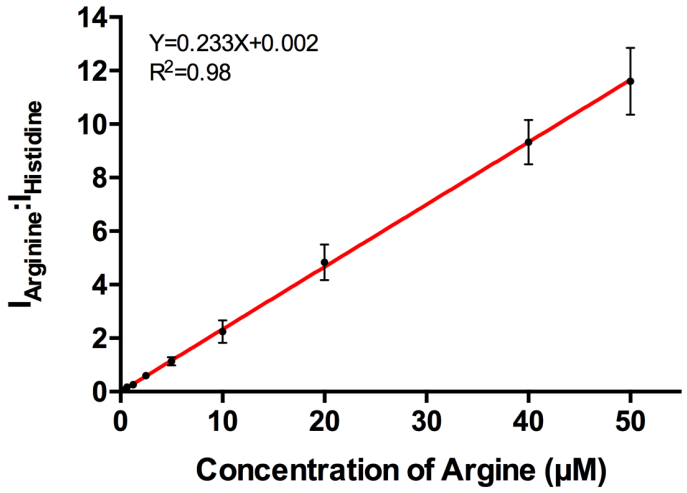

Figure 2-15: The internal standard calibration curve of arginine in aCSF sample containing amino acids mixture (20 µM lysine, cysteine, asparagine, tyrosine, serine, valine, threonine, and leucine in aCSF solution). 5 µM of histidine is used as the internal standard. The linear range is 0.5 ~ 50 µM. The error bar represents SD of 10 individual measurements.

The relative standard deviation in predicted concentration $\frac{\Delta concentration}{concentration}$ of pure samples, salts only aCSF samples, and aCSF with amino acid mixtures are ± 10.2%, ±12.4%, and ±11.0%, indicating the good accuracy of this method for analyzing biological sample with different matrices. The results also show the analytical performance is essentially independent of the two sample matrices tested, and of the method of labeling (individual versus mixed samples). Appendix A shows an analysis of the S/N *vs*. signal, for the data in Figure 2-13. The results show that for most of the data set, except the lowest signal strength, S/N is essentially constant, indicating the noise scales with the signal intensity. This is consistent with a flicker noise source for the sample signal observations.

2.4 Conclusion

Fluorous propanol offers high stability as a derivatization reagent. With the fluorous affinity tag, labeled amino acids show high intensity and clean background in SALDI-MS spectra, due to the raised mass and effective washing procedure. For small ionic metabolites, desalting methods other than chromatographic separation are difficult to use to selectively eliminate background electrolytes in biological samples. In this method, salts and unlabeled molecules can be removed through simple on-chip purification, while labeled amino acids are retained on fluorinated GLAD chips. In SALDI-MS measurements, fluorous derivatized amino acids have high and stable S/N even at μM level. This method provides good quantitative results in pure samples and artificial samples with high sensitivity and good stability, shows great potential for real sample detection.

Chapter 3 Quantitative analysis of amino acids in serum samples using fluorous derivatization and surface assisted laser desorption/ionization mass spectrometry (SALDI-MS)

3.1 Introduction

Amino acids play essential roles for proper function and growth of the human body and are of great clinical importance in the diagnosis of many diseases, such as cancer and Alzheimer's disease.[88,91,93–95] The basal level of amino acids in biological samples is at μM level, therefore it is important to develop a sensitive and selective method for the simultaneous determination of amino acids in biofluid samples. A variety of methods have been reported for determining amino acid levels by liquid chromatography (LC) with fluorescence, UV, or mass spectrometry (MS).[97–104] In LC-MS, chromatography can be optimized for effective separation of analytes, however being distinguishable by mass can be measured simultaneously.[103] In addition, derivatization has often been applied in LC-MS to label target molecules with high selectivity, and dramatically improve the sensitivity in MS detection.[116,117] Nohta and Hayama reported a series of studies using fluorous reagents to derivatize the analytes of interest, including amino acids and amines.[112,119,118,114,120,121,113,104] The fluorophilic interaction between fluorinated derivatives and a perfluorinated stationary phase leads to strong retention of fluorinated compounds.[104,112,119,134] The non-fluorinated molecules are eluted early, the derivatives are more eluted on the column and detected by MS.[119] Compared

with these LC-MS based techniques, direct mass spectrometric characterization of derivatives provides more rapid analysis of targeted analytes.[133] Many laser desorption/ionization techniques have been reported for analyzing target molecules directly without the need for chromatography.[133,145–147] Siuzdak's group developed a method utilizing a silylated nanoporous silicon surface for desorption/ionization on silicon (DIOS) mass spectrometry.[37,133] A previous report has described target molecules labeled with fluorous affinity tags being retained on the surface of perfluoro coated DIOS chips, leading to simple purification through on-target washing and direct analysis for MS.[133] However, no quantitative results for fluorinated amino acids in complex biological samples measuring by SALDI-MS have been reported so far.

In this chapter, we present a fluorous derivatization method for the determination of amino acids in serum. The method involves sample preparation by C18 beads solubilized in methanol, combined with fluorous labeling of amino acids, followed by SALDI-MS detection on perfluoro coated GLAD films. C18 beads in methanol provide effective removal of proteins, lipids, and other biomolecules in serum samples. The deproteinated sample is then labeled with 3-(perfluorohexyl)propan-1-ol as the derivatization reagent. The derivatization reaction provides high selectivity and good stability. The SALDI-MS detection utilizes glancing angle deposition (GLAD) prepared chips, which have a controllable nanoporous silicon surface with long shelf life. The nanoporous surface is silylated by simple soaking in reactive silane solution. The non-fluorous interference can be removed through simple on-chip washes, while the fluoro-labeled derivatives are retained on the chips. Our method offers rapid and easy to apply detection for SALDI-MS. The quantitative results show good

consistency with expected normal human ranges, and are consistent with the concentrations determined by LC-MS and NMR. The results indicate this method works well for accurate quantification of amino acids in serum samples, and can provide an important method for the study of human diseases.

3.2 Experimental section

3.2.1 Materials and reagents

Methanol (purity > 99.9%), HCl (hydrochloric acid), arginine, asparagine, glutamic acid, valine, histidine, and (1H, 1H, 2H, 2H-perfluorooctyl) trichlorosilane ($pFSiCl_3$) were purchased from Sigma-Aldrich Chemical Company (St. Louis, MO, USA). 3-(Perfluorohexyl)propan-1-ol was purchased from Fluorous Technologies, Inc. (Pittsburgh, PA, USA). C18 beads were purchased from Silicycle Inc. (SiliaSphere Spherical Silica Gel, C18 monomeric, 10 μm, 60 Å, Quebec, Canada). Isotope labeled ^{13}C arginine ($H_2N^*C(=NH)NH(CH_2)_3CH(NH_2)COOH \cdot HCl$) was from Cambridge Isotope Laboratories, Inc. (Tewksbury, MA, USA). Pooled normal human serum samples were purchased from Cedarlane (Burlington, Ontario, Canada).

Ultrapure water used for sample preparation was from a deionizing system (Millipore Canada, Mississauga, ON, Canada). Stock solutions of analyte standards were prepared as aqueous solutions and diluted in water.

1% (v/v) silane/methanol solution for GLAD film silanization was prepared by

adding 50 μL $pFSiCl_3$ into 5 mL methanol (purity > 99.9%), followed by 1 min of vortex mixing.

3.2.2 Serum sample preparation

100 μL of pooled normal human serum was mixed with C18 beads in methanol to achieve 5.0% (w/v) of C18 beads in the mixture for deproteination. The mixture was then spun at 13000 rpm for 2 min in a centrifuge (Sanyo MSE Micro Centaur). For some samples, the supernatant was collected and acidified with HCl to 0.2 M to denature any remaining proteins and acidic lipids for further derivatization reaction. For other samples, these steps were not used. No appreciable differences were observed.

The deproteinated sample was dried in a small vial and 150 μL of 3-(perfluorohexyl)propan-1-ol and 50 μL of concentrated HCl were added for the fluorous derivatization reaction. The reaction mixture was incubated at 65 °C for 1 hour and then evaporated to dryness to remove excess reagent. The derivatized samples were reconstituted with 100 μL of 1:1 (v/v) methanol/H_2O.

The standard solutions of 5 mM isotope labeled ^{13}C arginine, arginine, valine, asparagine, histidine, and glutamic acid were prepared in water. Stock solutions were further diluted so that 2 ~ 8 μL could be added into 100 μL of human serum to provide the required concentrations, followed by the deproteination and derivatization procedures, as described above. The standard solutions were added before sample preparation to allow for any interference from sample loss during

deproteination or labeling.

3.2.3 Quantitative analysis by SALDI-MS, LC-MS, and NMR

3.2.3.1 Quantitative analysis by SALDI-MS

SALDI chips were generated and modified with (1H, 1H, 2H, 2H-perfluorooctyl) trichlorosilane ($pFSiCl_3$, Gelest) as described in chapter 2. Reconstituted derivatized samples in 1 μL aliquots were spotted on perfluoro coated SALDI chips and then rinsed with 1:1 (v/v) methanol/H_2O. Each sample spot on SALDI chips was rinsed by applying 1 μL of 1:1 (v/v) methanol/H_2O as a standing droplet for 40 seconds, the droplet was then blown away to dryness by nitrogen gas.

MS measurements were performed on an AB Sciex Voyager Elite MALDI-TOF mass spectrometer equipped with a pulsed nitrogen laser (wavelength 337 nm, 3 ns pulse) at a repetition rate of 3.0 Hz. Spectra were acquired in positive ion mode in reflector, delayed ion extraction. Grid voltage was set at 69% and extraction delay time was 250 ns. Each spectrum consists of 100 laser shots.

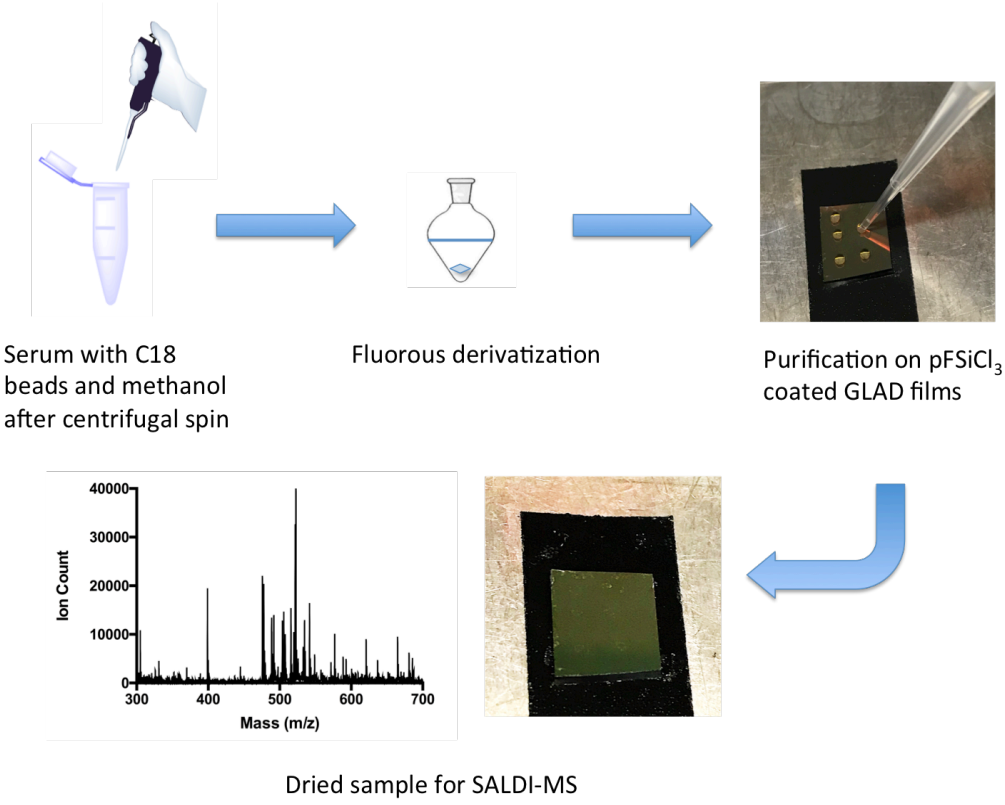

Figure 3-1: Workflow of serum sample preparation, on-chip purification, and SALDI-MS detection.

3.2.3.2 Quantitative analysis by LC-MS

Pooled normal serum and standard addition serum samples (100 µL serum with 0.5-300 µM arginine, valine, asparagine, histidine, and glutamic acid, or blank serum) were deproteinated with C18 beads and then detected by LC-MS.

The LC-MS system (Agilent Technologies 1100 HPLC with G1946A MSD, Agilent Technologies, Santa Clara, CA, USA) was composed of an autosampler

(G1313A ALS), a solvent delivery pump (G1312A Binary HPLC Pump), a single quadrupole, and a UV-Vis detector (G1314A VWD Variable Wavelength Detector). ChemStation LC/MSD version B.04.03 was used to process data. Chromatographic separation was performed on an Agilent Poroshell 120 Hilic-Z column (2.1 × 100 mm, 2.7 μm) using a gradient elution consisting of mobile phase A (20 mM NH_4Formate, pH 3.1 in water) and mobile phase B (20 mM ammonium formate in 90% acetonitrile with 10% water). Flow rate and gradient elution time were adjusted until amino acid resolution was achieved. The final flow rate was 0.5 mL/min with a linear gradient at the following conditions: 0 ~ 10 min 100% to 70% B, 10 ~ 11 min return to 100% B. The injection volume was 2 μL. The mass spectrometer was operated in a single ion monitoring (SIM) mode.

3.2.3.3 Quantitative analysis by ^{1}H-NMR spectroscopy

Serum samples were measured by ^{1}H-NMR spectroscopy for comparison. Before ^{1}H-NMR measurement, the serum sample was ultrafiltered by a 3 kDa molecular weight cut-off (MWCO) filter (Amicon Ultra-4, EMD Millipore, Etobicoke, Ontario, Canada). Each unit was pre-rinsed by adding 4 mL of deionized water, followed by a 10 minute spin at 4,000 g with a swinging bucket rotor (Beckman Coulter, Allegra X-22), to remove trace glycerin from the ultrafiltration membranes. The serum sample was then transferred into the pre-washed centrifugal filter units and spun at 4,000 g and 4 °C for 30 min to remove remaining proteins.

285 μL of downstream serum filtrate was mixed with 35 μL of D_2O and 30 μL of a standard buffer solution. The buffer solution was prepared with 11.7 mM sodium

2,2-dimethyl-2-silapentane-5-sulfonate (DSS), 730 mM imidazole, and 0.47% NaN_3 in water. The mixture was then transferred into a standard NMR tube for spectral acquisition.[148] The spectra of ^{1}H-NMR were collected on a 500 MHz Inova spectrometer (Varian Inc.) equipped with a 5 mm Z-gradient pulsed-field gradient (PFG) probe.[35,148] A standard presaturation ^{1}H-NOESY experiment was acquired at 25 °C using the first increment of the presaturation pulse sequence. The internal standard for chemical shift reference was the singlet produced by methyl groups of DSS. Chenomx NMR Suite Professional Software package version 7.1 (Chenomx Inc) was used to analyze ^{1}H-NMR spectra, and the standard Chenomx 500 MHz metabolite library was applied for the spectral fitting of metabolites. Suspected analytes were additionally spiked to check the signal change in NMR spectra, in order to confirm the identities. The samples for NMR analysis were prepared and detected by Rupasri Mandal.

3.3 Results and discussion

3.3.1 Serum sample preparation

Our group reported an on-chip sample preparation method using C18 beads in methanol and silica nanoparticles (SNP) to remove proteins and lipids from serum samples.[78] Herein, serum samples prepared with different densities of C18 beads were compared. C18 beads suspended in methanol were added into serum with a 3:1 (v/v) ratio to obtain overall densities of C18 beads in the mixture at 2.5%, 5.0%, 7.5%, and 10% (m/v). As shown in Figure 3-2, after treatment with 2.5% C18, signal to noise ratio (S/N) of arginine, valine, asparagine, and histidine are

improved. With the increase of C18 densities, the intensities of all four amino acids increased to the maximum at 5.0% C18. The SALDI-MS spectra are clean in the background with a high response of target peaks, indicating the preparation with C18 in methanol provides sufficient removal of proteins. When 7.5% and 10% C18 beads are used for sample preparation, S/N for four amino acids are decreased compared with 5.0% C18 beads. For valine and histidine, the S/N is even lower than no C18 treated samples. Therefore, 5.0% (m/v) C18 beads in 1:3 (v/v) serum/methanol mixture was selected for removing proteins and lipids.

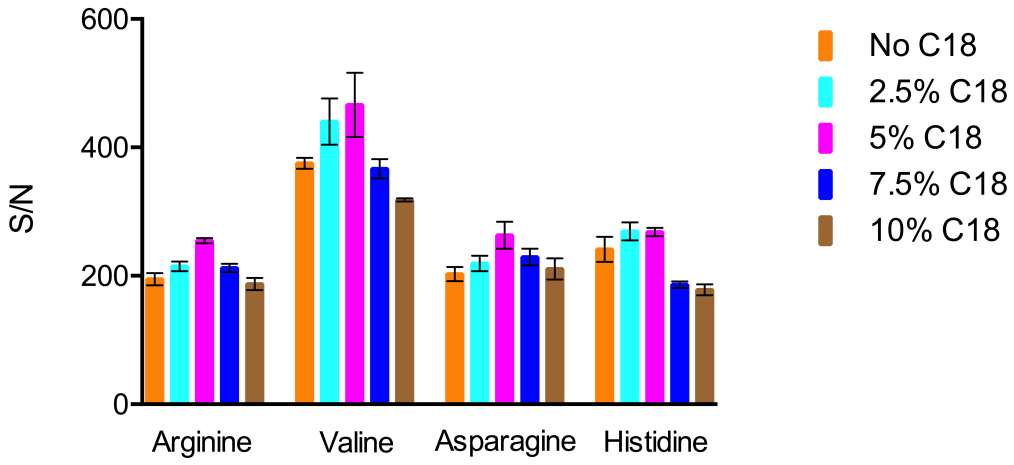

Figure 3-2: S/N of different labeled amino acids in serum samples prepared with different densities of C18 beads to remove proteins.

In Zhao's work, 235 nm silica nanoparticles were selected as a second extraction

phase to further clean the samples.[78] Here silica nanoparticles were also evaluated in this method. After the preparation with 5.0% C18 beads, the supernatant containing the analytes was transferred into a vial and heated in a water bath at 80 °C to dry the supernatant. 100 μL aqueous suspensions of silica nanoparticles with different densities were then added to re-dissolve the dried sample. The re-dissolved sample solution was transferred into a microcentrifuge tube, followed by a 5 min spin at 2000 rpm to separate silica nanoparticles. The sample was then dried, derivatized with 3-(perfluorohexyl)propan-1-ol, and reconstituted with 100 μL of 1:1 (v/v) methanol/H_2O following the previous procedure.

Different densities of SNP were used for sample preparation after methanol precipitation and C18 beads extraction, the density of SNP ranged from 0 to 0.25% (m/v). As shown in Figure 3-3, the MS response of valine and asparagine was reduced when 0.05% SNP was used, and the S/N was further decreased using higher densities of SNP. For the four amino acids in Figure 3-3, no significant improvement was observed in SALDI-MS after applying SNP as the second extraction phase.

These results contrast with those of Zhao's work,[78] who found the SNP improved S/N, presumably due to the extraction of hydrophilic proteins and other biomolecules. Using the rinsing procedures described here, with the perfluoro interactions to retain the analytes, means the second extraction is not required. Therefore, only 5.0% (m/v) C18 beads suspended in methanol were selected for sample preparation in this method.

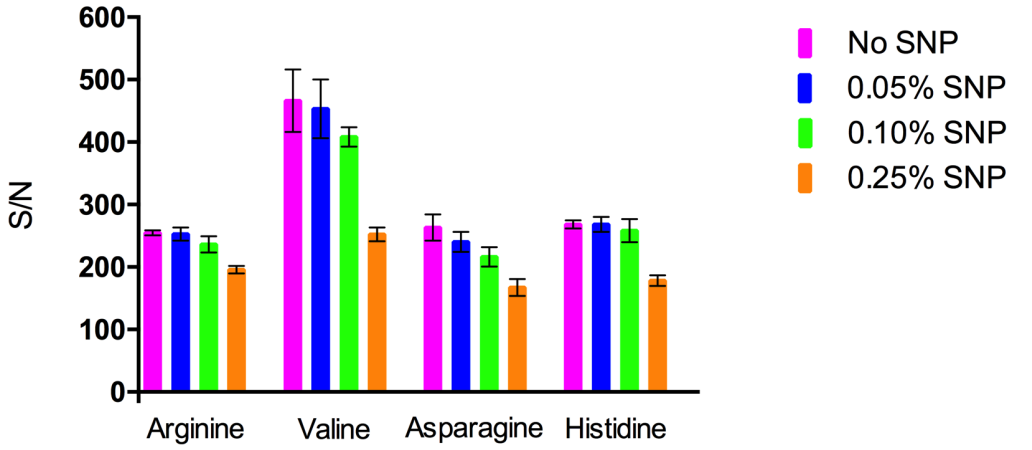

Figure 3-3: S/N of different amino acids in serum samples prepared with different densities of SNP to remove proteins.

3.3.2 Quantitative analysis by SALDI-MS, LC-MS, and NMR

3.3.2.1 Quantitative analysis by SALDI-MS

Fluorous labeled serum samples were detected by SALDI-MS. The perfluoro coated SALDI-MS spectra in positive and negative ion mode are compared in Figure 3-4. As shown in the spectra, the metabolites are raised in mass by derivatization. Notable SALDI-MS peaks are observed in positive ion mode (Figure 3-4a). The background is clean in the mass range from 100 to 700, and no salt related peaks are found in the spectra, showing the washing step is effective in removing salts and unlabeled molecules from serum samples. The identified amino acid peaks in the mass range of 460-560 are labeled with their m/z values in Figure 3-4b. In negative ion mode, the spectra were acquired in reflector, delayed ion

extraction mode with 78% of grid voltage and 150 ns of extraction delay time. Fewer peaks with lower intensities are obtained, as shown in Figure 3-4c. Valine, asparagine, histidine, and arginine are identified and labeled with their m/z values in the spectrum from left to right, in the mass range from 300 to 700. Based on this study, positive ion mode was applied for SALDI-MS quantitative analysis in this chapter.

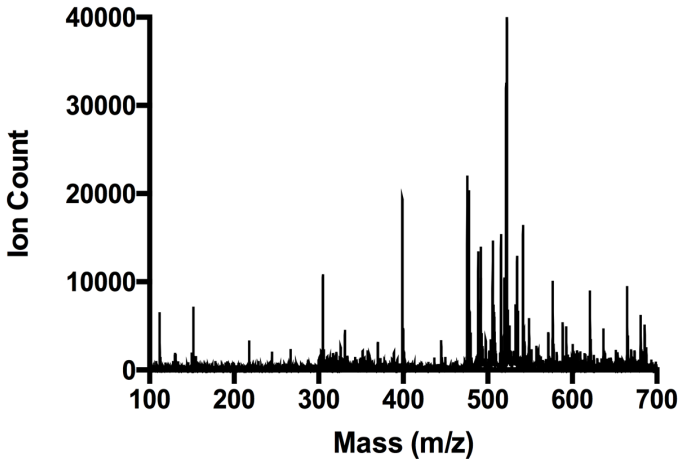

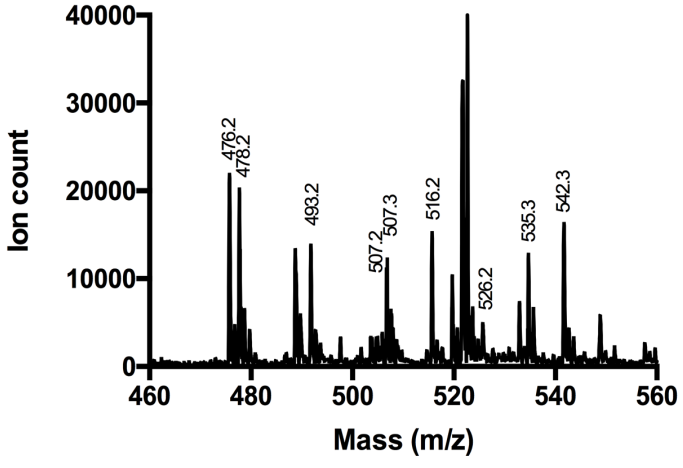

Continued on next page

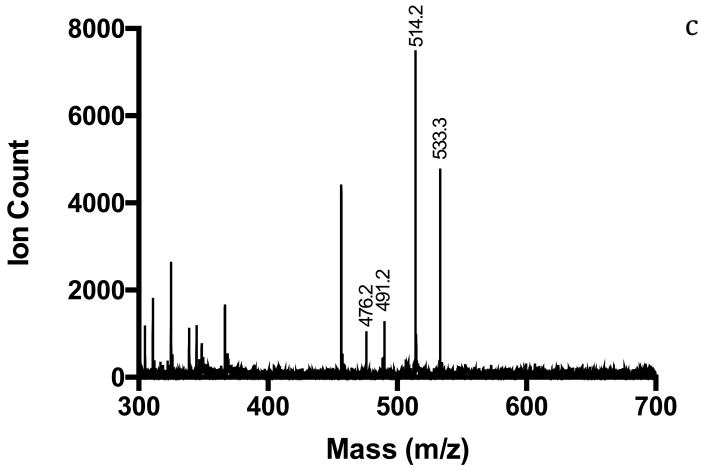

Figure 3-4: (a) SALDI-MS spectrum of derivatized serum in positive ion mode in the mass range of 100-700. (b) SALDI-MS spectrum of derivatized serum in positive ion mode with labeled peaks. Labeled peaks represent protonated amino acids with fluorous tag (C_6F_{13}), from left to right are proline: 476.2, valine: 478.2, asparagine: 493.2, glutamine: 507.2, lysine: 507.3, histidine: 516.2, phenylalanine: 526.2, arginine: 535.3, and tyrosine: 542.3. The mass range is 460-560. (c) SALDI-MS spectrum of derivatized serum in negative ion mode using reflector, delayed ion extraction mode with 78% of grid voltage and 150 ns of extraction delay time, labeled peaks represent deprotonated derivatives of valine: 476.2, asparagine: 491.2, histidine: 514.2, and arginine: 533.3 with fluorous tag (C_6F_{13}). The mass range is 300-700.

Silylated GLAD chips for SALDI-MS measurement were stored in petri dishes at room temperature before use. To test the shelf life of SALDI chips, 1% (v/v) $pFSiCl_3$ coated chips stored for 2 weeks, 1 month, and 3 months were compared.

As shown in Figure 3-5, perfluoro coated SALDI chips kept for a longer time yield slightly increased background noise in SALDI-MS analysis due to the interference arising from contamination by the environment during storage. (1H, 1H, 2H, 2H-perfluorooctyl) trichlorosilane coated SALDI chips become more hydrophobic during storage,[38] resulting in a smaller size of sample spots and a higher ion count of target peaks. For 6 different spots on newly prepared SALDI chips, the 95% confidence interval of S/N is 249.7±9.6 (n=6). For perfluoro-coated chips stored for over 3 months, the surface is too hydrophobic to spike 1:1 (v/v) methanol/water, thus adjustment for sample reconstitution by adding more methanol is required. A 2:1 methonal/water ratio was used. The overall S/N is slightly decreased with storage time, the 95% confidence interval of S/N is 227.5±6.3 (n=6) for SALDI chips stored for 3 months. Compared with newly prepared chips, a paired t-test showed $p < 0.05$. Based on this study, freshly modified SALDI chips are preferred for quantitative analysis, but the changes over time are not too severe. The most likely reason for the increased super-hydrophobicity over time is further curing of the siloxane bonds on the surface and between surface bound molecules. Slow loss of strongly bound surface water may also contribute.

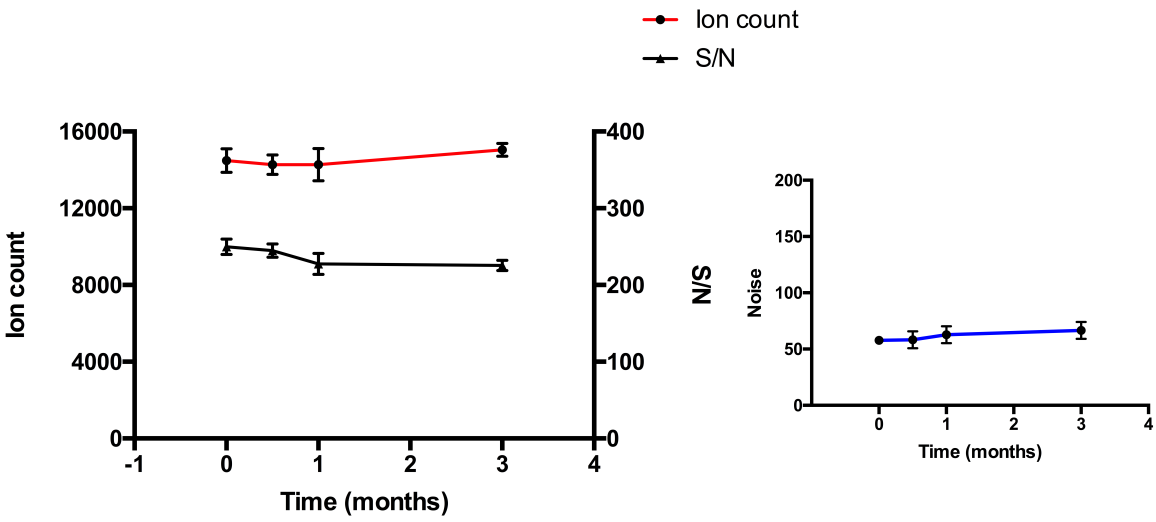

Figure 3-5: SALDI-MS signal (positive ion mode) of derivatized arginine in serum on 1% $pFSiCl_3$ coated GLAD film for 0-3 months. Red line represents ion count, black line represents signal to noise ratio (S/N), blue line represents noise in SALDI-MS measurements. The error bar represents SD of 6 individual measurements.

Four amino acids (arginine, valine, asparagine, and histidine) were quantified by adding different volumes of standard stock solutions into serum samples, using a standard addition method for quantification, followed by sample deproteination, fluorous derivatization, and on-chip purification procedures. The standard solutions were added before sample preparation to allow for any interference generated by sample loss during deproteination. The calibration curves are plotted in Figure 3-6. The concentration of arginine obtained from the quantitative results is 54.1±6.5 μM (95% confidence interval, n=7), and the concentrations of valine, asparagine, and

histidine are 209.3±21.0 µM (95% confidence interval, n=6), 102.6±15.9 µM (95% confidence interval, n=6), and 145.1±14.2 µM (95% confidence interval, n=7), respectively. The concentrations of these amino acids are within the concentration ranges of the Human Metabolome Database (HMDB, www.hmdb.ca).

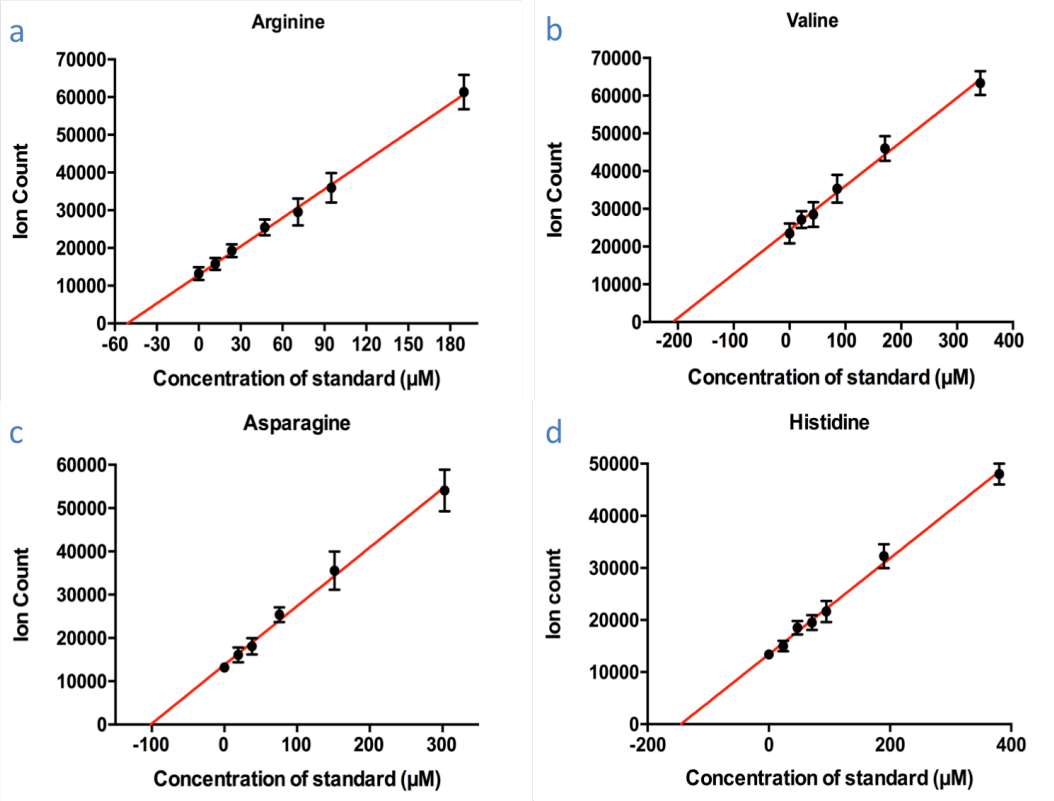

Figure 3-6: Standard addition calibration curves of (a) arginine, (b) valine, (c) asparagine, and (d) histidine in pooled normal human serum in SALDI-MS. The x-axis represents the concentration of the standard in serum samples before sample treatment. The error bar represents standard deviation (SD) of 6 individual measurements. The R^2 are 0.97 in (a), 0.96 in (b) & (c), and 0.98 in (d).

Arginine was also quantified by the standard addition method with an isotope labeled standard, as illustrated in Figure 3-7. Isotope labeled ^{13}C arginine was selected as the internal standard, since they have the same yield for the fluorous derivatization reaction and the same ionization efficiency in SALDI-MS detection. Isotope labeling provides optimal performance for quantitative studies of most MS work. Isotope labeled ^{13}C arginine stock solution was added before sample preparation to allow for the sample loss in the process of sample deproteination.

The relative intensity of the analyte to the internal standard gives better reproducibility, since it is less influenced by the variation due to the sample preparation and labeling process. Here 50 μM of isotope labeled ^{13}C arginine is used as the internal standard. The calibration curve of arginine is plotted as ion count ratio *vs.* concentration of standard arginine in Figure 3-7. A linear regression was achieved with a mass range from 0.5 to 500 μM and the R^2 of 0.99. The calculated concentration for arginine in serum is 53.2±12.0 μM (95% confidence interval, n=6), which is consistent with the concentration we observed from the traditional standard addition method in Figure 3-6a.

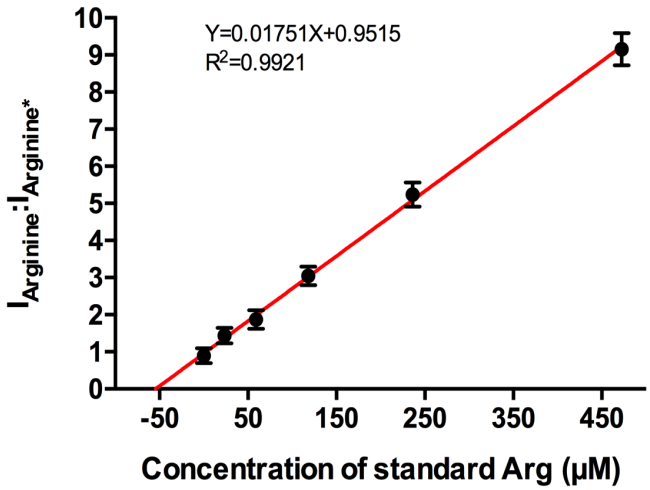

Figure 3-7: The calibration curve of arginine in serum samples with isotope labeled arginine as the internal standard in SALDI-MS. The linear range is 0.5-500 μM. The error bars represent SD of 6 individual measurements.

In the spectrum of derivatized serum in positive ion mode, two peaks are found at high mass region (m/z=854.2 and 868.2) as shown in Figure 3-8, which are assigned as protonated binary fluorous derivatized aspartic acid and glutamic acid.[133] Aspartic acid and glutamic acid have two carboxyl groups (α-COOH and side chain), both can be labeled with fluorous tags. Figure 3-9 shows the structural formula of di-derivatized aspartic acid and glutamic acid. To confirm the identities of these two peaks, pure aspartic and glutamic acid standard solutions were labeled with 3-(perfluorohexyl)propan-1-ol and detected by SALDI-MS. The peaks agreed with the spectra of pure samples, respectively. When different volumes of pure samples were spiked and labeled, the intensity of the binary peaks changed as expected. Therefore, the intensity of binary labeled peaks is used for determining

the concentration of these two acidic amino acids in serum.

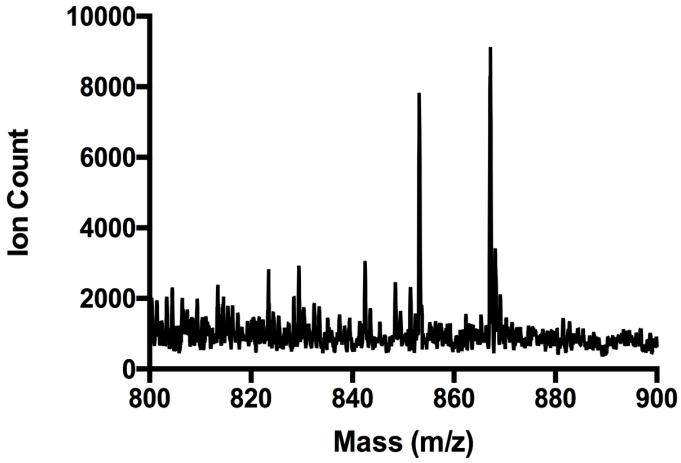

Figure 3-8: SALDI-MS spectrum of derivatized serum in positive ion mode in the mass range of 800-900.

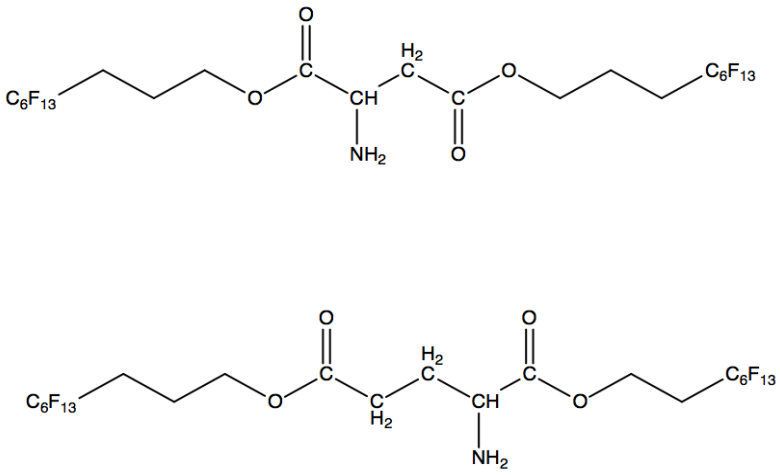

Figure 3-9: Structural formula of bi-fluorous derivatized aspartic acid and glutamic acid.

When the serum sample is spiked with additional aspartic and glutamic acid, the intensity of these two peaks in SALDI-MS linearly increases with increasing concentration of aspartic acid and glutamic acid from 0.5 μM to 500 μM. Herein glutamic acid was quantified by the standard addition method. A linear standard addition calibration curve is obtained in Figure 3-10 and the extrapolated concentration is 93.0±13.6 μM (95% confidence interval, n=6), within the normal concentration range of the database. This linear regression curve has an R^2 of 0.96, indicates that the yield of the binary fluorous reaction is stable in this concentration range since fluorous propanol is in large excess in our method. The binary labeled peaks of acidic amino acids provide reliable quantitative results for serum samples.

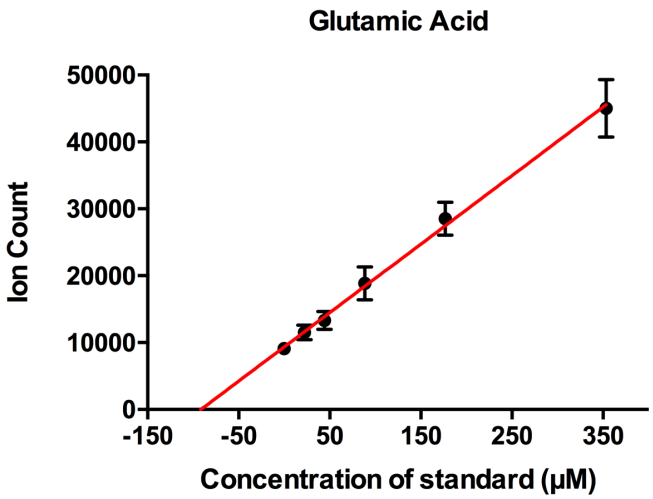

Figure 3-10: Calibration curve of glutamic acid in pooled normal human serum in SALDI-MS. The x-axis represents the concentration of glutamic acid added in serum samples before sample treatment. The error bar represents SD of 6 individual measurements. The R^2 is 0.96.

3.3.2.2 Quantitative analysis by LC-MS

To evaluate the sample preparation efficiency for removing proteins, serum samples prepared with C18 beads in methanol, verses ultrafiltration through centrifugal ultrafiltration tubes (Amicon Ultra-4, 3000 Dalton cut-off) were compared in hydrophilic interaction liquid chromatography (HILIC) MS. As is shown in Figure 3-11, the sample deproteinated by C18 beads in methanol has sharp peaks and clean baseline, while more tailing and other metabolite peaks are found in the chromatograph of a serum sample prepared through ultrafiltration. Besides, when ultrafiltration prepared serum samples were labeled with

3-(perfluorohexyl)propan-1-ol, yellow precipitates were formed at the bottom of the vial, which were easily carbonized in the evaporation step and were difficult to reconstitute in methanol/water. The results indicate C18 beads in methanol provide sufficient removal of proteins, lipids, and other interference from serum, while ultrafiltration prepared samples have more remaining biomolecules.

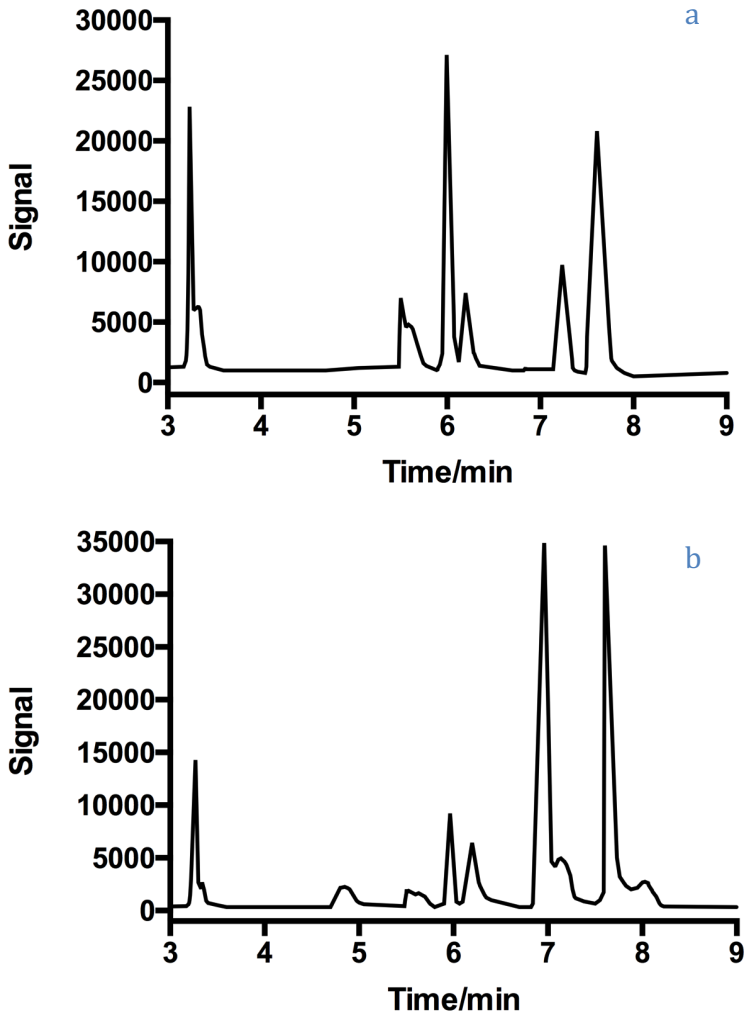

Figure 3-11: Ion chromatograms of five amino acids prepared by (a) C18 beads in methanol and (b) ultrafiltration using centrifugal ultrafiltration tubes on a Hilic-Z column. The retention times are 3.17 min for valine, 5.99 min for asparagine, 6.20 for glutamic acid, 7.24 min for histidine, and 7.68 min for arginine.

Pooled normal human serum samples spiked with additional standard solutions of

analytes were prepared through deproteination steps with 5.0% C18 beads. The samples without labeling were then measured by LC-MS as a comparison. A gradient elution method was designed to separate the target amino acids. The results of LC-MS were plotted as the area of target peak *vs.* concentration of standard added in serum, as shown in Figure 3-12. Linear regressions are obtained for five amino acids, and the extrapolated concentrations from Figure 3-12 are 53.9±5.4 μM of arginine, 197.6±9.4 μM of valine, 97.3±12.8 μM of asparagine, 146.8±11.4 μM of histidine, and 88.1±13.1 μM of glutamic acid (95% confidence interval, n=6), which are in agreement with the quantitative results from SALDI-MS. The data indicate that our method combining fluorous derivatization with perfluoro coated pSi surfaces in SALDI-MS detection, enables accurate determination of amino acids in serum.

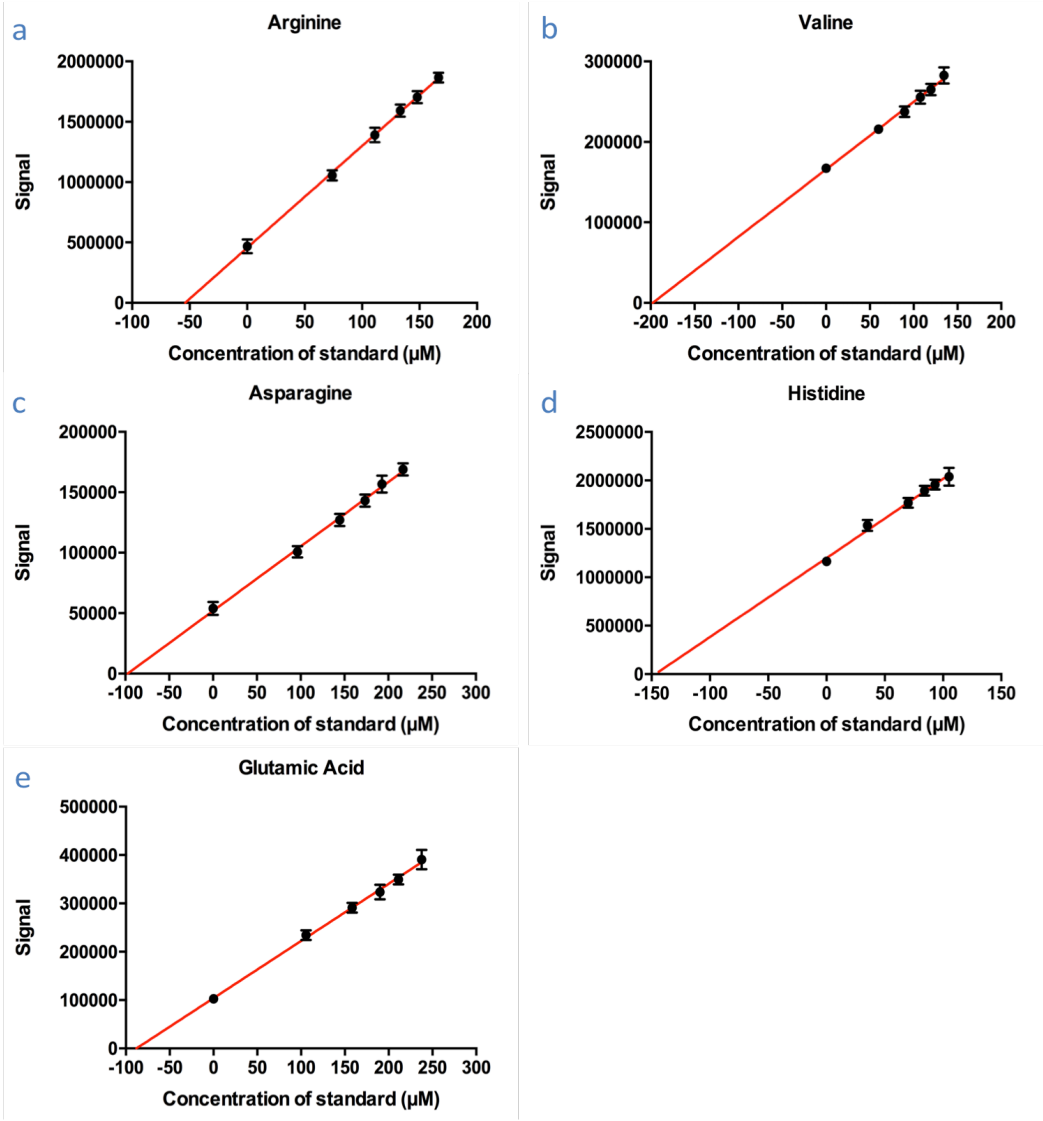

Figure 3-12: Calibration curves of (a) arginine, (b) valine, (c) asparagine, (d) histidine, and (e) glutamic acid in pooled normal human serum samples in LC-MS. The x-axis represents the concentration of the standard added in serum before sample treatment. The y-axis represents the peak area in the spectra. The error bar represents SD of 3 individual measurements. The R^2 are 0.99 in (a), 0.97 in (b), 0.98 in (c) & (e), and 0.96 in (d).

Isotope labeled chemicals are ideal internal standards widely used in LC-MS analysis. To explore the precision of our method, isotope labeled ^{13}C arginine was used as an internal standard for C18 beads based sample preparation of serum with LC-MS. 50 μM of isotope labeled ^{13}C arginine and different volumes of standard arginine solution were added in serum samples, followed by the same deproteination procedure. The standard addition calibration curve was observed by plotting signal (peak area) ratio *vs.* concentration of additional arginine in Figure 3-13. A good linear regression is achieved, with a calculated concentration of arginine of 56.6±8.4 μM (95% confidence interval, n=6), which agrees with the results we previously observed in LC-MS and SALDI-MS. The standard addition curve has an R^2 of 0.99, which is in agreement with the results of SALDI-MS, indicating a similar level of precision.

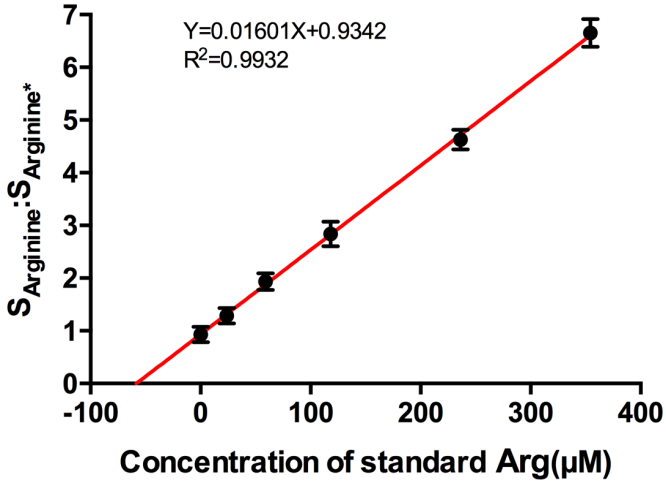

Figure 3-13: The calibration curve of arginine in serum samples using isotope labeled arginine as the internal standard in LC-MS. The linearity range is 0.5 ~ 360 μM with the R^2 of 0.99. The error bar represents SD of 3 individual measurements.

3.3.2.3 Quantitative analysis by ^{1}H-NMR spectroscopy

The NMR results are summarized in Table 3-1 and compared with SALDI-MS and LC-MS results, along with the Human Metabolome database (HMDB, www.hmdb.ca).

Table 3-1: The concentrations of amino acids in pooled normal human serum quantified by SALDI-MS, NMR, and LC-MS, compared with Metabolome database*.

Metabolite	MW (Dalton)	SALDI-MS (μM)	Database* (μM)	NMR (μM)	LC-MS (μM)
Arginine	174.20	54.1±6.5	17-130	61±3.0	53.9±5.4
Valine	117.15	209.3±21.0	71-385	345±17.2	197.6±9.4
Asparagine	132.12	102.6±15.9	4-132	112±5.6	97.3±12.8
Histidine	155.07	145.1±14.2	3-160	146±7.3	146.8±11.4
Glutamic acid	147.05	93.0±13.6	8-110	302±15.1	88.1±13.1

*Data are from Human Metabolome database (HMDB, www.hmdb.ca).

The concentrations of arginine, asparagine, and histidine observed by NMR are consistent with the quantitative results from LC-MS and SALDI-MS, respectively. For valine and glutamic acid, the concentrations by NMR are higher than the results from SALDI-MS and LC-MS. Bovee's work proved that NMR results of glutamic acid tend to be higher in complex samples.[149] However, the quantitative results of five amino acids observed by SALDI-MS and LC-MS are all within normal ranges of physiological samples, indicating the sample preparation and detection of our method offers clear advantages in quantifying amino acids in biofluid samples. A table for amino acids tested in various solutions is summarized in Appendix B. The labeling reaction produces distinguishable derivatives for most amino acids, however, for biological samples, SALDI has limitations for identifying isomers and some amino acids that have interference with close m/z (within ±0.1) in complex matrices.

3.4 Conclusion

In our method, serum samples were prepared after precipitation and solid phase extraction with C18 beads in methanol, and then derivatized by fluorous propanol, followed by SALDI-MS measurement. The comparison of precision for calibration curve versus different samples is list in the table of Appendix C. The sample preparation steps are effective in removing proteins, lipids, and other biomolecules from serum. The fluorous labeling of target molecules is highly selective with good stability. And the on-chip washing readily purifies the labeled derivatives. Our method provides simultaneous, direct analysis of amino acids in serum samples by SALDI-MS, the method is rapid with high selectivity and sensitivity in sample preparation and SALDI-MS detection. The results show good linear response from 0.5 to 500 μM for the five amino acids we explored detailed quantification with. These concentrations cover the normal range in human serum. The quantitative results show great consistency with the results observed by other preparation and detecting methods, respectively, indicating our method works well for determining amino acid levels in serum and has great potential for quantitative analysis of complex biological samples.

Chapter 4 Derivatization of amine groups with fluorous affinity tags for metabolite analysis

4.1 Introduction

Many biogenic amines and amine-related pathways have not been investigated in-depth due to a previous lack of sensitivity.[150] Recent advances in analytical technologies now render such analysis possible. Developing a sensitive and selective method for the quantification of amino acids and amines in biological samples is very meaningful. In recent studies, the combination of chemical derivatization techniques with liquid chromatography-mass spectrometry (LC-MS) analysis has become an attractive approach for determining trace amounts of amine-containing molecules.[113,114,118,119,151–155] However, for these highly sensitive methods, one common problem encountered in the analysis of biological analytes is the interference from complex matrices.[119] The matrix-induced ion suppression effects, which are caused by ionization competition between the analytes and coeluting components, prevent accurate quantitative analysis of biological compounds.[119] Direct mass spectrometric analysis by matrix-free surface assisted desorption/ionization (SALDI) strategies facilitates rapid and sensitive quantification of target molecules.

In chemical derivatization reactions, fluorous derivatization reagents have high electronegativity, low polarizability, and good thermal and chemical stabilities.[118] And the reactions can be simple, specific, and quantitative for analytes containing

functional groups.[115,119] Importantly, fluorous groups have a "fluorophilicity" for a fluorous environment, so the labeled species can be easily separated from non-fluorous species utilizing fluorous functionalized media.[29,139]

The objective of this work is to develop a selective labeling method of amine groups for direct spectrometric analysis by SALDI. Here we evaluate 4-chloro-3,5-dinitrobenzotrifluoride (CNBF) and 1H-perfluorohexane-1,1-diol as derivatization reagents to label amine groups in amino acids for SALDI-MS analysis on perfluoro coated GLAD films. The derivatization reaction is highly selective for amine groups, and the labeled analytes provide enhanced sensitivity in SALDI-MS. The quantitative analysis of 1H-perfluorohexane-1,1-diol derivatization by SALDI-MS shows great potential for determining amino acid levels in real samples. Moreover, this reaction is incubated at room temperature without heating, which enables further amenable combination with other on-chip sample preparation methods at room temperature for accurate quantification of amino acids in complex biological samples.

4.2 Experimental section

4.2.1 Materials and reagents

Methanol (purity > 99.9%), acetonitrile (purity > 99.9%), boric acid (H_3BO_3), sodium hydroxide (NaOH), 2-picoline borane, hydrochloric acid (HCl), histidine, valine, glutamic acid, tyrosine, tryptophan, (1H, 1H, 2H, 2H-perfluorooctyl) trichlorosilane ($pFSiCl_3$), and 4-chloro-3,5-dinitrobenzotrifluoride (CNBF) were

purchased from Sigma-Aldrich Chemical Company (St. Louis, MO, USA). 1H-Perfluorohexane-1,1-diol was purchased from Santa Cruz Biotechnology, Inc. (Dallas, Texas, USA).

Ultrapure water used for sample preparation was from a deionizing system (Millipore Canada, Mississauga, ON, Canada). Stock solutions were prepared to give 5 mM of amino acid standards as aqueous solutions and diluted in water.

1% (v/v) silane/methanol solution for GLAD film silanization was prepared by adding 50 μL $pFSiCl_3$ into 5 mL methanol (purity > 99.9%), followed by 1 min of vortex mixing.

4.2.2 Sample preparation

The derivatization reaction with CNBF was carried out in acetonitrile/buffer (1:2, v/v) solution. 200 μL of amino acid standards with concentrations from 1 μM to 5 mM were prepared in water, for poorly soluble amino acids, solutions were acidified with HCl. Aliquots of stock solutions were mixed with 1 mL of H_3BO_3-$Na_2B_4O_7$ buffer solution (pH 9.0), 600 μL of CNBF acetonitrile solution (70 mM) were added in that order into a vial. After vortex mixing for 1 min, the mixture was incubated at 60 °C for 30 min. The resulting solutions were diluted to 5 mL with H_3BO_3-$Na_2B_4O_7$ buffer.[141] The reaction of CNBF with the amine groups on amino acids was represented in Figure 4-1.

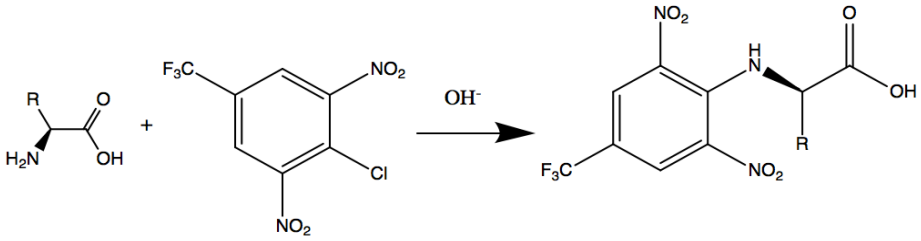

Figure 4-1: The reaction scheme of CNBF with amine groups on amino acids.

1H-Perfluorohexane-1,1-diol and 2-picoline borane solutions were prepared in acetonitrile. 100 µL of 1 M 1H-perfluorohexane-1,1-diol and 100 µL of 400 mM 2-picoline borane were added into 100 µL of amino acids (with concentrations ranging from 0.5 µM to 50 µM) dissolved in 1 mM HCl aqueous solution. The mixture was reacted at room temperature for 30 minutes. After the reaction, it was gently evaporated to dryness to remove excess reagent and then reconstituted with 100 µL of 1:1 (v/v) methanol/H_2O.

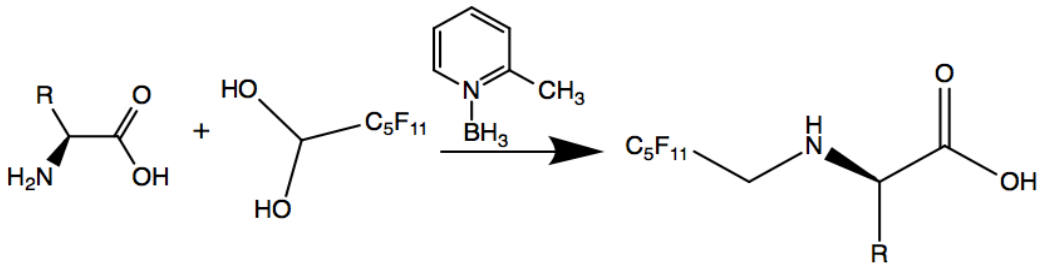

Figure 4-2: The reaction scheme of 1H-perfluorohexane-1,1-diol with amine groups on amino acids.

4.2.3 Mass spectrometry

SALDI chips were generated and modified with (1H, 1H, 2H, 2H-perfluorooctyl) trichlorosilane ($pFSiCl_3$, Gelest) as we mentioned previously. Reconstituted samples in 1 μL aliquots were spotted on $pFSiCl_3$ coated SALDI chips and open-air-dried for over 1 hour, then rinsed with 1 μL 1:1 (v/v) methanol/H_2O for 40 seconds.

MS measurements were performed on an AB Sciex Voyager Elite MALDI-TOF mass spectrometer equipped with a pulsed nitrogen laser (wavelength 337 nm, 3 ns pulse) at a repetition rate of 3.0 Hz. Spectra were acquired in positive ion mode using reflector, delayed ion extraction. Grid voltage was set at 69% and extraction delay time was 250 ns. Each spectrum consists of 100 laser shots.

4.3 Results and discussion

4.3.1 Derivatization by CNBF

At 60 °C for the reaction, the CNBF derivatization was rapid and stable. A uniform yellow solution was formed after the reaction. This derivative solution was diluted with the buffer solution, and then applied to the film. SALDI-MS measurements were performed to analyze the result.

The CNBF reagent can react with amino acids to form stable derivatives under basic conditions, and the excess reagent is hydrolyzed to the corresponding phenol without any by-products that cause interference.[142]

The addition of a buffer solution during reaction made many crystals form on the surface of perfluoro coated GLAD films, even with pure samples. After rinsing, most crystals were removed, however, the observed peaks for analytes in the SALDI-MS spectra were identified as sodium ion adduct peaks. CNBF labeled amino acids give strong SALDI-MS signals for standard solutions from 100 μM to 5 mM in positive ion mode as shown in Figure 4-3a. But below 100 μM, the intensity was low, and there was considerable background (Figure 4-3b).

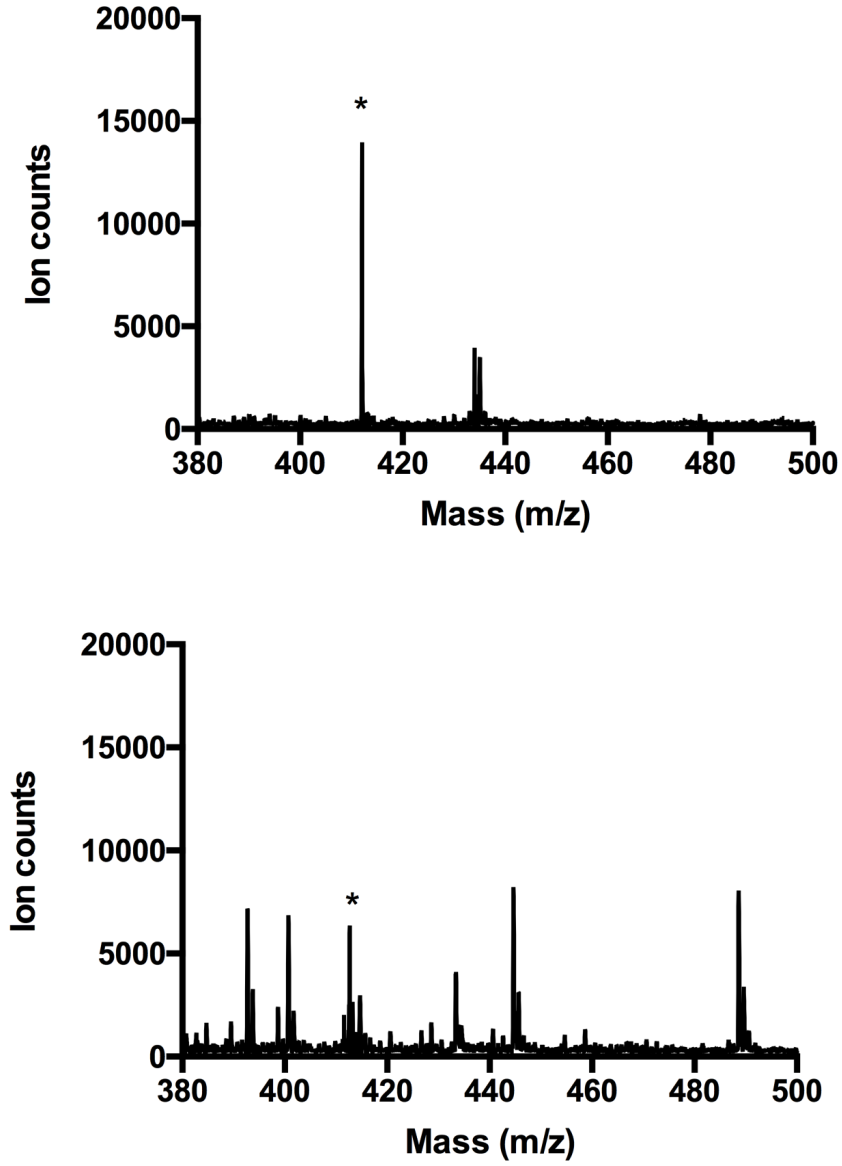

Figure 4-3: SALDI-MS spectra of (a) 5 mM and (b) 50 μM histidine standard solutions fluorous derivatized with CNBF in positive ion mode after 40 second rinse. The mass range is 380-500. The peak labeled with star (*) at m/z 412.3 is identified as sodium ion adduct peak of derivatized histidine [CNBF-His-Na^+].

As we can see from the structure of CNBF in Figure 4-1, there is only one $-CF_3$ group attached to the benzene ring as a single fluorinated label. This short fluorous label provides relatively weak fluorophilic affinity for perfluoro coated GLAD surfaces during rinsing. The quantitative results for CNBF labeled valine were analyzed, using histidine as the internal standard. Since 200 μL of the standard mixture was diluted to 5 mL in the final solution, the calibration curve of valine was plotted as the ion count ratio between valine and histidine *vs.* the final concentration of valine in the reation solution in Figure 4-4. The linear regression range was from 1.0 μM to 50 μM with the R^2 of 0.97. The limit of quantitation of valine in positive ion mode is 0.79 μM, which is higher than the 3-(perfluorohexyl)propan-1-ol labeling method.

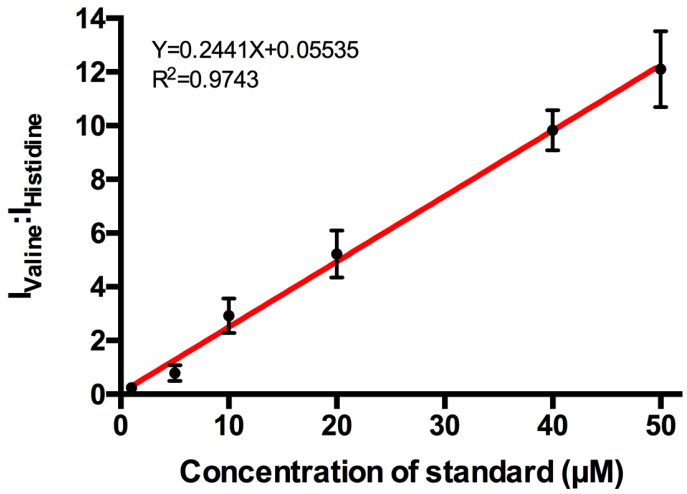

Figure 4-4: The internal standard calibration curve of valine derivatized with CNBF using 5 μM histidine as the internal standard. The linearity range is 1.0 ~ 50 μM. The error bar represents SD of 10 individual measurements. The concentration of the analyte and the internal standard represents the final concentration of valine and histidine in the reaction solution.

Compared with our previous work, these results identify that a labeling reagent with a larger fluorinated group will provide better retention of derivatives on the surface of perfluoro coated GLAD films. Meanwhile, a longer labeling tag with heavier molecular weight works better for raising the molar mass of the analyte to a higher mass region. Hence, labeling reagents with longer fluorinated chains are desired in our method.

4.3.2 Derivatization by fluorous diol in SALDI-MS

Hayama reported a method using fluorous aldehyde reagent to derivatize biogenic amines.[119] Primary amine groups were selectively binary labeled with fluorous groups, while secondary amine groups were derivatized with one fluorous tag. The reaction scheme of primary amine groups is shown in Figure 4-5. The derivatives were injected onto an LC column containing a perfluoroalkyl-modified stationary phase for LC-MS analysis, and the feasibility of their method was further evaluated by applying it to human plasma samples.[119] Unfortunately, the fluorous aldehyde of their method or some related aldehyde is no longer available for purchase.

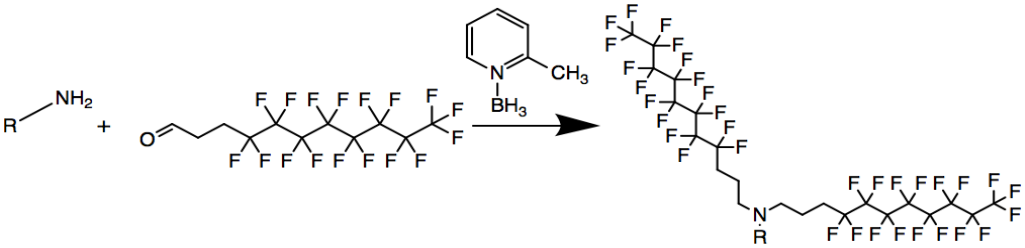

Figure 4-5: The reaction scheme of fluorous aldehyde 2H,2H,3H,3H-perfluoroundecan-1-al with primary amine groups.

In this work, a similar labeling reagent, 1H-perfluorohexane-1,1-diol, a hexanal hydrate was used for fluorous derivatization. This compound is in equilibrium with the aldehyde form. The reaction then proceeds through reductive amination, involving 2-picoline borane. The reaction solution was gently reacted at room

temperature. The derivatives of different amino acids were found to be ionizable in positive ion mode, forming protonated ions $[M + H]^+$. The SALDI-MS spectra of the protonated derivatives are shown in Figure 4-6. The MS data shows single perfluoro label per amine. The commercially available aldehyde yielded two labels per amine. The difference may be due to the amount of aldehyde form present in equilibrium with the hexanal hydrate form, as it is likely at lower concentration, due to the closer proximity of the CF_2 chain to the terminal carbon. However, the reaction mechanism of the metabolites with two or multiple amine groups is complicated and has not been fully investigated. Only a few amino acids are explored in this chapter.

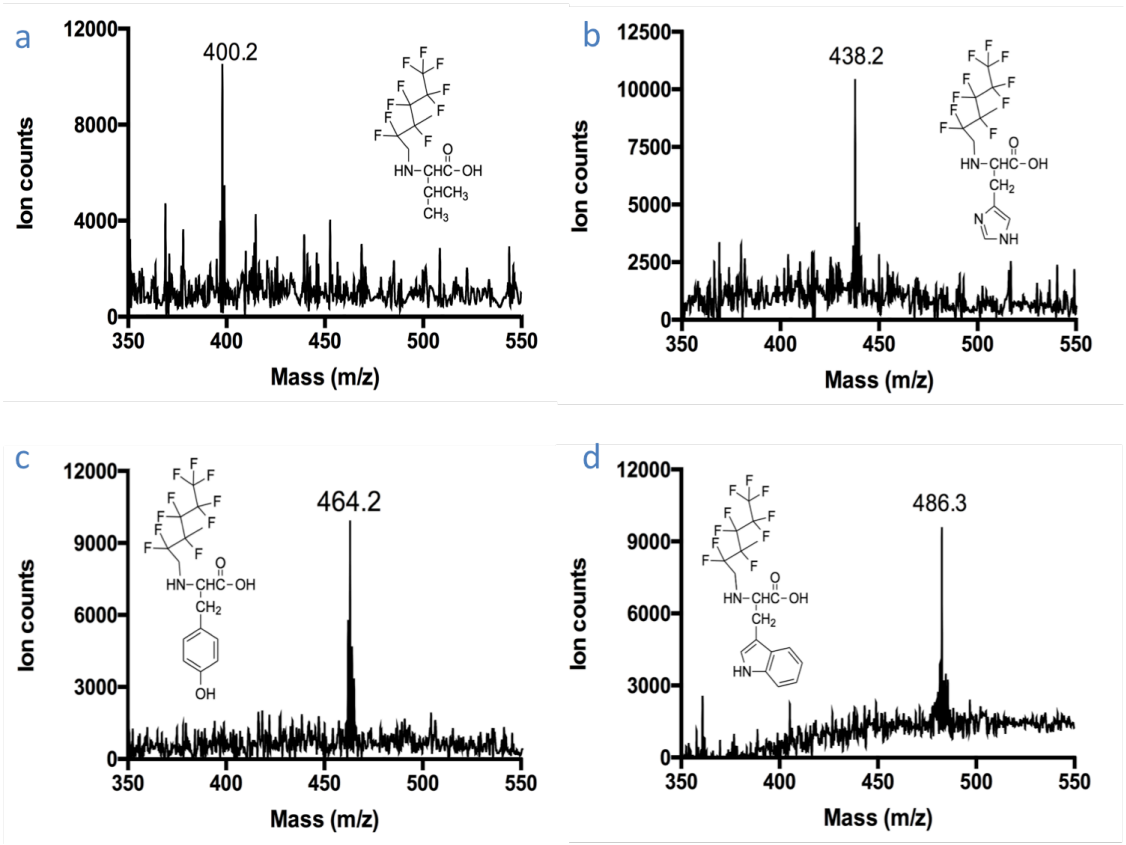

Figure 4-6: SALDI-MS spectra in positive ion mode of 1H-perfluorohexane-1,1-diol labeled amino acids: (a) valine, (b) histidine, (c) tyrosine, and (d) tryptophan. The labeled ions are protonated amino acids with fluorous tag (C_5F_{11}), the molar masses are (a) m/z 400.2, (b) m/z 438.2, (c) m/z 464.2, (d) m/z 486.3. The mass ranges are from 350 to 450.

A mixture of amino acids (50 μM of histidine, valine, glutamic acid, tyrosine, and tryptophan in 1 mM HCl) was labeled and identified by SALDI-MS in positive ion mode, as shown in Figure 4-7. In the SALDI-MS spectrum, the labeled peaks are

valine, glutamic acid, histidine, tyrosine, and tryptophan, from left to right. The target peaks of fluorous derivatized amino acids are raised to a higher mass region (> 400 Dalton). High intensity with a low and clean background is observed even at μM level, resulting in a higher signal to noise ratio in MS.

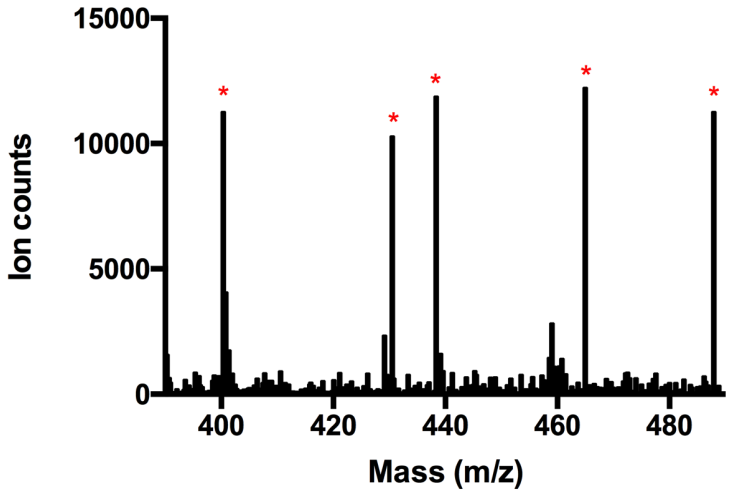

Figure 4-7: SALDI-MS spectra of sample (50 μM of histidine, valine, glutamic acid, tyrosine, and tryptophan in 1 mM HCl) derivatized with 1H-perfluorohexane-1,1-diol in positive ion mode after 40 second rinse. The mass range is 390-490. The peaks are identified and labeled with star (*), from left to right, the labeled peaks are valine (m/z 400.2), glutamic acid (m/z 430.2), histidine (m/z 438.2), tyrosine (m/z 464.2), and tryptophan (m/z 486.3).

Samples containing 5 μM histidine as the internal standard and valine at different

concentrations were prepared and derivatized with 1H-perfluorohexane-1,1-diol. In SALDI-MS, MS signals with high intensity and good reproducibility were obtained. Figure 4-8 shows the internal standard calibration curve of valine derivatized with 1H-perfluorohexane-1,1-diol using 5 μM histidine as the internal standard. The curve was constructed by plotting the relative peak intensity *vs*. the concentration of standard. The calibration curve shows a linear response from 0.5 μM to 50 μM with an R^2 of 0.99, and a limit of quantitation for valine of 0.41 μM, indicating this derivatization reaction works well in labeling and quantifying amino acids.

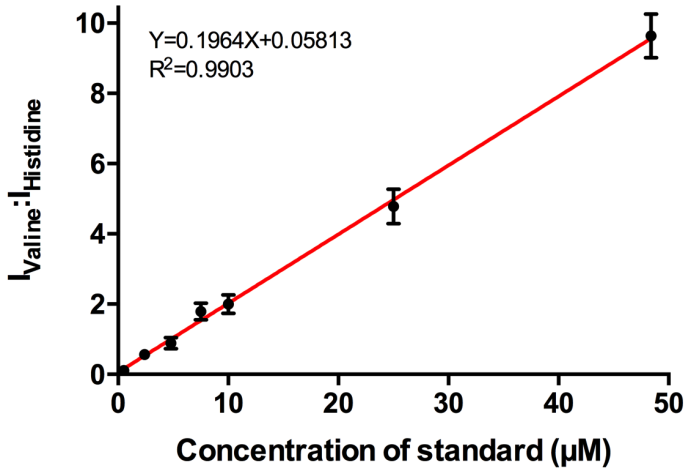

Figure 4-8: Internal standard calibration curve of valine derivatized with 1H-perfluorohexane-1,1-diol using 5 μM histidine as the internal standard. The linear range is 0.5 ~ 50 μM. The error bar represents SD of 10 individual measurements.

The reproducibility of different fluorous reagent (3-(perfluorohexyl)propan-1-ol, CNBF, and 1H-perfluorohexane-1,1-diol) labeled sample solutions was compared. 3-(Perfluorohexyl)propan-1-ol derivatized samples, in which the carboxyl group is derivatized, exhibited more uniform analyte ion signal intensities. The reproducibility between samples was monitored by calculating the relative standard deviation (RSD) values of the ion count ratios of two amino acids at a given concentration ratio on 6 different SALDI spots. A technique suitable for quantitative analysis should have low and consistent RSD values of measured signals. The measured RSD values for both 1H-perfluorohexane-1,1-diol and 3-(perfluorohexyl)propan-1-ol derivatization methods are less than 10% at given concentration ratios, indicating high sample-to-sample reproducibility, as seen in Table 4-1. However, for each concentration ratio, the RSD value (n=6) of the 1H-perfluorohexane-1,1-diol method is ~ 15% higher than the 3-(perfluorohexyl)propan-1-ol method. For the CNBF derivatization method, the RSD values are notably increased, especially at low concentration ratios (< 2.0) due to the poor retention efficiency of the derivatives. When the concentration ratios are over 2.0, the RSD values are also less than 10% for the CNBF method.

Table 4-1: Comparison of the reproducibility between different fluorous derivatization methods

	ratio	RSD (%, n=6)		
		3-(perfluorohexyl) propan-1-ol method	1H-perfluorohexane-1,1-diol method	CNBF method
val/his	0.1	2.46	3.57	17.0
	0.5	6.35	8.71	31.4
	1.0	5.66	6.72	18.3
	2.0	7.84	9.20	13.8
	4.0	5.84	6.78	7.23
	8.0	3.40	4.05	9.57

The correlation coefficients of the calibration curves are compared in Table 4-2. All correlation coefficients are greater than 0.9743. Among these three derivatization methods, the 3-(perfluorohexyl)propan-1-ol reagent gives a linear correlation coefficient of 0.9942 and the lowest RSD values, illustrating it is the best labeling method of those evaluated for determining amino acid levels in biological samples. In contrast, CNBF reagent gives the lowest R^2 of 0.9743 and the highest RSD values. Further optimization would be required before applying CNBF with SALDI-MS on GLAD films, but it is not clear it would be possible to improve the performance enough for this reagent.

Table 4-2. Comparison of the linear correlation coefficient (R^2) between different fluorous derivatization methods

Analyte	R^2		
	3-(perfluorohexyl) propan-1-ol method[a]	1H-perfluorohexane -1,1-diol method[a]	CNBF method[b]
val/his	0.9942	0.9903	0.9743

[a]Correlation coefficient of calibration curves in the range from 0.5 to 50 μM. [b]Correlation coefficient of calibration curves in the range from 1.0 to 50 μM.

For 1H-perfluorohexane-1,1-diol reagent, the linear correlation coefficient is 0.9903, which is suitable for accurate quantitative analysis of amino acids. The success of 1H-perfluorohexane-1,1-diol derivatization extends the application of fluorous derivatization reactions from carboxylic acids to amines. Because the reaction occurs at room temperature, the use of this reagent could enable automation of the sample preparation by combination with centrifugal fluidic devices. Complex biological samples can be purified and deproteinated through certain on-chip sample preparation steps and then reacted in another chamber for derivatization at room temperature on the same device. Hence the sample preparation and derivatization are performed on a single platform, which can simplify the whole process for quantitative analysis of complex biological samples.

4.4 Conclusion

In this chapter, 4-chloro-3,5-dinitrobenzotrifluoride (CNBF) and 1H-perfluorohexane-1,1-diol are evaluated as the derivatization reagents for amine groups in amino acids. In SALDI-MS measurements, CNBF labeled analytes show a stable SALDI-MS response after rinsing at high concentration levels (>100 μM). But at low concentrations (<100 μM), CNBF labeled derivatives have poor retention on perfluoro coated GLAD films. The intensity is relatively low, with considerable background noise. For 1H-perfluorohexane-1,1-diol labeled derivatives, the SALDI-MS results show high intensity and good reproducibility after rinsing. This 1H-perfluorohexane-1,1-diol derivatization reaction is fast and highly selective in labeling amine groups of amino acids.

The quantitative results of CNBF and 1H-perfluorohexane-1,1-diol derivatization methods are compared with 3-(perfluorohexyl)propan-1-ol derivatization method. The quantitative results of 3-(perfluorohexyl)propan-1-ol derivatization, which reacts with the carboxyl group and 1H-perfluorohexane-1,1-diol derivatization, which reacts with the amine group, provide reliable linear regressions. For both reagents, the relative standard deviations in the intensity ratio between the analyte and the internal standard are less than 10%, with a linear correlation coefficient of over 0.99. The results suggest great potential for precise quantitative analysis of amino acids in real samples.

In addition, this 1H-perfluorohexane-1,1-diol reaction labels amine groups, which extends the application of fluorous derivatization for metabolite analysis by SALDI with GLAD film MS. The reaction is incubated at room temperature, which is

suitable for further combination with other on-chip sample preparation methods.

Chapter 5 Concluding remarks and future work

5.1 Concluding remarks

In this thesis, different fluorous derivatization reagents were evaluated and compared using porous silicon based SALDI-MS for the analysis of amino acids in biological samples. The nanostructure of GLAD films assists the desorption/ionization process and improves the reproducibility and sensitivity in SALDI-MS detection.

In chapter 2 & 3, different fluorous propanol, 3-(perfluorobutyl)propan-1-ol, 3-(perfluorohexyl)propan-1-ol, and 3-(perfluorooctyl)propan-1-ol were compared as the derivatization reagents to label carboxyl groups of amino acids. The detection was measured by SALDI-MS on perfluoro coated GLAD films. We found 3-(perfluorohexyl)propan-1-ol to be the best labeling reagent. Based on this study, we developed a method using 3-(perfluorohexyl)propan-1-ol for quantitative analysis of amino acids by SALDI-MS. SALDI-MS results provide high sensitivity of low mass analytes. The analysis of artificial and serum samples shows reliable quantitative results, indicating this method works well for accurate quantification of amino acids in biological samples.

In chapter 4, 4-chloro-3,5-dinitrobenzotrifluoride (CNBF) and 1H-perfluorohexane-1,1-diol were evaluated as derivatization reagents to label amine groups in amino acids. The quantitative results were compared with

3-(perfluorohexyl)propan-1-ol derivatization method. The quantitative results of 1H-perfluorohexane-1,1-diol derivatization method provide good linear regression and low RSD values, suggesting this derivatization reaction has the potential for accurate quantitative analysis of amino acids in real samples.

Overall, fluorous derivatization reactions have been studied for labeling carboxyl groups and amine groups. Fluorous derivatization combined with perfluoro coated SALDI-MS provides efficient purification of unlabeled interference and improves the sensitivity of MS detection. The methods have great potential for precise quantification of amino acids in biological samples. For complex biological samples, sample preparation procedure is required before chemical derivatization, therefore the conjunction of fluorous derivatization with on-chip sample preparation methods is suggested for the next stage of development.

5.2 Future work

The combination of sample preparation on centrifugal devices and chemical derivatization can simplify the entire process for detecting biological samples and enhance the sensitivity of quantitative analysis. The multichannel centrifugal microfluidic device removes proteins and lipids from biological samples, thus amino acids can be detected by SALDI-MS in a clean matrix with high response and stable intensity.

At the end of this thesis work, we performed some preliminary experiments that coupled the 3-(perfluorohexyl)propan-1-ol derivatization method with centrifugal

fluidic technologies for whole blood detection as an initial attempt. After on-chip preparation of the blood sample, the sample was off-chip derivatized with 3-(perfluorohexyl)propan-1-ol and then measured by SALDI-MS. The concentration of arginine found in the blood was 52.5±11.6 μM (95% confidence interval, n=6), in agreement with the concentration range in human blood (Human Metabolome Database, HMDB, www.hmdb.ca). The concentrations of valine, asparagine, glutamic acid, and histidine were also detected and compared with normal concentration ranges, respectively (Table 5-1). The results indicate this method is competitive with chromatographic techniques, and may be well suited to batch, clinical analysis of samples.

Table 5-1: The concentrations of amino acids in human blood samples quantified by SALDI-MS, compared with Metabolome database*.

Metabolite	MW (Dalton)	Database (μM)	In Blood (μM)
Arginine	174.20	17-130	52.5±11.6
Valine	117.15	71-385	194.1±20.5
Asparagine	132.12	4-132	91.7±13.6
Histidine	155.07	3-160	147.1±16.1
Glutamic acid	147.05	8-110	73.1±6.6

*Data are from Human Metabolome database (HMDB, www.hmdb.ca).

In this study, the centrifugal prepared sample is fluorous derivatized off-chip since the reaction is incubated at 65 °C. Therefore additional sample loss is involved during the transfer and a larger sample volume is required for each test. As the next step, we propose to use 1H-perfluorohexane-1,1-diol for on-chip derivatization, since the reaction is incubated at room temperature, thus biological samples can be on-chip prepared and derivatized in the same centrifugal device. Combining 1H-perfluorohexane-1,1-diol derivatization method with centrifugal fluidic devices to achieve the sample preparation and chemical derivatization performed on a single platform will be the objective of future work in this project.

References

1. Siuzdak, G. An introduction to mass spectrometry ionization: an excerpt from the expanding role of mass spectrometry in biotechnology, ; MCC Press: San Diego, 2005. *JALA: Journal of the Association for Laboratory Automation* **9**, 50–63 (2004).

2. Villas‐Bôas, S. G., Mas, S., Åkesson, M., Smedsgaard, J. & Nielsen, J. Mass spectrometry in metabolome analysis. *Mass spectrometry reviews* **24**, 613–646 (2005).

3. Khan, M. F. *et al.* Proteomics by mass spectrometry—Go big or go home? *Journal of pharmaceutical and biomedical analysis* **55**, 832–841 (2011).

4. Fenner, N. C. & Daly, N. R. Laser used for mass analysis. *Review of Scientific Instruments* **37**, 1068–1070 (1966).

5. Vastola, F. J. & Pirone, A. J. Ionization of organic solids by laser irradiation. *Adv. mass spectrom* **4**, 107–111 (1968).

6. Vastola, F. J., Mumma, R. O. & Pirone, A. J. Analysis of organic salts by laser ionization. *Organic Mass Spectrometry* **3**, 101–104 (1970).

7. Gross, J. H. Matrix-assisted laser desorption/ionization. in *Mass Spectrometry* 507–559 (Springer, 2011).

8. Liu, L. K., Busch, K. L. & Cooks, R. G. Matrix-assisted secondary ion mass spectra of biological compounds. *Analytical Chemistry* **53**, 109–113 (1981).

9. Karas, M., Bachmann, D. & Hillenkamp, F. Influence of the wavelength in high-irradiance ultraviolet laser desorption mass spectrometry of organic molecules. *Analytical chemistry* **57**, 2935–2939 (1985).

10. Karas, M. & Hillenkamp, F. Laser desorption ionization of proteins with molecular masses exceeding 10,000 daltons. *Analytical chemistry* **60**, 2299–2301 (1988).

11. Barber, M., Bordoli, R. S., Sedgwick, R. D. & Tyler, A. N. Fast atom bombardment of solids as an ion source in mass spectrometry. *Nature* **293**, 270 (1981).

12. Tanaka, K. *et al.* Protein and polymer analyses up to m/z 100 000 by laser ionization time−of−flight mass spectrometry. *Rapid communications in mass spectrometry* **2**, 151–153 (1988).

13. Watanabe, T., Kawasaki, H., Yonezawa, T. & Arakawa, R. Surface−assisted laser desorption/ionization mass spectrometry (SALDI−MS) of low molecular weight organic compounds and synthetic polymers using zinc oxide (ZnO) nanoparticles. *Journal of mass spectrometry* **43**, 1063–1071 (2008).

14. Sunner, J., Dratz, E. & Chen, Y.-C. Graphite surface-assisted laser desorption/ionization time-of-flight mass spectrometry of peptides and proteins from liquid solutions. *Analytical chemistry* **67**, 4335–4342 (1995).

15. Law, K. P. & Larkin, J. R. Recent advances in SALDI-MS techniques and their chemical and bioanalytical applications. *Analytical and bioanalytical*

chemistry **399**, 2597–2622 (2011).

16. Wu, C.-Y., Lee, K.-C., Kuo, Y.-L. & Chen, Y.-C. Revisiting the quantitative features of surface-assisted laser desorption/ionization mass spectrometric analysis. *Philosophical Transactions of the Royal Society A: Mathematical, Physical and Engineering Sciences* **374**, 20150379 (2016).

17. Schürenberg, M., Dreisewerd, K. & Hillenkamp, F. Laser desorption/ionization mass spectrometry of peptides and proteins with particle suspension matrixes. *Analytical Chemistry* **71**, 221–229 (1999).

18. Marklein, G. *et al.* Matrix-assisted laser desorption ionization-time of flight mass spectrometry for fast and reliable identification of clinical yeast isolates. *Journal of clinical microbiology* **47**, 2912–2917 (2009).

19. Wei, J., Buriak, J. M. & Siuzdak, G. Desorption–ionization mass spectrometry on porous silicon. *Nature* **399**, 243 (1999).

20. Thomas, J. J., Shen, Z., Crowell, J. E., Finn, M. G. & Siuzdak, G. Desorption/ionization on silicon (DIOS): a diverse mass spectrometry platform for protein characterization. *Proceedings of the National Academy of Sciences* **98**, 4932–4937 (2001).

21. Chen, W.-Y. & Chen, Y.-C. Affinity-based mass spectrometry using magnetic iron oxide particles as the matrix and concentrating probes for SALDI MS analysis of peptides and proteins. *Analytical and bioanalytical chemistry* **386**, 699–704 (2006).

22. Yuan, M. *et al.* Preparation of highly ordered mesoporous WO3–TiO2 as matrix in matrix-assisted laser desorption/ionization mass spectrometry. *Microporous and Mesoporous Materials* **78**, 37–41 (2005).

23. McLean, J. A., Stumpo, K. A. & Russell, D. H. Size-selected (2− 10 nm) gold nanoparticles for matrix assisted laser desorption ionization of peptides. *Journal of the American Chemical Society* **127**, 5304–5305 (2005).

24. Huang, Y.-F. & Chang, H.-T. Nile red-adsorbed gold nanoparticle matrixes for determining aminothiols through surface-assisted laser desorption/ionization mass spectrometry. *Analytical chemistry* **78**, 1485–1493 (2006).

25. Chen, C.-T. & Chen, Y.-C. Fe3O4/TiO2 core/shell nanoparticles as affinity probes for the analysis of phosphopeptides using TiO2 surface-assisted laser desorption/ionization mass spectrometry. *Analytical chemistry* **77**, 5912–5919 (2005).

26. Kang, M.-J. *et al.* Nanowire−assisted laser desorption and ionization mass spectrometry for quantitative analysis of small molecules. *Rapid Communications in Mass Spectrometry: An International Journal Devoted to the Rapid Dissemination of Up−to−the−Minute Research in Mass Spectrometry* **19**, 3166–3170 (2005).

27. Daniels, R. H., Dikler, S., Li, E. & Stacey, C. Break free of the matrix: sensitive and rapid analysis of small molecules using nanostructured surfaces and LDI-TOF mass spectrometry. *JALA: Journal of the Association for*

Laboratory Automation **13**, 314–321 (2008).

28. Peterson, D. S. Matrix−free methods for laser desorption/ionization mass spectrometry. *Mass spectrometry reviews* **26**, 19–34 (2007).

29. Go, E. P. *et al.* Desorption/ionization on silicon time-of-flight/time-of-flight mass spectrometry. *Analytical chemistry* **75**, 2504–2506 (2003).

30. Kruse, R. A., Rubakhin, S. S., Romanova, E. V., Bohn, P. W. & Sweedler, J. V. Direct assay of Aplysia tissues and cells with laser desorption/ionization mass spectrometry on porous silicon. *Journal of mass spectrometry* **36**, 1317–1322 (2001).

31. Shen, Z. *et al.* Porous silicon as a versatile platform for laser desorption/ionization mass spectrometry. *Analytical Chemistry* **73**, 612–619 (2001).

32. Lewis, W. G., Shen, Z., Finn, M. G. & Siuzdak, G. Desorption/ionization on silicon (DIOS) mass spectrometry: background and applications. *International Journal of Mass Spectrometry* **226**, 107–116 (2003).

33. Okuno, S., Wada, Y. & Arakawa, R. Quantitative analysis of polypropyleneglycol mixtures by desorption/ionization on porous silicon mass spectrometry. *International Journal of Mass Spectrometry* **241**, 43–48 (2005).

34. Jemere, A. B., Bezuidenhout, L. W., Brett, M. J. & Harrison, D. J. Matrix−free laser desorption/ionization mass spectrometry using silicon glancing angle deposition (GLAD) films. *Rapid Communications in Mass*

Spectrometry **24**, 2305–2311 (2010).

35. Zhou, Y., Peng, C., Harris, K. D., Mandal, R. & Harrison, D. J. Salt segregation and sample cleanup on perfluoro-coated nanostructured surfaces for laser desorption ionization mass spectrometry of biofluid samples. *Analytical chemistry* **89**, 3362–3369 (2017).

36. Singh, R. N. Cobalt, Silicon and Silica GLAD films for SMALDI-MS, UTLC and Tissue Imaging. (2014).

37. Trauger, S. A. *et al.* High sensitivity and analyte capture with desorption/ionization mass spectrometry on silylated porous silicon. *Analytical chemistry* **76**, 4484–4489 (2004).

38. Peng, C. Thin Films for Solid Matrix Laser Desorption/Ionization for Biomarker Analysis. (2014).

39. Plawsky, J. L., Kim, J. K. & Schubert, E. F. Engineered nanoporous and nanostructured films. *Materials Today* **12**, 36–45 (2009).

40. Tang, H.-W., Ng, K.-M., Lu, W. & Che, C.-M. Ion desorption efficiency and internal energy transfer in carbon-based surface-assisted laser desorption/ionization mass spectrometry: desorption mechanism (s) and the design of SALDI substrates. *Analytical chemistry* **81**, 4720–4729 (2009).

41. Hsu, W.-Y., Lin, W.-D., Hwu, W.-L., Lai, C.-C. & Tsai, F.-J. Screening assay of very long chain fatty acids in human plasma with multiwalled carbon nanotube-based surface-assisted laser desorption/ionization mass

spectrometry. *Analytical chemistry* **82**, 6814–6820 (2010).

42. Amini, N., Shariatgorji, M. & Thorsén, G. SALDI-MS signal enhancement using oxidized graphitized carbon black nanoparticles. *Journal of the American Society for Mass Spectrometry* **20**, 1207–1213 (2009).

43. Lin, Z. *et al.* Negative ion laser desorption/ionization time-of-flight mass spectrometric analysis of small molecules using graphitic carbon nitride nanosheet matrix. *Analytical chemistry* **87**, 8005–8012 (2015).

44. Ugarov, M. V. *et al.* MALDI matrices for biomolecular analysis based on functionalized carbon nanomaterials. *Analytical chemistry* **76**, 6734–6742 (2004).

45. Shin, J. H., Song, J. Y. & Park, H. M. Growth of ZnO nanowires on a patterned Au substrate. *Materials Letters* **63**, 145–147 (2009).

46. Shariatgorji, M., Amini, N. & Ilag, L. L. Silicon nitride nanoparticles for surface-assisted laser desorption/ionization of small molecules. *Journal of nanoparticle research* **11**, 1509–1512 (2009).

47. Sato, H., Nemoto, A., Yamamoto, A. & Tao, H. Surface cleaning of germanium nanodot ionization substrate for surface−assisted laser desorption/ionization mass spectrometry. *Rapid Communications in Mass Spectrometry: An International Journal Devoted to the Rapid Dissemination of Up−to−the−Minute Research in Mass Spectrometry* **23**, 603–610 (2009).

48. Seino, T. *et al.* Matrix-free laser desorption/ionization-mass spectrometry

using self-assembled germanium nanodots. *Analytical chemistry* **79**, 4827–4832 (2007).

49. Guo, Z., Ganawi, A. A., Liu, Q. & He, L. Nanomaterials in mass spectrometry ionization and prospects for biological application. *Analytical and bioanalytical chemistry* **384**, 584–592 (2006).

50. Go, E. P., Shen, Z., Harris, K. & Siuzdak, G. Quantitative analysis with desorption/ionization on silicon mass spectrometry using electrospray deposition. *Analytical chemistry* **75**, 5475–5479 (2003).

51. Northen, T. R. *et al.* High surface area of porous silicon drives desorption of intact molecules. *Journal of the American Society for Mass Spectrometry* **18**, 1945–1949 (2007).

52. Brinker, C. J., Lu, Y., Sellinger, A. & Fan, H. Evaporation−induced self−assembly: nanostructures made easy. *Advanced materials* **11**, 579–585 (1999).

53. Nitta, S. V. *et al.* Surface modified spin-on xerogel films as interlayer dielectrics. *Journal of Vacuum Science & Technology B: Microelectronics and Nanometer Structures Processing, Measurement, and Phenomena* **17**, 205–212 (1999).

54. Jain, A. *et al.* Porous silica materials as low-k dielectrics for electronic and optical interconnects. *Thin Solid Films* **398**, 513–522 (2001).

55. Ojha, M., Gill, W. N., Plawsky, J. L. & Cho, W. Fabrication of ultrathin (~

100 nm), low-index nanoporous silica films for photonic devices: Role of substrate adhesion on the film thickness. *Journal of Vacuum Science & Technology B: Microelectronics and Nanometer Structures Processing, Measurement, and Phenomena* **24**, 1109–1116 (2006).

56. Luo, G., Chen, Y., Siuzdak, G. & Vertes, A. Surface modification and laser pulse length effects on internal energy transfer in DIOS. *The Journal of Physical Chemistry B* **109**, 24450–24456 (2005).

57. Grill, A. Plasma enhanced chemical vapor deposited SiCOH dielectrics: from low-k to extreme low-k interconnect materials. *Journal of Applied Physics* **93**, 1785–1790 (2003).

58. Taschuk, M. T., Hawkeye, M. M. & Brett, M. J. Glancing angle deposition. in *Handbook of Deposition Technologies for Films and Coatings* 621–678 (Elsevier, 2010).

59. Robbie, K. & Brett, M. J. Sculptured thin films and glancing angle deposition: Growth mechanics and applications. *Journal of Vacuum Science & Technology A: Vacuum, Surfaces, and Films* **15**, 1460–1465 (1997).

60. Robbie, K., Sit, J. C. & Brett, M. J. Advanced techniques for glancing angle deposition. *Journal of Vacuum Science & Technology B: Microelectronics and Nanometer Structures Processing, Measurement, and Phenomena* **16**, 1115–1122 (1998).

61. Hawkeye, M. M., Taschuk, M. T. & Brett, M. J. Introduction: glancing angle

deposition technology. *Glancing Angle Deposition of Thin Films* 1–30 (2014).

62. Schubert, M. F., Xi, J.-Q., Kim, J. K. & Schubert, E. F. Distributed Bragg reflector consisting of high-and low-refractive-index thin film layers made of the same material. *Applied physics letters* **90**, 141115 (2007).

63. Alimpiev, S., Nikiforov, S., Karavanskii, V., Minton, T. & Sunner, J. On the mechanism of laser-induced desorption–ionization of organic compounds from etched silicon and carbon surfaces. *The Journal of Chemical Physics* **115**, 1891–1901 (2001).

64. Dubin, V. M., Vieillard, C., Ozanam, F. & Chazalviel, J.-N. Preparation and Characterization of Surface−Modified Luminescent Porous Silicon. *physica status solidi (b)* **190**, 47–52 (1995).

65. Buriak, J. M. & Allen, M. J. Lewis acid mediated functionalization of porous silicon with substituted alkenes and alkynes. *Journal of the American Chemical Society* **120**, 1339–1340 (1998).

66. Buriak, J. M. *et al.* Lewis acid mediated hydrosilylation on porous silicon surfaces. *Journal of the American Chemical Society* **121**, 11491–11502 (1999).

67. Stewart, M. P. *et al.* Three methods for stabilization and functionalization of porous silicon surfaces via hydrosilylation and electrografting reactions. *physica status solidi (a)* **182**, 109–115 (2000).

68. Stewart, M. P. & Buriak, J. M. Exciton-mediated hydrosilylation on

photoluminescent nanocrystalline silicon. *Journal of the American Chemical Society* **123**, 7821–7830 (2001).

69. Xu, D. *et al.* Hydrolysis and silanization of the hydrosilicon surface of freshly prepared porous silicon by an amine catalytic reaction. *New Journal of Chemistry* **27**, 300–306 (2003).

70. Zhou, Y. Biomolecules in Nanoporous Structures. (2017).

71. Okuno, S. & Wada, Y. Measurement of serum salicylate levels by solid-phase extraction and desorption/ionization on silicon mass spectrometry. *Journal of Mass Spectrometry* **40**, 1000–1004 (2005).

72. Vaidyanathan, S. *et al.* A laser desorption ionisation mass spectrometry approach for high throughput metabolomics. *Metabolomics* **1**, 243–250 (2005).

73. Liu, Q., Guo, Z. & He, L. Mass Spectrometry Imaging of Small Molecules Using Desorption/Ionization on Silicon. *Analytical Chemistry* **79**, 3535–3541 (2007).

74. Woo, H.-K., Northen, T. R., Yanes, O. & Siuzdak, G. Nanostructure-initiator mass spectrometry: a protocol for preparing and applying NIMS surfaces for high-sensitivity mass analysis. *Nature Protocols* **3**, 1341–1349 (2008).

75. Yanes, O. *et al.* Nanostructure initiator mass spectrometry: tissue imaging and direct biofluid analysis. *Analytical chemistry* **81**, 2969–2975 (2009).

76. Northen, T. R. *et al.* Clathrate nanostructures for mass spectrometry. *Nature* **449**, 1033–1036 (2007).

77. Greving, M. P., Patti, G. J. & Siuzdak, G. Nanostructure-Initiator Mass Spectrometry Metabolite Analysis and Imaging. *Analytical Chemistry* **83**, 2–7 (2011).

78. Zhao, Y. *et al.* Sample preparation in centrifugal microfluidic discs for human serum metabolite analysis by surface assisted laser desorption/ionization mass spectrometry. *Analytical chemistry* (2019).

79. Kawasaki, H., Shimomae, Y., Watanabe, T. & Arakawa, R. Desorption/ionization on porous silicon mass spectrometry (DIOS-MS) of perfluorooctane sulfonate (PFOS). *Colloids and Surfaces A: Physicochemical and Engineering Aspects* **347**, 220–224 (2009).

80. Reviews, C. T. I. *Medical Biochemistry: Biology, Biochemistry*. (Cram101 Textbook Reviews, 2016).

81. Fonteh, A. N., Harrington, R. J., Tsai, A., Liao, P. & Harrington, M. G. Free amino acid and dipeptide changes in the body fluids from Alzheimer's disease subjects. *Amino acids* **32**, 213–224 (2007).

82. Tsujimoto, T. *et al.* Both high and low plasma glutamine levels predict mortality in critically ill patients. *Surgery today* **47**, 1331–1338 (2017).

83. Gu, Y. *et al.* Perioperative dynamics and significance of amino acid profiles in patients with cancer. *Journal of translational medicine* **13**, 35 (2015).

84. Gar, C. *et al.* Serum and plasma amino acids as markers of prediabetes, insulin resistance, and incident diabetes. *Critical reviews in clinical laboratory sciences* **55**, 21–32 (2018).

85. Duskova, K. *et al.* Differences in urinary amino acid patterns in individuals with different types of urological tumor urinary amino acid patterns as markers of urological tumors. *in vivo* **32**, 425–429 (2018).

86. Stoessel, D. *et al.* Promising Metabolite Profiles in the Plasma and CSF of Early Clinical Parkinson's Disease. *Frontiers in aging neuroscience* **10**, 51 (2018).

87. Tan, B. *et al.* Metabonomics identifies serum metabolite markers of colorectal cancer. *Journal of proteome research* **12**, 3000–3009 (2013).

88. Zheng, P. *et al.* A novel urinary metabolite signature for diagnosing major depressive disorder. *Journal of proteome research* **12**, 5904–5911 (2013).

89. Suliman, M. E. *et al.* Hyperhomocysteinemia in relation to plasma free amino acids, biomarkers of inflammation and mortality in patients with chronic kidney disease starting dialysis therapy. *American journal of kidney diseases* **44**, 455–465 (2004).

90. Lai, H.-S., Lee, J.-C., Lee, P.-H., Wang, S.-T. & Chen, W.-J. Plasma free amino acid profile in cancer patients. in *Seminars in cancer biology* **15**, 267–276 (Elsevier, 2005).

91. Poschke, I., Mao, Y., Kiessling, R. & de Boniface, J. Tumor-dependent

increase of serum amino acid levels in breast cancer patients has diagnostic potential and correlates with molecular tumor subtypes. *Journal of translational medicine* **11**, 1 (2013).

92. Miyagi, Y. *et al.* Plasma free amino acid profiling of five types of cancer patients and its application for early detection. *PloS one* **6**, e24143 (2011).

93. Xu, X.-J. *et al.* 2, 4-Dihydroxypyrimidine is a potential urinary metabolite biomarker for diagnosing bipolar disorder. *Molecular bioSystems* **10**, 813–819 (2014).

94. Kawai, N. *et al.* Plasma free amino acid (PFAA) profile is a potential blood-based biomarker for Alzheimer's disease. *Alzheimer's & Dementia: The Journal of the Alzheimer's Association* **10**, P886–P887 (2014).

95. Olson, L. & Humpel, C. Growth factors and cytokines/chemokines as surrogate biomarkers in cerebrospinal fluid and blood for diagnosing Alzheimer's disease and mild cognitive impairment. *Experimental gerontology* **45**, 41–46 (2010).

96. Tessari, P., Lante, A. & Mosca, G. *Sci Rep* **6**, (2016).

97. Neurauter, G. *et al.* Simultaneous measurement of phenylalanine and tyrosine by high performance liquid chromatography (HPLC) with fluorescence detection. *Clinical biochemistry* **46**, 1848–1851 (2013).

98. Jámbor, A. & Molnár-Perl, I. Quantitation of amino acids in plasma by high performance liquid chromatography: Simultaneous deproteinization and

derivatization with 9-fluorenylmethyloxycarbonyl chloride. *Journal of Chromatography A* **1216**, 6218–6223 (2009).

99. Jaworska, M. *et al.* New approach for amino acid profiling in human plasma by selective fluorescence derivatization. *Amino acids* **43**, 1653–1661 (2012).

100. Wu, X. *et al.* Determination of amino acid neurotransmitters in rat hippocampi by HPLC−UV using NBD−F as a derivative. *Biomedical Chromatography* **28**, 459–462 (2014).

101. Mo, X., Li, Y., Tang, A. & Ren, Y. Simultaneous determination of phenylalanine and tyrosine in peripheral capillary blood by HPLC with ultraviolet detection. *Clinical biochemistry* **46**, 1074–1078 (2013).

102. Shimbo, K. *et al.* Automated precolumn derivatization system for analyzing physiological amino acids by liquid chromatography/mass spectrometry. *Biomedical Chromatography* **24**, 683–691 (2010).

103. Ziegler, J. & Abel, S. Analysis of amino acids by HPLC/electrospray negative ion tandem mass spectrometry using 9-fluorenylmethoxycarbonyl chloride (Fmoc-Cl) derivatization. *Amino Acids* **46**, 2799–2808 (2014).

104. Tamashima, E. *et al.* Direct tandem mass spectrometric analysis of amino acids in plasma using fluorous derivatization and monolithic solid-phase purification. *Journal of pharmaceutical and biomedical analysis* **115**, 201–207 (2015).

105. Knapp, D. R. *Handbook of analytical derivatization reactions*. (John Wiley &

Sons, 1979).

106. Orata, F. Derivatization reactions and reagents for gas chromatography analysis. in *Advanced gas chromatography-Progress in agricultural, biomedical and industrial applications* (IntechOpen, 2012).

107. Garcia, B. A. *et al.* Chemical derivatization of histones for facilitated analysis by mass spectrometry. *Nature protocols* **2**, 933 (2007).

108. Keough, T., Youngquist, R. S. & Lacey, M. P. A method for high-sensitivity peptide sequencing using postsource decay matrix-assisted laser desorption ionization mass spectrometry. *Proceedings of the National Academy of Sciences* **96**, 7131–7136 (1999).

109. Keough, T., Lacey, M. P. & Youngquist, R. S. Derivatization procedures to facilitate de novo sequencing of lysine−terminated tryptic peptides using postsource decay matrix−assisted laser desorption/ionization mass spectrometry. *Rapid Communications in Mass Spectrometry* **14**, 2348–2356 (2000).

110. Standing, K. G. Peptide and protein de novo sequencing by mass spectrometry. *Current opinion in structural biology* **13**, 595–601 (2003).

111. Halket, J. M. & Zaikin, V. G. Derivatization in mass spectrometry—1. Silylation. *European Journal of Mass Spectrometry* **9**, 1–21 (2003).

112. Hayama, T. *et al.* Fluorous derivatization combined with liquid chromatography/tandem mass spectrometry: a method for the selective and

sensitive determination of sialic acids in biological samples. *Rapid Communications in Mass Spectrometry* **24**, 2868–2874 (2010).

113. Sakaguchi, Y. *et al.* Selective liquid-chromatographic determination of native fluorescent biogenic amines in human urine based on fluorous derivatization. *Journal of Chromatography A* **1218**, 5581–5586 (2011).

114. Sakaguchi, Y. *et al.* Selective and sensitive liquid chromatographic determination method of 5-hydroxyindoles with fluorous and fluorogenic derivatization. *Journal of pharmaceutical and biomedical analysis* **114**, 348–354 (2015).

115. Halket, J. M. & Zaikin, V. G. Derivatization in mass spectrometry–3. Alkylation (arylation). *European Journal of Mass Spectrometry* **10**, 1–19 (2004).

116. De Jesús, V. R., Chace, D. H., Lim, T. H., Mei, J. V. & Hannon, W. H. Comparison of amino acids and acylcarnitines assay methods used in newborn screening assays by tandem mass spectrometry. *Clinica chimica acta* **411**, 684–689 (2010).

117. Hardy, D. T., Hall, S. K., Preece, M. A. & Green, A. Quantitative determination of plasma phenylalanine and tyrosine by electrospray ionization tandem mass spectrometry. *Annals of clinical biochemistry* **39**, 73–75 (2002).

118. Hayama, T. Development of Analytical Methods Utilizing Selectivity of Fluorous Affinity and Their Applications. *Chromatography* **37**, 1–8 (2016).

119. Hayama, T. *et al.* Binary fluorous alkylation of biogenic primary amines with perfluorinated aldehyde followed by fluorous liquid chromatography–tandem mass spectrometry analysis. *Analytical chemistry* **84**, 8407–8414 (2012).

120. Sakaguchi, Y., Kinumi, T., Yamazaki, T. & Takatsu, A. A novel amino acid analysis method using derivatization of multiple functional groups followed by liquid chromatography/tandem mass spectrometry. *Analyst* **140**, 1965–1973 (2015).

121. Sakaguchi, Y., Yoshida, H., Todoroki, K., Nohta, H. & Yamaguchi, M. Separation-oriented derivatization of native fluorescent compounds through fluorous labeling followed by liquid chromatography with fluorous-phase. *Analytical chemistry* **81**, 5039–5045 (2009).

122. Pierce, A. E. Silylation of Organic Compounds, Pierce Chem. *Co., Rockford* **111**, 438 (1968).

123. van Look, G. Silylating Agents. *Fluka Chemika: Buchs: Fluka Chemie AG* (1988).

124. Kataoka, H. Gas chromatography of amines as various derivatives. in *Journal of Chromatography Library* **70**, 364–404 (Elsevier, 2005).

125. Halket, J. M. *et al.* Deconvolution gas chromatography/mass spectrometry of urinary organic acids–potential for pattern recognition and automated identification of metabolic disorders. *Rapid communications in mass spectrometry* **13**, 279–284 (1999).

126. Zenkevich, I. G. Hydroxy compounds: derivatization for GC analysis. *Encyclopedia of chromatography.* **CRC Press**, 1165-1172. (2009).

127. Zaikin, V. G. & Halket, J. M. Derivatization in mass spectrometry—2. Acylation. *European Journal of Mass Spectrometry* **9**, 421–434 (2003).

128. Halket, J. M. & Zaikin, V. G. Derivatization in mass spectrometry—5. Specific derivatization of monofunctional compounds. *European Journal of Mass Spectrometry* **11**, 127–160 (2005).

129. Black, R. M. & Muir, B. Derivatisation reactions in the chromatographic analysis of chemical warfare agents and their degradation products. *Journal of Chromatography A* **1000**, 253–281 (2003).

130. Zaikin, V. G. & Halket, J. M. Derivatization in mass spectrometry—4. Formation of cyclic derivatives. *European Journal of Mass Spectrometry* **10**, 555–568 (2004).

131. Spitellek, G. Mass spectrometry of heterocyclic compounds. in *Advances in Heterocyclic Chemistry* **7**, 301–376 (Elsevier, 1967).

132. Budzikiewicz, H., Djerassi, C. & Williams, D. H. Mass spectrometry of organic compounds. (1967).

133. Go, E. P. *et al.* Selective metabolite and peptide capture/mass detection using fluorous affinity tags. *Journal of proteome research* **6**, 1492–1499 (2007).

134. Brittain, S. M., Ficarro, S. B., Brock, A. & Peters, E. C. Enrichment and

analysis of peptide subsets using fluorous affinity tags and mass spectrometry. *Nature biotechnology* **23**, 463 (2005).

135. Hawkeye, M. M. & Brett, M. J. Glancing angle deposition: fabrication, properties, and applications of micro-and nanostructured thin films. *Journal of Vacuum Science & Technology A: Vacuum, Surfaces, and Films* **25**, 1317–1335 (2007).

136. Yang, J. *et al.* Potential metabolite markers of schizophrenia. *Molecular psychiatry* **18**, 67 (2013).

137. Todoroki, K., Etoh, H., Yoshida, H., Nohta, H. & Yamaguchi, M. A fluorous tag-bound fluorescence derivatization reagent, F-trap pyrene, for reagent peak-free HPLC analysis of aliphatic amines. *Analytical and bioanalytical chemistry* **394**, 321–327 (2009).

138. Xu, Z., Gibson, G. T. & Oleschuk, R. D. Development of fluorous porous polymer monolith (FPPM) for the capillary electrochromatographic separation of fluorous analytes based on fluorous–fluorous interaction. *Analyst* **138**, 611–619 (2013).

139. Curran, D. P. Fluorous reverse phase silia gel. A new tool for preparative separations in synthetic organic and organofluorine chemistry. *Synlett* **2001**, 1488–1496 (2001).

140. Northen, T. R. *et al.* Clathrate nanostructures for mass spectrometry. *Nature* **449**, 1033 (2007).

141. Sweetman, M. J. *et al.* Rapid, metal-free hydrosilanisation chemistry for porous silicon surface modification. *Chemical Communications* **51**, 10640–10643 (2015).

142. Shi, T. *et al.* High-performance liquid chromatographic method for determination of amino acids by precolumn derivatization with 4-chloro-3, 5-dinitrobenzotrifluoride. *Analytica chimica acta* **654**, 154–161 (2009).

143. Raider, S. I., Flitsch, R. & Palmer, M. J. Oxide growth on etched silicon in air at room temperature. *Journal of the Electrochemical Society* **122**, 413–418 (1975).

144. Morita, M., Ohmi, T., Hasegawa, E., Kawakami, M. & Ohwada, M. Growth of native oxide on a silicon surface. *Journal of Applied Physics* **68**, 1272–1281 (1990).

145. Dick Jr, L. W., Swinteck, B. J. & McGown, L. B. Albumins as a model system for investigating separations of closely related proteins on DNA stationary phases in capillary electrochromatography. *Analytica chimica acta* **519**, 197–205 (2004).

146. Lin, Y.-S., Tsai, P.-J., Weng, M.-F. & Chen, Y.-C. Affinity capture using vancomycin-bound magnetic nanoparticles for the MALDI-MS analysis of bacteria. *Analytical chemistry* **77**, 1753–1760 (2005).

147. Meng, J., Siuzdak, G. & Finn, M. G. Affinity mass spectrometry from a tailored porous silicon surface. *Chemical Communications* 2108–2109 (2004).

148. Ravanbakhsh, S. *et al.* Accurate, fully-automated NMR spectral profiling for metabolomics. *PloS one* **10**, e0124219 (2015).

149. Bovee, W. Quantification of glutamate, glutamine, and other metabolites in in vivo proton NMR spectroscopy. *NMR in biomedicine* **4**, 81–84 (1991).

150. Yuan, W., Zhang §, J., Li, S. & Edwards, J. L. Amine metabolomics of hyperglycemic endothelial cells using capillary LC–MS with isobaric tagging. *Journal of proteome research* **10**, 5242–5250 (2011).

151. Yang, W.-C., Mirzaei, H., Liu, X. & Regnier, F. E. Enhancement of amino acid detection and quantification by electrospray ionization mass spectrometry. *Analytical Chemistry* **78**, 4702–4708 (2006).

152. Xu, F., Zou, L., Liu, Y., Zhang, Z. & Ong, C. N. Enhancement of the capabilities of liquid chromatography–mass spectrometry with derivatization: general principles and applications. *Mass spectrometry reviews* **30**, 1143–1172 (2011).

153. Shimbo, K., Yahashi, A., Hirayama, K., Nakazawa, M. & Miyano, H. Multifunctional and highly sensitive precolumn reagents for amino acids in liquid chromatography/tandem mass spectrometry. *Analytical Chemistry* **81**, 5172–5179 (2009).

154. Iwasaki, Y. *et al.* A new strategy for ionization enhancement by derivatization for mass spectrometry. *Journal of Chromatography B* **879**, 1159–1165 (2011).

155. Guo, K., Ji, C. & Li, L. Stable-isotope dimethylation labeling combined with LC− ESI MS for quantification of amine-containing metabolites in biological samples. *Analytical chemistry* **79**, 8631–8638 (2007).

Appendix A

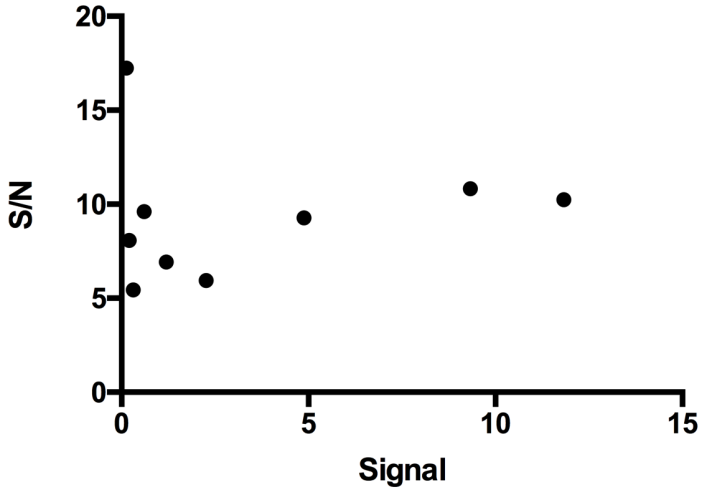

Figure: S/N *vs.* signal for arginine in aCSF solution using 5 μM histidine as the internal standard (data in Figure 2-13).

Appendix B

Table: Amino acids tested in various samples. The amino acid that is distinguishable in SALDI-MS by its fluorous derivatives is marked with ✓ in the table.

Amino acid	Aqueous	aCSF	Serum
Gly	✓	✓	
Ala	✓	✓	
Ser	✓	✓	
Thr	✓	✓	
Cys	✓	✓	
Val	✓	✓	✓
Leu	✓	✓	
Ile			
Met			
Pro	✓	✓	
Phe	✓	✓	✓
Tyr	✓	✓	✓
Trp	✓	✓	
Asp	✓	✓	✓
Glu	✓	✓	✓
Asn	✓	✓	✓
Gln	✓	✓	✓
His	✓	✓	✓

Lys	✓	✓	✓
Arg	✓	✓	✓

Appendix C

Table: Comparison of relative standard deviation in predicted concentration in different samples.

Metabolite	SALDI-MS combined with derivatization	Other SALDI-MS method[a]
Arginine (pure samples with histidine as IS)	±8.42%	
Arginine (salts only aCSF samples with histidine as IS)	±12.4 %	
Arginine (aCSF samples containing amino acids with histidine as IS)	±11.0 %	
Arginine (serum with ^{13}C arginine* as IS)	±10.2 %	
Arginine (serum)	±8.53 %	
Valine (serum)	±9.67 %	
Asparagine (serum)	±15.5 %	
Histidine (serum)	±12.2 %	±29 % with IS
Glutamic acid (serum)	±10.9 %	
Glutamine (serum)		±21 % with IS

a) Data from reference [38].

Appendix D

The error of estimating the concentration of an unknown, S_x, is given from the measured value y and the calibration curve using the least-squares method.

$$S_x = \frac{S_y}{|m|}\sqrt{\frac{1}{k}+\frac{1}{n}+\frac{(y-\bar{y})^2}{m^2\sum(x_i-\bar{x})^2}}$$

where

$$S_y = \sqrt{\frac{\sum(y_i - mx_i - b)^2}{n-2}}$$

m is the slope of the line, k is the number of measurements of the unknown, n is the number of data points for the calibration curve, y is the average y value for k measurements of the unknown, $\bar{y}$ is the mean value of y for the points on the calibration curve, x_i are the individual values of x for the points on the calibration curve, and $\bar{x}$ is the mean value of x for the points on the calibration curve.

95% confidence interval for an unknown is given by $x \pm tS_x$, where t is Student's t value.